Mathematics

https://www.aimspress.com/journal/Math

AIMS Mathematics, 11(6): 16837–16886.
DOI: 10.3934/math.2026691
Received: 31 January 2026
Revised: 13 April 2026
Accepted: 13 May 2026
Published: 11 June 2026

Research article

A flexible hyperbolic secant-B family of distributions with applications to lifetime and stress-strength data

Aijaz Ahmad[1], Ahmed R. El-Saeed[2], Taha Radwan[3,*], Manzoor A. Khanday[4] and Ahlam H. Tolba[5,*]

[1] Lincoln University College, Petaling Jaya-47301, Selangor, Malaysia

[2] Department of Mathematics and Statistics, Faculty of Science, Imam Mohammad Ibn Saud Islamic University (IMSIU), Riyadh 11432, Saudi Arabia

[3] Department of Management Information Systems, College of Business and Economics, Qassim University, Buraydah 51452, Saudi Arabia

[4] Department of Mathematics, Lovely Professional University, Punjab, India

[5] Department of Mathematics, Faculty of Science, Mansoura University, Mansoura 35516, Egypt

* **Correspondence:** Email: t.radwan@qu.edu.sa, dr_ahmady156@mans.edu.eg; Tel: +201008782195.

Abstract: Despite the availability of continuous distributions, few utilize the modeling potential of trigonometric functions, and none are based on the hyperbolic secant function. To fill this gap, we introduce the hyperbolic Sec-B family of trigonometric distributions. As a specific application, we introduce an adapted half-power logistic distribution (HS-PHLD) that retains a simple two-parameter form while offering greater versatility, particularly in tail behavior and skewness. Our research comprehensively explores this, establishing its fundamental mathematical properties, providing series expansions for its functions, and using both non-Bayesian and Bayesian estimation techniques. Monte Carlo simulations are used to validate the effectiveness of these estimators. Practically speaking, the HS-PHLD outperforms well-established models on three real-world datasets from the engineering and survival domains.

Keywords: hyperbolic secant function; moments; statistical model; acturial indicators; Bayesian analysis; simulation; estimations; data analysis
Mathematics Subject Classification: 62A86, 62D05, 62F12, 62F25, 62G07, 62L05, 62L10, 62L12

1. Introduction

Probability distributions have been used extensively in industries such as engineering, health, insurance, and economics to model, analyze, and predict data patterns. The success of statistical inference is strongly dependent on how well the chosen probability distribution matches the underlying data patterns. However, standard distributions often lack the versatility and accuracy needed to accurately describe complex data. This constraint has culminated in the development of more adaptive and complex distributional models that better explain the behavior of real-world data.

Trigonometric functions have been utilized extensively in probability and statistics, notably for modeling periodic patterns and signal processing. Their cyclical character is critical for investigating and replicating oscillations and recurrent trends in empirical data. These functions are vital in probability theory for stochastic processes and temporal data processing. For example, sine and cosine functions form the basis of the Fourier transform, which decomposes complex signals into their constituent frequencies. This is essential for understanding and anticipating data patterns. Statistical distributions have attracted an enormous amount of attention in developing adaptable frameworks for analyzing diverse datasets. In the past few years, researchers in this field have created several generators to improve plausibility within traditional probability distributions. This flexibility is often achieved by introducing new parameters into established distribution structures. Contemporary research has primarily concentrated on creating novel generators from continuous classical distributions. Recently, researchers have created a number of probability generators that utilize trigonometric functions. These functions have been found to significantly improve the performance of traditional distributions, particularly when dealing with complicated data across several scientific areas. Overall, trigonometric function-based probability generators represent a significant advance in statistical modeling. They provide researchers with powerful tools for addressing complex data analysis challenges, enabling discoveries and insights across various disciplines. As a consequence, these sophisticated distributions increase the adaptability and efficiency of data handling.

The following are some derived families of distributions. Sine transformations based on trigonometric functions are proposed by Anwar et al. [1], Alomair et al. [2], Chesneau et al. [3], Souza et al. [4], Jammal et al. [5], Kumar et al. [6], Lone et al. [7], Muzamil et al. [8], Odhah et al. [9].

In the area of probability distribution theory, various generator methods have been developed to enhance the flexibility of basic distributions. These generators include the Marshall-Olkin generator, the alpha power generator, the beta family generated, the Kumaraswamy family generated, and the Topp-Leone generator. These models have been successfully applied in reliability theory, survival analysis, and risk modeling because of their ability to change the skewness, tail, and hazard rate functions. One thing that is common to all these generators is that their flexibility is mainly achieved through the addition of new shape parameters, which can be considered as a reparameterization of the original model. Although the addition of parameters can be beneficial in terms of goodness of fit, it often results in model complexity, identifiability problems, and instability, especially when working with small to moderate samples; see Mahmoud et al. [10], and Ramadan et al. [11].

Some recent studies in probability theory have focused on generators based on trigonometric functions, such as the sine-G, cosine-G, and tan-G generators [12]. In contrast to parameter-augmented generators, these models directly operate on the basic cumulative distribution function (CDF) using bounded trigonometric functions. This approach keeps the original parameter space's dimensionality but provides better flexibility using functional transformation instead of parameter augmentation. The results show that these generators can greatly enhance the modeling capability for complex lifetime and reliability data. Given these advances, it is necessary to explore other functional transformations that can keep the same level of parsimony but provide better distributional flexibility. However, secant-based hyperbolic generators have not yet been considered in the literature. Although the smooth and bounded form, and the strong tail-modulating abilities, of hyperbolic functions make them very attractive, the hyperbolic secant function, in particular, has not been sufficiently investigated in the context of distributional generation yet. This reveals a gap for developing a compact generator based on the nonlinear transformation of the CDF, which enhances the tail and hazard rate modeling capabilities without increasing the number of parameters.

Aijaz et al. [13] recently suggested a novel hyperbolic sine generator that uses the Rayleigh distribution as an example; the CDF of this generator is expressed as:

$$F(z;\theta,\zeta)=\frac{2e^{\bar{\theta}}}{(e^{\bar{\theta}}-1)^2}\left(\cosh(\theta^{G(z;\zeta)}-1)-1\right);\quad z\in\mathbb{R},\theta>1,\zeta>0.$$

In the literature on probability distribution theory, Aijaz et al. [14] developed a novel arc- cosine-Ψ class of distribution designed to enhance the efficiency of traditional distributions. The CDF of the arc-cosine generator is expressed as:

$$F(z;\zeta)=1-\frac{2}{\pi}\cos^{-1}\left(\frac{\pi^{\Psi(z;\zeta)}-\bar{\Psi}(z;\zeta)}{\pi}\right);\quad z\in\mathbb{R},\zeta>0.$$

Among others, Souza et al. [15] established the sec-G class of distribution with the CDF stated as

$$F(z;\zeta)=\sec\left(\frac{\pi}{3}G(z;\zeta)\right)-1;\quad z\in\mathbb{R},\zeta>0.$$

This paper presents a hyperbolic secant (as defined by an exponential function) distribution as the basis of a flexible and non-linear CDF. The proposed distribution demonstrates a wide variety of failure rates and probability density functions (PDFs), making it an innovative addition to the literature on distribution generators.

1.1. Definition

Assuming that $F(x;\Theta)$ symbolizes the CDF and $f(x;\Theta)$ is the related PDF for a random variable X, the CDF of the hyperbolic sech-B family of distribution can be described as follows.

$$\begin{aligned}F(x;\Theta)=&\frac{e^{2\bar{e}}+1}{(e^{\bar{e}}-1)^2}\int_0^{\left(e-e^{\bar{B}(x;\Theta)}\right)}\operatorname{sech}(t)\tanh(t)dt\\=&\frac{e^{2\bar{e}}+1}{(e^{\bar{e}}-1)^2}\left(1-\operatorname{sech}\left(e-e^{\bar{B}(x;\Theta)}\right)\right);\quad x\in\mathbb{R},2<e<3,\ \Theta>0.\end{aligned}\tag{1.1}$$

The relevant PDF of Eq (1.1) is expressed as

$$f(x;\Theta)=\frac{e^{2\bar{e}}+1}{(e^{\bar{e}}-1)^2}b(x;\Theta)e^{\bar{B}(x;\Theta)}\operatorname{sech}\left(e-e^{\bar{B}(x;\Theta)}\right)\tanh\left(e-e^{\bar{B}(x;\Theta)}\right);\quad x\in\mathbb{R},2<e<3,\ \Theta>0.\tag{1.2}$$

The function, which $B(x;\Theta)$ represents the baseline CDF, whose behavior is governed by the parameter vector Θ. Furthermore, the derivative of $B(x;\Theta)$ with respect to x is expressed as $b(x;\Theta)$ and $\bar{B}(x;\Theta) = 1 - B(x;\Theta)$.

Construction flowchart of the hyperbolic sech-B CDF.

Start: Random variable X with the baseline CDF $B(x;\Theta)$

Define the survival function: $\bar{B}(x;\Theta) = 1 - B(x;\Theta)$

Apply exponential transformation: $e - e^{\bar{B}(x;\Theta)}$

Construct integral form of CDF:

$$F(x;\Theta) = \frac{e^{2\bar{e}} + 1}{(e^{\bar{e}} - 1)^2} \int_0^{e-e^{\bar{B}(x;\Theta)}} \operatorname{sech}(t)\tanh(t)\,dt$$

Evaluate the integral: $\int_0^u \operatorname{sech}(t)\tanh(t)\,dt = 1 - \operatorname{sech}(u)$

Final closed-form CDF of hyperbolic sech-B family:

$$F(x;\Theta) = \frac{e^{2\bar{e}} + 1}{(e^{\bar{e}} - 1)^2}\left(1 - \operatorname{sech}\left(e - e^{\bar{B}(x;\Theta)}\right)\right); \quad x \in \mathbb{R}$$

The proposed generator introduces several key innovations.

- The hyperbolic secant CDF mechanism is structurally different from other types of generators that have been developed, such as the beta-G, Kumaraswamy-G, Marshall-Olkin-G, alpha power-G, and trigonometric-based generators, and provides a method that has never been used before. Control over the shape of the tail and the failure rate through hyperbolic mapping allows for different forms of monotonic/non-monotonic shapes
- This is the first generator to embed sech within a cumulative distribution framework. Applying the term $e - e^{B(x;\Theta)}$ "inside" sech introduces a non-linear reshaping of the baseline distribution, allowing for richer tail and modality behaviors.
- The generator does not add extra shape parameters beyond those of the baseline distribution $B(x;\Theta)$, aiming for parsimony. The resulting PDF and hazard rate can exhibit symmetric, skewed, heavy-tailed, reverse-J, and various non-monotonic failure patterns.
- The CDF and other important properties of the distribution have been derived mathematically. The quantile function has also been derived as an explicit expression, which makes it easier to use for statistical or simulation purposes and to generate random variations efficiently.

The generator's dependability is measured by the accompanying functions: The reliability $R(x;\Theta)$, the hazard rate $h(x;\Theta)$, the reverse hazard rate $r(x;\Theta)$, and the cumulative hazard rate $H(x;\Theta)$. These attributes are frequently utilized in a variety of scientific and engineering domains, including reliability engineering, survival evaluation, risk assessment, and maintenance planning, to analyze and enhance systems' effectiveness and endurance.

$$\begin{aligned}
R(x;\Theta) =&\bar{F}(x;\Theta) = 1 - \frac{e^{2\bar{e}}+1}{(e^{\bar{e}}-1)^2}\left(1-\operatorname{sech}\left(e-e^{\bar{B}(x;\Theta)}\right)\right),\\
h(x;\Theta) =&\frac{f(x;\Theta)}{R(x;\Theta)} = \frac{\left(e^{2\bar{e}}+1\right)b(x;\Theta)e^{\bar{B}(x;\Theta)}\operatorname{sech}\left(e-e^{\bar{B}(x;\Theta)}\right)\tanh\left(e-e^{\bar{B}(x;\Theta)}\right)}{(e^{\bar{e}}-1)^2-(e^{2\bar{e}}+1)\left(1-\operatorname{sech}\left(e-e^{\bar{B}(x;\Theta)}\right)\right)},\\
r(x;\Theta) =&\frac{f(x;\Theta)}{F(x;\Theta)} = \frac{b(x;\Theta)e^{\bar{B}(x;\Theta)}\operatorname{sech}\left(e-e^{\bar{B}(x;\Theta)}\right)\tanh\left(e-e^{\bar{B}(x;\Theta)}\right)}{\left(1-\operatorname{sech}\left(e-e^{\bar{B}(x;\Theta)}\right)\right)},\\
H(x;\Theta) =&-\ln[\bar{F}(x;\Theta)] = -\ln\left\{1-\frac{e^{2\bar{e}}+1}{(e^{\bar{e}}-1)^2}\left(1-\operatorname{sech}\left(e-e^{\bar{B}(x;\Theta)}\right)\right)\right\}.
\end{aligned}$$

The quantile function of the specified generator, which is accomplished by the inversion of Eq (1.1), is an additional valuable tool for assessing various statistical characteristics, including the median, Bowley's skewness, Moor's kurtosis, and other comparable metrics.

$$Q(u;\Theta) = Q_*\left(1-\log\left(e-\operatorname{sech}^{-1}\left(1-\frac{(e^{\bar{e}}-1)^2}{e^{2\bar{e}}+1}u\right)\right)\right);\quad u\in(0,1).$$

The quantile function Q_* relates to the distribution $B(x;\Theta)$.

1.2. Concaveness and asymptotic evaluation

Concavity is used to detect a function's curvature and peaks, and it also serves to locate modes (peaks) and inflection points (locations where concavity varies). While asymptotics dictate tail behavior, which influences risk, and outlier analysis aids in classifying distributions as light- or heavy-tailed. They are essential for statistical simulation, economics, and engineering.

We investigate the curvature of the constructed generator's PDF and hazard rate function (HRF). By implementing logarithmic differentiation to the PDF, we acquire the following expression:

$$\frac{d}{dx}\log(f(x;\Theta)) =\frac{b^{'}(x;\Theta)}{b(x;\Theta)} - b(x;\Theta) + b(x;\Theta)e^{\bar{B}(x;\Theta)}\left(\tanh\left(e-e^{\bar{B}(x;\Theta)}\right)+2\operatorname{csch}\left(2e-2e^{\bar{B}(x;\Theta)}\right)\right).$$

To evaluate the concavity of the PDF, and whether it is concave upward or downward, we need to calculate its second derivative. Putting the second derivative to zero i.e., $\frac{d^2}{dx^2}\log(f(x;\Theta)) = 0$, which enables us to compute the inflection point(s), revealing where the concavity changes. Assuming that I is an interval. Then the PDF is concave upward (or convex) in this interval if the second derivative of its log adheres to the following: $\frac{d^2}{dx^2}\log(f(x;\Theta)) > 0,\ \ \forall\ x\in I$. On the other hand, the PDF is concave downwards if $\frac{d^2}{dx^2}\log(f(x;\Theta)) < 0,\ \ \forall\ x\in I$.

We apply an analogous technique. After evaluating the first derivative of the HRF, we obtain the following expression:

$$\frac{d}{dx}\log(h(x;\Theta)) =\frac{b^{'}(x;\Theta)}{b(x;\Theta)} - b(x;\Theta) + b(x;\Theta)e^{\bar{B}(x;\Theta)}\left(\tanh\left(e-e^{\bar{B}(x;\Theta)}\right)+2\operatorname{csch}\left(2e-2e^{\bar{B}(x;\Theta)}\right)\right)$$

$$-\frac{\left(e^{2\bar{e}}+1\right)b(x;\Theta)e^{\bar{B}(x;\Theta)}\operatorname{sech}\left(e-e^{\bar{B}(x;\Theta)}\right)\tanh\left(e-e^{\bar{B}(x;\Theta)}\right)}{\log\left((e^{\bar{e}}-1)^2-(e^{2\bar{e}}+1)\left(1-\operatorname{sech}\left(e-e^{\bar{B}(x;\Theta)}\right)\right)\right)}.$$

Similarly, we investigate the concavity of the HRF, we evaluate its second derivative, and then we set it to zero $\left\{\frac{d^2}{dx^2}\log(h(x;\Theta))\right\}=0$. This expression aids in determining the points of inflection, which demonstrate changes in the concave shape of the HRF. Suppose that I^* indicates the interval. Then the HRF is concave upward (or convex) in this interval if the second derivative of its log adheres to the following: $\frac{d^2}{dx^2}\log(h(x;\Theta))>0,\ \forall\ x\in I^*$. On the other hand, the HRF is described as being concave downwards if $\frac{d^2}{dx^2}\log(h(x;\Theta))<0,\ \ \forall\ x\in I^*$.

Afterwards, we will compute some asymptotic observations for these functions. Adapting Taylor's series to the CDF described in Eq (1.1) yields the corresponding equivalencies. If $B(x;\Theta)\to 0$, we have

$$\begin{aligned}
F(x;\Theta) &\sim \frac{e^{2\bar{e}}+1}{(e^{\bar{e}}-1)^2}\left(B(x;\Theta)\right)^2,\\
f(x;\Theta) &\sim \frac{2\left(e^{2\bar{e}}+1\right)}{(e^{\bar{e}}-1)^2}b(x;\Theta)B(x;\Theta),\\
h(x;\Theta) &\sim \frac{2\left(e^{2\bar{e}}+1\right)b(x;\Theta)B(x;\Theta)}{(e^{\bar{e}}-1)^2-(e^{2\bar{e}}+1)\left(B(x;\Theta)\right)^2}.
\end{aligned}$$

Following that, given $B(x;\Theta)\to 1$, we acquire the following equivalencies:

$$\begin{aligned}
&F(x;\Theta)\sim 1-\frac{2e^{\bar{e}}\left(e^{\bar{e}}+1\right)}{(e^{\bar{e}}-1)\left(e^{\bar{e}}+1\right)}\left(1-B(x;\Theta)\right),\\
&f(x;\Theta)\sim \frac{2e^{\bar{e}}\left(e^{\bar{e}}+1\right)}{(e^{\bar{e}}-1)\left(e^{\bar{e}}+1\right)}b(x;\Theta),\quad h(x;\Theta)\sim\frac{b(x;\Theta)}{1-B(x;\Theta)}.
\end{aligned}$$

These investigations examine the asymptotic behavior of the PDF and HRF of the resulting distribution, utilizing a baseline CDF $B(x;\Theta)$. The subsequent subsection demonstrates this notion by looking at a specific hyperbolic secant-B class model.

1.3. Useful expansion of CDF

Applying the following expansion to the CDF in Eq (1.1), we have

$$\operatorname{sech}(y)=\sum_{p=0}^{\infty}\frac{(-1)^pE_p}{(2p)!}y^{2p};\quad |y|<\frac{\pi}{2},$$

where E_p represents the p-th Euler number,

$$E_1=1,E_2=5,E_3=61,E_4=1385,E_5=50521,...$$

$$F(x;\Theta)=\frac{e^{2\bar{e}}+1}{(e^{\bar{e}}-1)^2}\left(1-\sum_{p=0}^{\infty}\frac{(-1)^pE_p}{(2p)!}\left(e-e^{\bar{B}(x;\Theta)}\right)^{2p}\right)$$

$$=\frac{e^{2\bar{e}}+1}{(e^{\bar{e}}-1)^2}\left(1-\sum_{p,q=0}^{\infty}\frac{(-1)^p E_p}{(2p)!}e^{2p}\left(1-\frac{e^{\bar{B}(x;\Theta)}}{e}\right)^{2p}\right). \tag{1.3}$$

Since we know that $(1-u)^a = \sum_{n=0}^{\infty}(-1)^n\binom{a}{n}u^n$; $|u|<1$, using this expansion in Eq (1.3), we have the following:

$$F(x;\Theta)=\frac{e^{2\bar{e}}+1}{(e^{\bar{e}}-1)^2}\left(1-\sum_{p,q=0}^{\infty}\frac{(-1)^{p+q}E_p}{(2p)!}e^{2p-q}\binom{2p}{q}e^{q\bar{B}(x;\Theta)}\right). \tag{1.4}$$

Now, we make use of the following expansion in Eq (1.4):

$$e^{bu}=\sum_{r=0}^{\infty}\frac{b^r}{r!}u^r;\quad u\in\mathbb{R},$$

$$F(x;\Theta)=\frac{e^{2\bar{e}}+1}{(e^{\bar{e}}-1)^2}\left(1-\sum_{p,q,r=0}^{\infty}\frac{(-1)^{p+q}E_p}{(2p)!r!}e^{2p-q}\binom{2p}{q}q^r(\bar{B}(x;\Theta))^r\right). \tag{1.5}$$

In order to establish the related PDF in the linear form of Eq (1.5), we differentiate it as

$$\begin{aligned} f(x;\Theta)=&\frac{e^{2\bar{e}}+1}{(e^{\bar{e}}-1)^2}\sum_{p,q,r=0}^{\infty}\frac{(-1)^{p+q}E_p}{(2p)!r!}e^{2p-q}\binom{2p}{q}q^r\, b(x;\Theta)(\bar{B}(x;\Theta))^{r-1}\\ =&\sum_{p,q,r=0}^{\infty}\eta_{p,q,r}\, b(x;\Theta)(\bar{B}(x;\Theta))^{r-1}, \end{aligned} \tag{1.6}$$

where $\eta_{p,q,r}=\frac{e^{2\bar{e}}+1}{(e^{\bar{e}}-1)^2}\frac{(-1)^{p+q}E_p}{(2p)!r!}e^{2p-q}\binom{2p}{q}q^r$.

1.4. *Identifiability of the hyperbolic secant-B family*

Identifiability ensures that distinct parameter values correspond to distinct probability distributions. A parametric family with the CDF $F(x;\Theta)$ is identifiable if

$$F(x;\Theta_1)=F(x;\Theta_2),\quad \forall x\in\mathbb{R}, \tag{1.7}$$

imply $\Theta_1=\Theta_2$. If the baseline distribution $B(x;\Theta)$ is identifiable, then the hyperbolic secant-B family is identifiable. Assume that for two parameter vectors Θ_1 and Θ_2, by substituting Eq (1.2) into Eq (1.8) we have

$$\frac{e^{2\bar{e}}+1}{(e^{\bar{e}}-1)^2}\left(1-\operatorname{sech}\left(e-e^{\bar{B}(x;\Theta_1)}\right)\right)=\frac{e^{2\bar{e}}+1}{(e^{\bar{e}}-1)^2}\left(1-\operatorname{sech}\left(e-e^{\bar{B}(x;\Theta_2)}\right)\right),$$

$$\operatorname{sech}\left(e-e^{\bar{B}(x;\Theta_1)}\right)=\operatorname{sech}\left(e-e^{\bar{B}(x;\Theta_2)}\right).$$

The hyperbolic secant function $\operatorname{sech}(T)$ is strictly monotone for $T>0$. Under the conditions $2<e<3$ and $0<B(x;\Theta)<1$, the argument $e-e^{\bar{B}(x;\Theta)}$ lies in a region where the function is one-to-one. Hence, we have

$$e-e^{\bar{B}(x;\Theta_1)}=e-e^{\bar{B}(x;\Theta_2)}.$$

Therefore

$$e^{\bar{B}(x;\Theta_1)} = e^{\bar{B}(x;\Theta_2)}.$$

Applying a logarithm function on both sides yields the following:

$$\bar{B}(x;\Theta_1) = \bar{B}(x;\Theta_2),$$

which implies

$$B(x;\Theta_1) = B(x;\Theta_2), \quad \forall x.$$

Since the baseline distribution $B(x;\Theta)$ is identifiable, which indicates that

$$\Theta_1 = \Theta_2.$$

Therefore, the hyperbolic secant-B family is identifiable.

1.5. Hyperbolic secant-power half-logistic distribution and properties

This section highlights the flexibility and wide applicability of the proposed generator, defined by its CDF in Eq (1.2), by adopting the power half-logistic distribution (PHLD) as the foundation distribution.

In parametric models, the half-logistic distribution (HLD) is a well-known type of distribution that is often used in statistical studies across various fields. It has a decreasing PDF and an increasing failure rate. It exhibits a declining PDF and a rising failure rate. As a consequence, the HLD's main disadvantage is its inability to accommodate non-monotone failure rates and unimodal density shapes. However, because of its broad application, various authors have developed adaptations to increase its applicability to a variety of modeling settings. The CDF of HLD is stated as

$$G(y;\beta_1) = 1 - \frac{2e^{-\beta_1 y}}{1 + e^{-\beta_1 y}}; \quad y \geq 0, \beta_1 > 0. \tag{1.8}$$

The associated PDF of HLD is stated as follows

$$g(y;\beta_1) = \frac{2\beta_1 e^{-\beta_1 y}}{(1 + e^{-\beta_1 y})^2}; \quad y \geq 0, \beta_1 > 0.$$

The HRF of HLD is stated as follows

$$h(y;\beta_1) = \left(1 + e^{-\beta_1 y}\right)^{-1}; \quad y \geq 0, \beta_1 > 0.$$

Consider a random variable Y distributed according to the HLD, where its CDF is defined in Eq (1.9). By introducing the transformation $X^{\beta_2} = Y$, we derive the CDF of the PHLD, as

$$B(x;\beta_1,\beta_2) = 1 - \frac{2e^{-\beta_1 x^{\beta_2}}}{1 + e^{-\beta_1 x^{\beta_2}}}; \quad x \geq 0, \beta_1, \beta_2 > 0. \tag{1.9}$$

The related PDF of the PHLD is stated as follows

$$b(x;\beta_1,\beta_2) = \frac{2\beta_1\beta_2 x^{\beta_2-1}e^{-\beta_1 x^{\beta_2}}}{\left(1+e^{-\beta_1 x^{\beta_2}}\right)^2}; \quad x \geq 0, \beta_1, \beta_2 > 0. \tag{1.10}$$

Moving forward, we adopt the PHLD as our baseline model for the formulated generator. By incorporating Eq (1.10), we derive the CDF of the hyperbolic secant-power half logistic distribution (HS-PHLD), as presented in Eq (1.12). Our primary objective is to address the limitations of both the PHLD and HLD when analyzing complex datasets across diverse scientific fields. Additionally, we explore its key analytical properties to enhance its applicability.

$$F(x;\beta_1,\beta_2) = \frac{e^{2\bar{e}}+1}{(e^{\bar{e}}-1)^2}\left(1-\operatorname{sech}\left(e-e^{\frac{2e^{-\beta_1 x^{\beta_2}}}{(1+e^{-\beta_1 x^{\beta_2}})}}\right)\right) \quad ; x \geq 0, \beta_1, \beta_2 > 0. \tag{1.11}$$

In Figure 1, the CDF plots of the HS-PHLD, derived with various parameter choices, illustrate that the function consistently stays within the (0, 1) range. This validates that the stated distribution adheres to the essential requirements of a proper CDF.

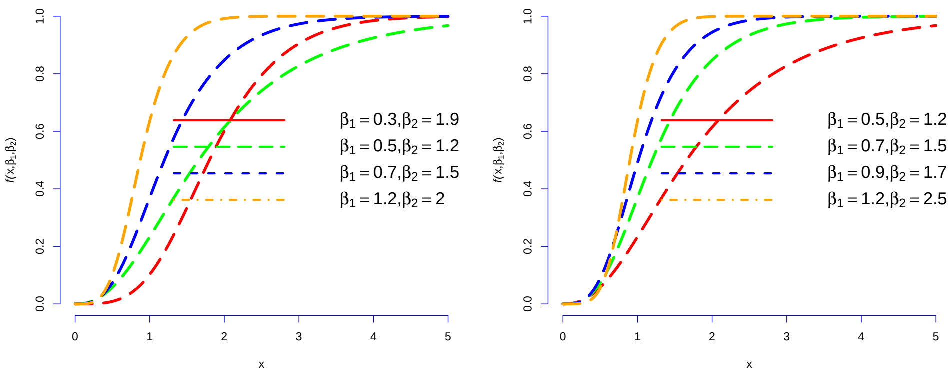

Figure 1. The CDF plots of the HS-PHLD.

The PDF of Eq (1.12) is described as follows:

$$f(x;\beta_1,\beta_2) = \frac{2(e^{2\bar{e}}+1)\beta_1\beta_2 x^{\beta_2-1}e^{-\beta_1 x^{\beta_2}}}{(e^{\bar{e}}-1)^2\left(1+e^{-\beta_1 x^{\beta_2}}\right)^2} e^{\frac{2e^{-\beta_1 x^{\beta_2}}}{(1+e^{-\beta_1 x^{\beta_2}})}} \operatorname{sech}\left(e-e^{\frac{2e^{-\beta_1 x^{\beta_2}}}{(1+e^{-\beta_1 x^{\beta_2}})}}\right)\tanh\left(e-e^{\frac{2e^{-\beta_1 x^{\beta_2}}}{(1+e^{-\beta_1 x^{\beta_2}})}}\right);$$
$$x \geq 0, \beta_1, \beta_2 > 0. \tag{1.12}$$

The PDF plots (Figure 2) of the HS-PHLD exhibit a wide range of flexible shapes, including symmetric, skewed, heavy-tailed, and reverse-J forms, depending on the chosen parameters. This distribution is consistently unimodal, with variations in the peak heights and tail behaviors, demonstrating its ability to adapt to diverse data patterns. These characteristics highlight the HS-PHLD as a highly versatile model for various statistical applications.

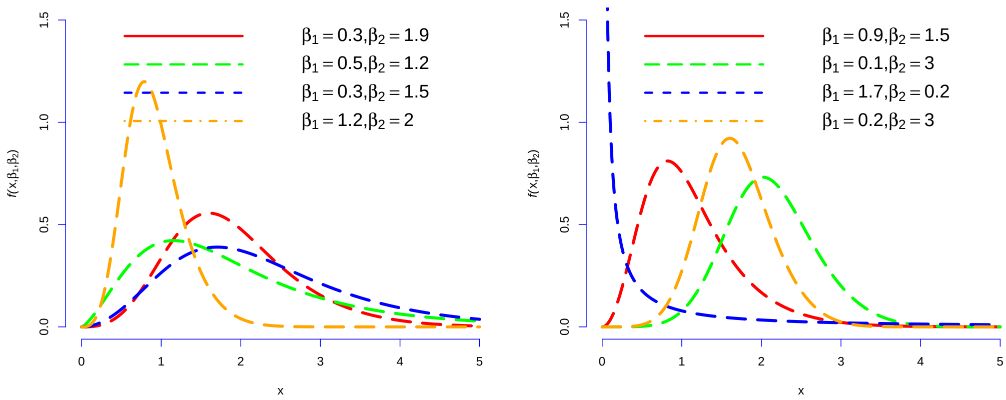

Figure 2. The PDF plots of the HS-PHLD.

The HS-PHLD has excellent shape flexibility and can represent many different PDF shapes depending on the parameters used (e.g., lef-skewed, symmetric, right-skewed, and heavy-tailed) (see Figure 3). Although it is always unimodal, changes in the peak sharpness and tail weight (which indicate how heavy a distribution's tails are) provide evidence of its capacity to describe a broad range of data behavior. Therefore, the HS-PHLD is an incredibly useful tool for statistical modeling.

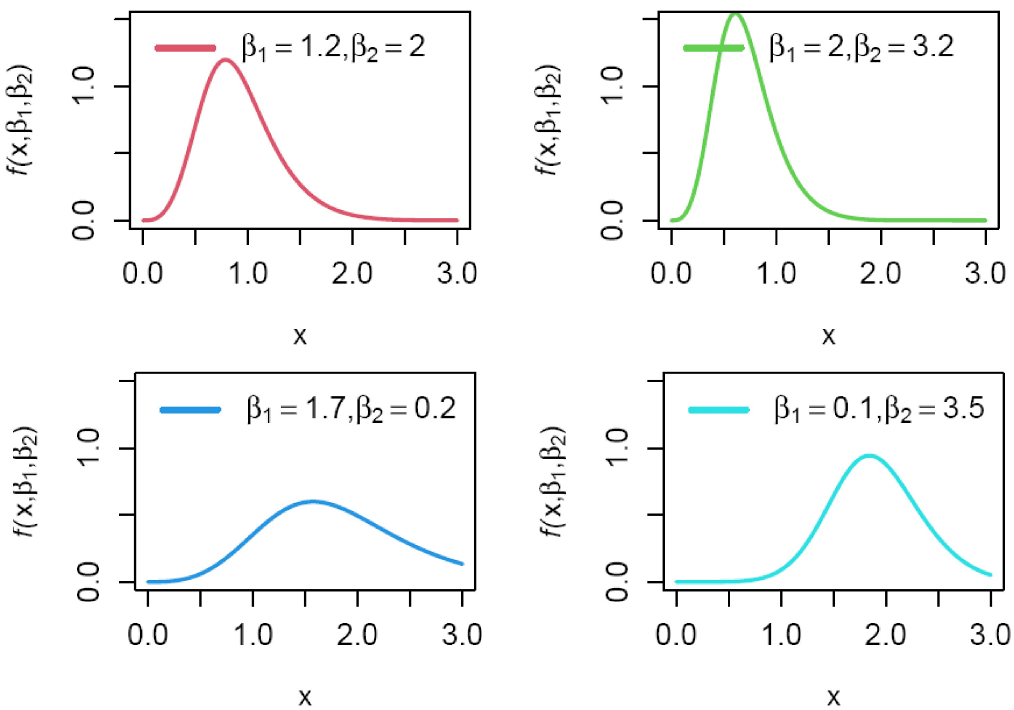

Figure 3. The PDF plots of the HS-PHLD.

1.6. Asymptotic measures

We will develop asymptotic expansions for the HS-PHLD. Based on Section 1, we derive the following equivalences if $x \to 0$:

$$F(x;\beta_1,\beta_2) \sim \frac{e^{2\bar{e}}+1}{(e^{\bar{e}}-1)^2}\frac{\beta_1^2 x^{2\beta_2}}{4},\quad f(x;\beta_1,\beta_2) \sim \frac{\left(e^{2\bar{e}}+1\right)}{(e^{\bar{e}}-1)^2}\frac{\beta_1^2\beta_2 x^{2\beta_2-1}}{2},$$
$$h(x;\beta_1,\beta_2) \sim \frac{2\left(e^{2\bar{e}}+1\right)\beta_1^2\beta_2 x^{2\beta_2-1}}{4\,(e^{\bar{e}}-1)^2-(e^{2\bar{e}}+1)\,\beta_1^2 x^{2\beta_2}}.$$

Hence, from these equivalences, we obtain.

$$f(x;\beta_1,\beta_2) \to -\infty;\ \text{if}\beta_2<1, f(x;\beta_1,\beta_2) \to 0;\ \text{if}\beta=1, \text{and}\quad f(x;\beta_1,\beta_2) \to 0;\ \text{if}\beta_2>1.$$

Now, for $x \to +\infty$, we have

$$F(x;\beta_1,\beta_2) \sim 1-\frac{4e^{\bar{e}}\,(e^{\bar{e}}+1)}{(e^{\bar{e}}-1)\,(e^{\bar{e}}+1)}e^{-\beta_1 x^{\beta_2}},$$
$$f(x;\beta_1,\beta_2) \sim \frac{4e^{\bar{e}}\,(e^{\bar{e}}+1)}{(e^{\bar{e}}-1)\,(e^{\bar{e}}+1)}\beta_1\beta_2 x^{\beta_2-1}e^{-\beta_1 x^{\beta_2}},$$
$$h(x;\beta_1,\beta_2) \sim \beta_1\beta_2 x^{\beta_2-1}.$$

Subsequently, we have

$f(x;\beta_1,\beta_2) \to 0$, in all cases; however, $h(x;\beta_1,\beta_2) \to 0;\text{if}\beta_2<1, h(x;\beta_1,\beta_2) \to \beta_1;\text{if}\beta_2=1,$ and $h(x;\beta_1,\beta_2) \to +\infty;\text{if}\beta_2>1.$

1.7. Moments

Let $X \sim$ HS-PHLD be a random variable; Then the k^{th} moment is denoted as μ_k' and is stated as

$$\mu_k' = \mathbb{E}(x^k) = \int_0^\infty x^k f(x;\Theta)dx. \tag{1.13}$$

Using Eq (1.6) in Eq (1.14), we have

$$\begin{aligned}
\mu_k' &= \sum_{p,q,r=0}^{\infty}\eta_{p,q,r}\int_0^\infty b(x;\Theta)(\bar{B}(x;\Theta))^{r-1}dx \\
&= \sum_{p,q,r=0}^{\infty}\eta_{p,q,r}\ 2\beta_1\beta_2\int_0^\infty \frac{x^{k+\beta_2-1}e^{-\beta_1 x^{\beta_2}}}{\left(1+e^{-\beta_1 x^{\beta_2}}\right)^2}\left(\frac{2e^{-\beta_1 x^{\beta_2}}}{1+e^{-\beta_1 x^{\beta_2}}}\right)^{r-1}dx \\
&= \sum_{p,q,r=0}^{\infty}\eta_{p,q,r}\ 2^r\beta_1\beta_2\int_0^\infty \frac{x^{k+\beta_2-1}e^{-\beta_1 r x^{\beta_2}}}{\left(1+e^{-\beta_1 x^{\beta_2}}\right)^{r+1}}dx.
\end{aligned}$$

We now make use of the generalized binomial theorem $\frac{1}{(1+u)^{a+1}} = \sum_{s=0}^{\infty}(-1)^s\binom{a+s}{s}u^s$, we have

$$\mu_k' = \sum_{p,q,r,s=0}^{\infty}(-1)^s\eta_{p,q,r}\binom{r+s}{s}2^r\beta_1\beta_2\int_0^{\infty}x^{k+\beta_2-1}e^{-\beta_1(r+s)x^{\beta_2}}dx.$$

Through substitution with $\beta_1(r+s)x^{\beta_2} = t$, so that $0 < t < \infty$, we have

$$\mu_k' = \sum_{p,q,r,s=0}^{\infty}(-1)^s\eta_{p,q,r}\binom{r+s}{s}2^r\frac{\beta_1}{(\beta_2(r+s))^{\frac{k}{\beta_2}+1}}\int_0^{\infty}t^{\frac{k}{\beta_2}}e^{-t}dt.$$

By integrating, we obtain

$$\mu_k' = \sum_{p,q,r,s=0}^{\infty}(-1)^s\eta_{p,q,r}\binom{r+s}{s}2^r\frac{\beta_1}{(\beta_2(r+s))^{\frac{k}{\beta_2}+1}}\Gamma\left(\frac{k}{\beta_2}+1\right),$$

where $\Gamma(.)$ denotes the gamma function, and by taking $k = -1$, we acquire the harmonic mean. Moreover, by setting $k = 1, 2, 3, 4$, we obtain the first four moments of the specialized distribution. The first moment, μ_1' is known as the mean. The variance and the coefficient of variation (CV) are then derived on the basis of these moments

$$Var = \mu_2 = \mu_2' - \mu_1'^2,$$

and

$$CV = \frac{\sqrt{\mu_2' - \mu_1'^2}}{\mu_1'}.$$

The moment-generating function $M_X(t)$ characterizes the distribution of the random variable X is described as

$$\begin{aligned}
M_X(t) = E(e^{tx}) &= \int_0^{\infty}e^{tx}f(x;\Theta)dx \\
&= \sum_{k=0}^{\infty}\frac{t^k}{k!}\int_0^{\infty}x^kf(x;\Theta)dx = \sum_{k=0}^{\infty}\frac{t^k}{k!}E(x^k) \\
&= \sum_{p,q,r,s=0}^{\infty}(-1)^s\eta_{p,q,r}\binom{r+s}{s}\frac{t^k2^r\beta_1}{k!\,(\beta_2(r+s))^{\frac{k}{\beta_2}+1}}\Gamma\left(\frac{k}{\beta_2}+1\right).
\end{aligned}$$

1.8. Incomplete moments

In probability and statistics, incomplete moments are a more generalized version of ordinary moments. They are especially beneficial when working with shortened or censored data, or when evaluating distributions over a narrow range rather than over the full support. These moments find their application in fields such as econometrics, survival analysis, and reliability engineering. They assist in calculating the projected deficit beyond a specific quantile. In the field of economics, the distribution of wealth is represented by incomplete moments. For the HS-PHLD, the v^{th} incomplete moment can be expressed as

$$\begin{aligned}
I_k(v) &= \int_0^v x^k f(x;\Theta)dx \\
&= \sum_{p,q,r=0}^{\infty} \eta_{p,q,r}\, 2^r \beta_1\beta_2 \int_0^v \frac{x^{k+\beta_2-1}e^{-\beta_1 r x^{\beta_2}}}{\left(1+e^{-\beta_1 x^{\beta_2}}\right)^{r+1}}dx \\
&= \sum_{p,q,r,s=0}^{\infty} (-1)^s \eta_{p,q,r,s}\, 2^r \binom{r+1}{s} \beta_1\beta_2 \int_0^v x^{k+\beta_2-1} e^{-\beta_1(r+s)x^{\beta_2}} dx.
\end{aligned}$$

By substitution with $\beta_1(r+s)x^{\beta_2} = t$, so that $0 < t < \beta_1(r+s)v^{\beta_2}$, we have

$$I_k(v) = \sum_{p,q,r,s=0}^{\infty} (-1)^s \eta_{p,q,r,s}\, 2^r \binom{r+1}{s} \frac{\beta_1}{(\beta_1(r+s))^{\frac{k}{\beta_2}+1}} \int_0^{\beta_1(r+s)v^{\beta_2}} t^{\frac{k}{\beta_2}} e^{-t} dt.$$

By integrating we have

$$I_k(v) = \sum_{p,q,r,s=0}^{\infty} (-1)^s \eta_{p,q,r,s}\, 2^r \binom{r+1}{s} \frac{\beta_1}{(\beta_1(r+s))^{\frac{k}{\beta_2}+1}} \gamma\left(\frac{k}{\beta_2}+1, \beta_1(r+s)v^{\beta_2}\right),$$

where $\gamma(d,w) = \int_0^w z^{d-1}e^{-z}dz$ denotes the lower incomplete gamma function.

1.9. Quantile function

Let X be a random variable with the following CDF. The quantile function of the HS-PHLD can be derived by inverting this CDF as follows:

$$F(x;\beta_1,\beta_2) = \frac{e^{2\bar{e}}+1}{(e^{\bar{e}}-1)^2}\left(1 - \operatorname{sech}\left(e - e^{\frac{2e^{-\beta_1 x^{\beta_2}}}{(1+e^{-\beta_1 x^{\beta_2}})}}\right)\right) = q,$$

$$x = \left(\frac{-1}{\beta_1}\log\left(\frac{\log\left(e - \operatorname{sech}^{-1}\left(1 - \frac{(e^{\bar{e}}-1)^2}{(e^{2\bar{e}}+1)}q\right)\right)}{2 - \log\left(e - \operatorname{sech}^{-1}\left(1 - \frac{(e^{\bar{e}}-1)^2}{(e^{2\bar{e}}+1)}q\right)\right)}\right)\right)^{\frac{1}{\beta_2}}.$$

Since the CDF given in (1.12) is a one-to-one function, it is invertible. By substituting $q = u$ and $u \in (0,1)$, we obtain the random number generation function for the HS-PHLD. Additionally, quantile-based measures like Bowley skewness and Moors kurtosis can be used to assess skewness and kurtosis variations. Bowley's skewness, which relies on quartiles, is defined as

$$\gamma_3 = \frac{Q(0.75) + Q(0.25) - 2Q(0.5)}{Q(0.75) - Q(0.25)}.$$

The Moors kurtosis involving octiles is

$$\gamma_4 = \frac{Q(0.37) + Q(0.12) + Q(0.87) - Q(0.62)}{Q(0.75) - Q(0.25)}.$$

Table 1 illustrates that when the parameter selected is fewer than one, the variance increases, suggesting a greater data dispersion. Furthermore, higher skewness indicates a right-tailed distribution, but increasing kurtosis indicates a heavy-tailed and peaked form. In contrast, when the parameter choice improves, the variance falls, indicating that data points cluster more tightly around the mean, which indicates greater consistency and lower variability. Lower skewness keeps the distribution symmetric, while kurtosis values greater than three imply leptokurtic behavior (sharper peaks and heavier tails). Owing to its adaptability, this distribution could potentially be applied to a wide variety of datasets.

Table 1. Numerical evaluation for μ, σ^2, CV,γ_3, and γ_4 of the HS-PHLD for distinct combinations of β_1 and β_2.

β_1	β_2	μ	σ^2	CV	γ_3	γ_4
0.5	0.75	3.511031	15.67326	1.127574	3.084338	19.12338
0.75	1.0	1.565004	1.59612	0.8072671	2.012444	9.461875
1.5	1.2	0.7842101	0.2701312	0.6627579	1.559557	6.772077
2.0	1.5	0.6581844	0.1197461	0.5257547	1.141572	4.95481
2.5	2.0	0.6375225	0.06306644	0.393916	0.7433861	3.790106
3.0	2.5	0.640582	0.04103191	0.3162176	0.5069472	3.354429
3.5	3.0	0.6508259	0.02965936	0.2646159	0.3476409	3.168419
4.0	3.5	0.6632248	0.02280923	0.2277165	0.2319814	3.088229
4.5	4.0	0.6759525	0.01826945	0.1999616	0.1437403	3.058535
5.0	4.5	0.6882964	0.01506089	0.1782994	0.07398246	3.054638

2. Actuarial indicators

This part delves into essential risk indicators in actuarial science connected to the suggested HS-PHLD. The HS-PHLD offers a robust framework for assessing the volatility and tail risk associated with various financial instruments. By identifying key risk indicators, actuaries can better quantify potential losses and make informed decisions regarding risk management strategies. Risk managers typically evaluate these indicators to assess their firms' vulnerability to possible hazards caused by fluctuations in fundamental factors such as market pricing, interest rates, or currency exchange rates. Various actuarial risk metrics have been investigated in previous studies for this purpose.

2.1. Value at risk indicator

The value at risk ((VaR)) indicator is a statistical instrument that calculates the risk of loss on a portfolio of investments over a period of time and at a given confidence level. It estimates the highest possible loss (in monetary terms or as a percentage) that might occur in normal market conditions. To determine the VaR (υ_1), we acquire the inversion of the CDF for our offered HS-PHLD. The complete form of the VaR value is expressed as

$$\upsilon_1 = F^{-1}(u);\ 0 < u < 1 = \left(\frac{-1}{\alpha}\log\left(\frac{\log\left(e - \operatorname{sech}^{-1}\left(1 - \frac{(e^{\bar{e}}-1)^2}{(e^{2\bar{e}}+1)}u\right)\right)}{2 - \log\left(e - \operatorname{sech}^{-1}\left(1 - \frac{(e^{\bar{e}}-1)^2}{(e^{2\bar{e}}+1)}u\right)\right)}\right)\right)^{\frac{1}{\beta_2}}.$$

2.2. Tail value-at-risk indicator

The tail value-at-risk (TVaR), formerly referred to as the expected shortfall (ES) or conditional (CVaR), is a risk metric that measures the probable loss in worst-case situations over a certain confidence level. Whereas VaR, which simply offers a threshold loss at a certain confidence level, TVaR accounts for the mean of the losses that surpass that threshold, rendering it more susceptible to the tail of the loss distribution. The TVaR measure (υ_2) is determined through the expression below:

$$\begin{aligned}\upsilon_2 =& \frac{1}{1-u}\int_{\upsilon_1}^{\infty} x f(x;\Theta)dx \\ =& \frac{1}{1-u}\sum_{p,q,r=0}^{\infty} \eta_{p,q,r}\, 2^r\beta_1\beta_2 \int_{\upsilon_1}^{\infty} \frac{x^{\beta_2} e^{-\beta_1 r x^{\beta_2}}}{\left(1 + e^{-\beta_1 x^{\beta_2}}\right)^{r+1}}dx \\ =& \frac{1}{1-u}\sum_{p,q,r,s=0}^{\infty} (-1)^s \eta_{p,q,r,s}\, 2^r\binom{r+1}{s}\beta_1\beta_2 \int_{\upsilon_1}^{\infty} x^{\beta_2} e^{-\beta_1 (r+s) x^{\beta_2}}dx.\end{aligned}$$

By substitution with $\beta_1(r+s)x^{\beta_2} = t$, so that $\beta_1(r+s)\upsilon_1^{\beta_2} < t < \infty$, we have

$$\upsilon_2 = \frac{1}{1-u}\sum_{p,q,r,s=0}^{\infty} (-1)^s \eta_{p,q,r,s}\, 2^r\binom{r+1}{s}\frac{\beta_1}{(\beta_1(r+s))^{\frac{1}{\beta_2}+1}}\int_{\beta_1(r+s)\upsilon_1^{\beta_2}}^{\infty} t^{\frac{1}{\beta_2}} e^{-t}dt.$$

By integrating, we obtain

$$\upsilon_2 = \frac{1}{1-u}\sum_{p,q,r,s=0}^{\infty} (-1)^s \eta_{p,q,r,s}\, 2^r\binom{r+1}{s}\frac{\beta_1}{(\beta_1(r+s))^{\frac{1}{\beta_2}+1}}\Gamma\left(\frac{1}{\beta_2}+1, \beta_1(r+s)\upsilon_1^{\beta_2}\right),$$

where $\Gamma(d,w) = \int_w^{\infty} z^{d-1}e^{-z}dz$ denotes the upper incomplete gamma function.

2.3. Tail variance premium indicator

The tail variance premium (TVP) (υ_3) is a risk metric that evaluates the variability of losses in a distribution's tail (beyond a particular limit, generally the VaR. Subsequently, it has a strong relationship with tail conditional variance (TCV) and ES. It is expressed mathematically by the following formula:

$$\upsilon_3 = \upsilon_2 + u\upsilon_4,$$

where

$$\upsilon_4 = \frac{1}{1-u}\int_{\upsilon_1}^{\infty} x^2 f(x;\Theta)dx - (\upsilon_2)^2$$

$$= \frac{1}{1-u}\sum_{p,q,r=0}^{\infty}\eta_{p,q,r}\,2^r\beta_1\beta_2\int_{\upsilon_1}^{\infty}\frac{x^{\beta_2+1}e^{-\beta_1 r x^{\beta_2}}}{\left(1+e^{-\beta_1 x^{\beta_2}}\right)^{r+1}}dx-(\upsilon_2)^2$$
$$= \frac{1}{1-u}\sum_{p,q,r,s=0}^{\infty}(-1)^s\eta_{p,q,r,s}\,2^r\binom{r+1}{s}\beta_1\beta_2\int_{\upsilon_1}^{\infty}x^{\beta_2+1}e^{-\beta_1(r+s)x^{\beta_2}}dx-(\upsilon_2)^2.$$

By substitution with $\beta_1(r+s)x^{\beta_2}=t$, so that $\beta_1(r+s)\upsilon_1^{\beta_2}<t<\infty$, we have

$$\upsilon_4 = \frac{1}{1-u}\sum_{p,q,r,s=0}^{\infty}(-1)^s\eta_{p,q,r,s}\,2^r\binom{r+1}{s}\frac{\beta_1}{(\beta_1(r+s))^{\frac{2}{\beta_2}+1}}\int_{\beta_1(r+s)\upsilon_1^{\beta_2}}^{\infty}t^{\frac{2}{\beta_2}}e^{-t}dt-(\upsilon_2)^2,$$

by integrating with, we obtain

$$\upsilon_4 = \frac{1}{1-u}\sum_{p,q,r,s=0}^{\infty}(-1)^s\eta_{p,q,r,s}\,2^r\binom{r+1}{s}\frac{\beta_1}{(\beta_1(r+s))^{\frac{2}{\beta_2}+1}}\Gamma\left(\frac{2}{\beta_2}+1,\beta_1(r+s)\upsilon_1^{\beta_2}\right)-(\upsilon_2)^2,$$

where $\Gamma(d,w)=\int_w^{\infty}z^{d-1}e^{-z}dz$ denotes the upper incomplete gamma function.

Tables 2 and 3 indicate that the HS-PHLD has lower VAR, TVAR, and TVP values than the PHLD, implying a smaller tail and less severe risk exposure. Despite both distributions following the pattern $\upsilon_1<\upsilon_2<\upsilon_3$, the continuously higher values for the PHLD indicate an expanded tail, suggesting a higher risk of severe losses. This makes the HS-PHLD a more conservative choice for risk modeling, since it indicates less severe losses, whereas the PHLD requires more capital reserves due to its higher tail risk.

Table 2. Numerical evaluation of $\upsilon_1,\ \upsilon_2,$ and υ_3 for the models HS-PHLD and PHLD.

Model	Parameter	u	υ_1	υ_2	υ_3
HS-PHLD	$\beta_1=0.5,\ \beta_2=0.75$	0.2	0.872976	4.268727	7.615536
		0.3	1.266897	4.726129	9.960842
		0.5	2.245445	5.925796	15.605716
		0.6	2.920632	6.765253	19.165391
		0.7	3.841830	7.902333	23.554766
		0.8	5.251731	9.609469	29.382305
PHLD	$\beta_1=0.5,\ \beta_2=0.75$	0.2	0.7562139	5.491605	10.65788
		0.3	1.3294261	6.128466	14.01034
		0.5	2.8564893	7.762099	21.44413
		0.6	3.8950581	8.863783	25.73225
		0.7	5.2517753	10.305260	30.69147
		0.8	7.1979019	12.380007	36.87169

Table 3. Numerical evaluation of $\upsilon_1,\ \upsilon_2,$ and υ_3 for the models HS-PHLD and PHLD.

Model	Parameter	u	υ_1	υ_2	υ_3
HS-PHLD	$\beta_1 = 0.75,\ \beta_2 = 1.2$	0.2	0.6552149	1.637235	1.793206
		0.3	0.8269337	1.765161	1.993159
		0.5	1.1825548	2.071038	2.437213
		0.6	1.3937354	2.267507	2.700413
		0.7	1.6542212	2.517173	3.014736
		0.8	2.0111586	2.865110	3.423319
PHLD	$\beta_1 = 0.75,\ \beta_2 = 1.2$	0.2	0.5989771	1.908065	2.128078
		0.3	0.8522115	2.076939	2.385431
		0.5	1.3745250	2.464072	2.917092
		0.6	1.6685088	2.700444	3.211280
		0.7	2.0111692	2.989114	3.548148
		0.8	2.4491252	3.374218	3.970280

3. Reliability indicators

This section focuses on different reliability indicators.

3.1. Survival function

The survival function is essential in survival analysis to comprehend the distribution of survival periods or durations, such as the time until a machine fails, an organism's lifespan, or the time until an event happens. It offers information about the likelihood of survival after certain time points. Let us assume that X is a random variable with the CDF $F()x$. Then its survival function is described as follows:

$$S(x) = \int_x^\infty f(x;\Theta)dx = 1 - F(x).$$

Therefore, the survival function for the HS-PHLD is stated as follows:

$$S(x;\beta_1,\beta_2) = 1 - \frac{e^{2\bar{e}}+1}{(e^{\bar{e}}-1)^2}\left(1 - \operatorname{sech}\left(e - e^{\frac{2e^{-\beta_1 x^{\beta_2}}}{(1+e^{-\beta_1 x^{\beta_2}})}}\right)\right). \tag{3.1}$$

3.2. Cumulative HRF

The cumulative HRF of a random variable x is defined as

$$\begin{aligned} H(x;\beta_1,\beta_2) &= -\ln[\bar{F}(x;\beta_1,\beta_2)] \\ &= -\ln\left\{1 - \frac{e^{2\bar{e}}+1}{(e^{\bar{e}}-1)^2}\left(1 - \operatorname{sech}\left(e - e^{\frac{2e^{-\beta_1 x^{\beta_2}}}{(1+e^{-\beta_1 x^{\beta_2}})}}\right)\right)\right\}. \end{aligned} \tag{3.2}$$

By differentiating Eq (3.2), we acquire the following HRF:

$$h(x;\beta_1,\beta_2)=\frac{2(e^{2\bar{e}}+1)\beta_1\beta_2 x^{\beta_2-1}e^{-\beta_1 x^{\beta_2}}e^{\frac{2e^{-\beta_1 x^{\beta_2}}}{(1+e^{-\beta_1 x^{\beta_2}})}}\operatorname{sech}\left(e-e^{\frac{2e^{-\beta_1 x^{\beta_2}}}{(1+e^{-\beta_1 x^{\beta_2}})}}\right)\tanh\left(e-e^{\frac{2e^{-\beta_1 x^{\beta_2}}}{(1+e^{-\beta_1 x^{\beta_2}})}}\right)}{\left(1+e^{-\beta_1 x^{\beta_2}}\right)^2\left((e^{\bar{e}}-1)^2-(e^{2\bar{e}}+1)\left(1-\operatorname{sech}\left(e-e^{\frac{2e^{-\beta_1 x^{\beta_2}}}{(1+e^{-\beta_1 x^{\beta_2}})}}\right)\right)\right)}.$$

The HRF plots of the HS-PHLD display increasing, decreasing, and unimodal shapes, reflecting a wide range of failure behaviors (see Figure 4). This versatility enables the modeling of early failures, wear-out patterns, and periods of peak risk in real-world datasets. Such adaptability makes the HS-PHLD well-suited for applications in survival analysis, reliability engineering, and risk assessment.

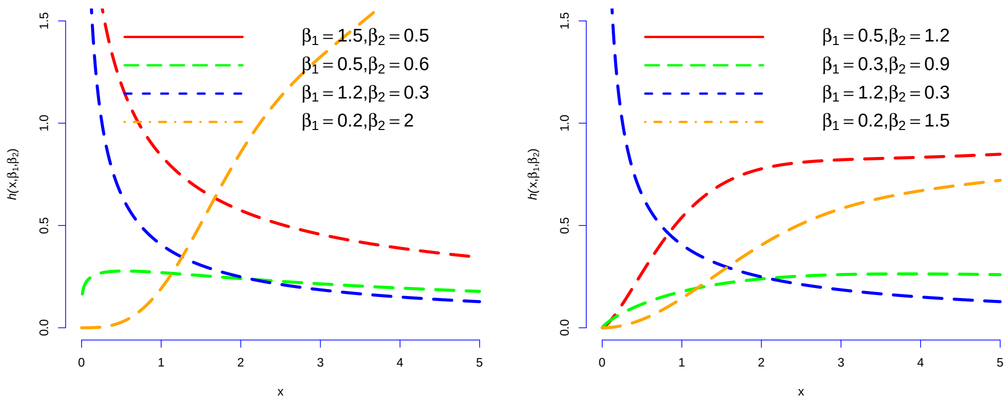

Figure 4. The HRF plots of the HS-PHLD (for various parameter selections).

The HRF of the HS-PHLD provides the ability to model a wide variety of failure modes via multiple hazard rates, including increasing, decreasing, bathtub-shaped, and J-shaped hazard rate shapes (see Figure 5). Therefore, the HS-PHLD describes the broad range of essential failure behaviors, including early-stage failure, wear-out due to aging, elevated-risk time periods, etc. Thus, the HS-PHLD generates a highly applicable distribution for survival analysis, reliability engineering, and risk evaluation.

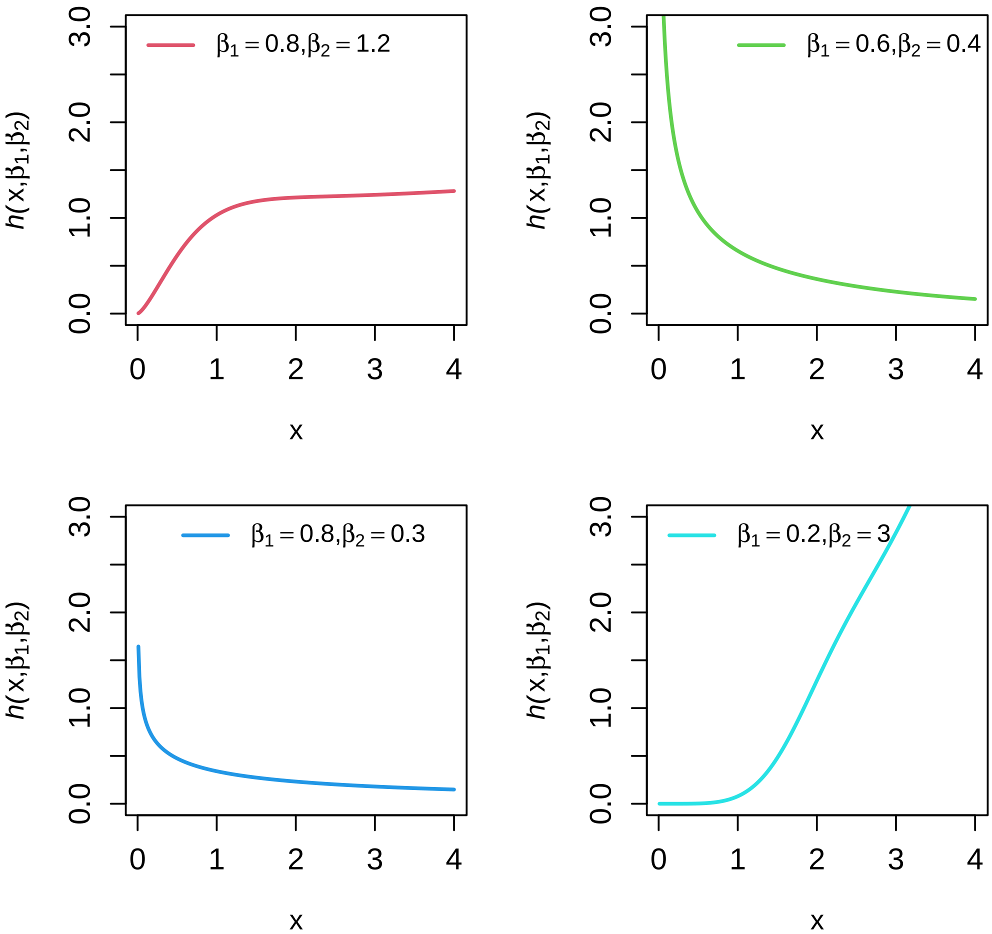

Figure 5. The HRF plots of the HS-PHLD (for various parameter selections).

3.3. Reverse HRF

The reverse HRF of a random variable X is stated as follows:

$$r(x;\beta_1,\beta_2)=\frac{f(x;\beta_1,\beta_2)}{F(x;\beta_1,\beta_2)}.$$

Therefore, the reverse HRF for the HS-PHLD is stated as

$$r(x;\beta_1,\beta_2)=\frac{2\beta_1\beta_2 x^{\beta_2-1}e^{-\beta_1 x^{\beta_2}}e^{\frac{2e^{-\beta_1 x^{\beta_2}}}{(1+e^{-\beta_1 x^{\beta_2}})}}\operatorname{sech}\left(e-e^{\frac{2e^{-\beta_1 x^{\beta_2}}}{(1+e^{-\beta_1 x^{\beta_2}})}}\right)\tanh\left(e-e^{\frac{2e^{-\beta_1 x^{\beta_2}}}{(1+e^{-\beta_1 x^{\beta_2}})}}\right)}{\left(1+e^{-\beta_1 x^{\beta_2}}\right)^2\left(1-\operatorname{sech}\left(e-e^{\frac{2e^{-\beta_1 x^{\beta_2}}}{(1+e^{-\beta_1 x^{\beta_2}})}}\right)\right)}.$$

3.4. Mean residual function

The mean residual lifespan is the mean amount of remaining time an item is projected to have after having lived up to a particular age x. This statistic is very useful in reliability and survival analyses.

If we assume the HS-PHLD $\sim X$, then the mean residual function is defined as

$$m(x;\beta_1,\beta_2) = \frac{1}{S(x;\beta_1,\beta_2)} \int_x^\infty t f(t,\beta_1,\beta_2)dt - x$$
$$= \frac{\left(e^{\bar{e}}-1\right)^2}{\left(e^{2\bar{e}}+1\right)\left(1-\operatorname{sech}\left(e-e^{\frac{2e^{-\beta_1 x^{\beta_2}}}{(1+e^{-\beta_1 x^{\beta_2}})}}\right)\right)} \sum_{p,q,r=0}^{\infty} \eta_{p,q,r}\, 2^r \beta_1\beta_2 \int_x^\infty \frac{t^{\beta_2} e^{-\beta_1 r t^{\beta_2}}}{\left(1+e^{-\beta_1 t^{\beta_2}}\right)^{r+1}} dt - x$$
$$= \sum_{p,q,r,s=0}^{\infty} \frac{\left(e^{\bar{e}}-1\right)^2 (-1)^s \eta_{p,q,r,s}\, 2^r}{\left(e^{2\bar{e}}+1\right)\left(1-\operatorname{sech}\left(e-e^{\frac{2e^{-\beta_1 x^{\beta_2}}}{(1+e^{-\beta_1 x^{\beta_2}})}}\right)\right)} \binom{r+1}{s} \beta_1\beta_2 \int_x^\infty t^{\beta_2} e^{-\beta_1 (r+s) t^{\beta_2}} dt - x.$$

By substitution with $\beta_1(r+s)t^{\beta_2} = y$, so that $\beta_1(r+s)x^{\beta_2} < t < \infty$, we have

$$m(x;\beta_1,\beta_2) = \sum_{p,q,r,s=0}^{\infty} \frac{\left(e^{\bar{e}}-1\right)^2 (-1)^s \eta_{p,q,r,s}\, 2^r}{\left(e^{2\bar{e}}+1\right)\left(1-\operatorname{sech}\left(e-e^{\frac{2e^{-\beta_1 x^{\beta_2}}}{(1+e^{-\beta_1 x^{\beta_2}})}}\right)\right)} \binom{r+1}{s} \frac{\beta_1}{(\beta_1(r+s))^{\frac{1}{\beta_2}+1}}$$
$$\times \int_{\beta_1(r+s)x^{\beta_2}}^\infty t^{\frac{1}{\beta_2}} e^{-t} dt - x.$$

By integrating, we have

$$m(x;\beta_1,\beta_2) = \sum_{p,q,r,s=0}^{\infty} \frac{\left(e^{\bar{e}}-1\right)^2 (-1)^s \eta_{p,q,r,s}\, 2^r}{\left(e^{2\bar{e}}+1\right)\left(1-\operatorname{sech}\left(e-e^{\frac{2e^{-\beta_1 x^{\beta_2}}}{(1+e^{-\beta_1 x^{\beta_2}})}}\right)\right)} \binom{r+1}{s} \frac{\beta_1}{(\beta_1(r+s))^{\frac{1}{\beta_2}+1}}$$
$$\times \Gamma\left(\frac{1}{\beta_2}+1, \beta_1(r+s)x^{\beta_2}\right) - x,$$

where $\Gamma(d,w) = \int_w^\infty z^{d-1}e^{-z}dz$ denotes the upper incomplete gamma function.

4. Inferences

The likelihood function is the joint probability of the observed data given the parameters Θ. If the data points are $X_1, X_2, X_3, ..., X_n$ and assuming they are independent and identically distributed (i.i.d.), the likelihood function is:

$$L = \prod_{i=1}^{n} f(X = x_i|\Theta) = \prod_{i=1}^{n} \left\{ \frac{2\left(e^{2\bar{e}}+1\right)\beta_1\beta_2 x_i^{\beta_2-1} e^{-\beta_1 x_i^{\beta_2}}}{\left(e^{\bar{e}}-1\right)^2 \left(1+e^{-\beta_1 x_i^{\beta_2}}\right)^2} e^{\frac{2e^{-\beta_1 x_i^{\beta_2}}}{(1+e^{-\beta_1 x_i^{\beta_2}})}} \operatorname{sech}\left(e-e^{\frac{2e^{-\beta_1 x_i^{\beta_2}}}{(1+e^{-\beta_1 x_i^{\beta_2}})}}\right) \tanh\left(e-e^{\frac{2e^{-\beta_1 x_i^{\beta_2}}}{(1+e^{-\beta_1 x_i^{\beta_2}})}}\right) \right\}.$$

The log-likelihood function, which is given as

$$\ell = n\log\left(2(e^{2\bar{e}}+1)\right) - 2n\log\left(e^{\bar{e}}-1\right) + n\log(\beta_1) + n\log(\beta_2) - \beta_1\sum_{i=1}^{n} x_i^{\beta_1} - \sum_{i=1}^{n}\log\left(1+e^{-\beta_1 x_i^{\beta_2}}\right)^2$$
$$+2\sum_{i=1}^{n}\frac{e^{-\beta_1 x_i^{\beta_2}}}{\left(1+e^{-\beta_1 x_i^{\beta_2}}\right)} + \sum_{i=1}^{n}\log\left(\operatorname{sech}\left(e - e^{\frac{2e^{-\beta_1 x_i^{\beta_2}}}{(1+e^{-\beta_1 x_i^{\beta_2}})}}\right)\right) + \sum_{i=1}^{n}\log\left(\tanh\left(e - e^{\frac{2e^{-\beta_1 x_i^{\beta_2}}}{(1+e^{-\beta_1 x_i^{\beta_2}})}}\right)\right).$$

The Anderson-Darling estimation technique (δ_2) is another approach that requires minimizing the given equation as follows:

$$\begin{aligned} AD &= -n - \frac{1}{n}\sum_{i=1}^{n}(2i-1)[\log F(x_i) + \log S(x_i)] \\ &= -n - \frac{1}{n}\sum_{i=1}^{n}(2i-1)\left[\log\left(\frac{e^{2\bar{e}}+1}{(e^{\bar{e}}-1)^2}(\mathcal{A})\right) + \log\left(1 - \frac{e^{2\bar{e}}+1}{(e^{\bar{e}}-1)^2}(\mathcal{A})\right)\right], \end{aligned}$$

where

$$\mathcal{A} = 1 - \operatorname{sech}\left(e - e^{\frac{2e^{-\beta_1 x^{\beta_2}}}{(1+e^{-\beta_1 x^{\beta_2}})}}\right).$$

The objective of the Cramér-von Mises criterion (δ_3) is to enhance statistical analysis through the minimization of the following expression:

$$\begin{aligned} CVM &= -\frac{1}{12n} + \sum_{i=1}^{n}\left[F(x_i) - \frac{2i-1}{2n}\right]^2 \\ &= -\frac{1}{12n} + \sum_{i=1}^{n}\left[\frac{e^{2\bar{e}}+1}{(e^{\bar{e}}-1)^2}\left(1 - \operatorname{sech}\left(e - e^{\frac{2e^{-\beta_1 x^{\beta_2}}}{(1+e^{-\beta_1 x^{\beta_2}})}}\right)\right) - \frac{2i-1}{2n}\right]^2. \end{aligned}$$

The maximum product of the spacing estimation (MPS) which is (δ_4) in the tables is derived by optimizing the following equation,which is a standard approach in statistical analysis for parameter estimation:

$$T = \frac{1}{n+1}\sum i = 1^{n+1}\log D_i, \quad D_i = F\left(x_{(i)}\right) - F\left(x_{(i-1)}\right).$$

Unlike other methods, least-squares estimation (δ_5) optimizes the model by reducing the total squared error between the observed and expected values to obtain the best possible fit.

$$LS = \sum_{i=1}^{n}\left[F(x_i) - \frac{i}{n+1}\right]^2 = \sum_{i=1}^{n}\left[\frac{e^{2\bar{e}}+1}{(e^{\bar{e}}-1)^2}\left(1 - \operatorname{sech}\left(e - e^{\frac{2e^{-\beta_1 x^{\beta_2}}}{(1+e^{-\beta_1 x^{\beta_2}})}}\right)\right) - \frac{i}{n+1}\right]^2.$$

Weighted least squares estimation (δ_6) aims to minimize the equation by incorporating weights that reduce the effect of particular observations on the final estimation,

$$WLS = \sum_{i=1}^{n}\frac{(n+1)^2(n+2)}{i(n-i+1)}\left[F(x_i) - \frac{i}{n+1}\right]^2$$

$$= \sum_{i=1}^{n} \frac{(n+1)^2(n+2)}{i(n-i+1)} \left[\frac{e^{2\bar{e}}+1}{(e^{\bar{e}}-1)^2} \left(1 - \operatorname{sech}\left(e - e^{\frac{2e^{-\beta_1 x^{\beta_2}}}{(1+e^{-\beta_1 x^{\beta_2}})}}\right)\right) - \frac{i}{n+1} \right]^2 .$$

4.1. Simulation investigation

This section analyzes the performance of multiple estimation approaches for estimating the parameters of the proposed model with considerable amounts of simulated data. In our simulation investigation, we created random datasets with varing sample sizes (n = 25, 75, 150, 200, 250, and 400) using the suggested model's quantile function. Our objective is to evaluate the behavior and efficiency of the model's estimators in various scenarios. We also examine the performance of several estimating approaches across many statistical criteria. To assess the estimation accuracy, we compute the following performance measures:

$|\mathrm{Bias}(\zeta)| = \frac{1}{L}\sum_{i=1}^{L} |\hat{\Theta} - \Theta|$;

Mean squared error $(MSE) = \frac{1}{L}\sum_{i=1}^{L}(\hat{\Theta} - \Theta)^2$;

mean relative errors $(MRE) = \frac{1}{L}\sum_{i=1}^{L} \frac{|\hat{\Theta}-\Theta|}{\Theta}$;

Average absolute difference $(D_{\text{abs}}) = \frac{1}{nL}\sum_{i=1}^{L}\sum_{j=1}^{n} |F(x_{ij}|\boldsymbol{\Theta}) - F(x_{ij}|\hat{\boldsymbol{\Theta}})|$;

Maximum absolute difference $(D_{\max}) = \frac{1}{L}\sum_{i=1}^{L} \max_j |F(x_{ij}|\boldsymbol{\Theta}) - F(x_{ij}|\hat{\boldsymbol{\Theta}})|$;

Average squared absolute error $(ASAE) = \frac{1}{n}\sum_{i=1}^{n} \frac{|x_i - \hat{x}_i|}{x_n - x_1}$.

The observations x_i are in ascending order and $\Theta = (\beta_1, \beta_2)$. Tables 4–8 offer the simulation results for the selected model parameters using six estimating approaches. The results show that all parameter estimations for the proposed distribution are extremely trustworthy and close to their real values. As the sample size (n) increases, the expected measures for each scenario fall consistently. Overall, all estimation approaches are effective in estimating the model parameters. Table 9 illustrates the overall ranks of the estimating techniques, with the MPS estimate receiving the lowest rank, indicating it as the most effective approach in our investigation.

Table 4. Numerical values of the simulation evaluation for $\beta_1 = 0.5,\ \beta_2 = 0.7$.

n	Est.	δ_1	δ_2	δ_3	δ_4	δ_5	δ_6
30	BIAS(β_1)	0.064459$^{\{5\}}$	0.059225$^{\{1\}}$	0.061641$^{\{4\}}$	0.061373$^{\{3\}}$	0.068886$^{\{6\}}$	0.059731$^{\{2\}}$
	BIAS(β_2)	0.062912$^{\{2\}}$	0.062212$^{\{1\}}$	0.080034$^{\{5\}}$	0.065692$^{\{3\}}$	0.083197$^{\{6\}}$	0.068350$^{\{4\}}$
	MSE(β_1)	0.006529$^{\{5\}}$	0.005608$^{\{1\}}$	0.005652$^{\{2\}}$	0.006137$^{\{4\}}$	0.007461$^{\{6\}}$	0.005841$^{\{3\}}$
	MSE(β_2)	0.006144$^{\{1\}}$	0.006347$^{\{2\}}$	0.009890$^{\{5\}}$	0.006372$^{\{3\}}$	0.010335$^{\{6\}}$	0.007624$^{\{4\}}$
	MRE(β_1)	0.128917$^{\{5\}}$	0.118451$^{\{1\}}$	0.123282$^{\{4\}}$	0.122746$^{\{3\}}$	0.137772$^{\{6\}}$	0.119462$^{\{2\}}$
	MRE(β_2)	0.089875$^{\{2\}}$	0.088874$^{\{1\}}$	0.114334$^{\{5\}}$	0.093845$^{\{3\}}$	0.118853$^{\{6\}}$	0.097643$^{\{4\}}$
	D_{abs}	0.03812$^{\{3\}}$	0.03588$^{\{2\}}$	0.03858$^{\{5\}}$	0.03840$^{\{4\}}$	0.04426$^{\{6\}}$	0.03457$^{\{1\}}$
	D_{max}	0.06117$^{\{3\}}$	0.05845$^{\{2\}}$	0.06434$^{\{5\}}$	0.06120$^{\{4\}}$	0.07239$^{\{6\}}$	0.05678$^{\{1\}}$
	ASAE	0.02399$^{\{4\}}$	0.02326$^{\{2\}}$	0.02528$^{\{5\}}$	0.02349$^{\{3\}}$	0.02631$^{\{6\}}$	0.02096$^{\{1\}}$
	$\sum Ranks$	30$^{\{3.5\}}$	13$^{\{1\}}$	40$^{\{5\}}$	30$^{\{3.5\}}$	54$^{\{6\}}$	22$^{\{2\}}$
70	BIAS(β_1)	0.042119$^{\{4\}}$	0.041411$^{\{3\}}$	0.038409$^{\{1\}}$	0.041123$^{\{2\}}$	0.043758$^{\{6\}}$	0.043592$^{\{5\}}$
	BIAS(β_2)	0.044904$^{\{3\}}$	0.042579$^{\{2\}}$	0.038409$^{\{1\}}$	0.049078$^{\{4\}}$	0.053263$^{\{6\}}$	0.051904$^{\{5\}}$
	MSE(β_1)	0.002809$^{\{4\}}$	0.002743$^{\{3\}}$	0.002423$^{\{1\}}$	0.002502$^{\{2\}}$	0.002940$^{\{5\}}$	0.003048$^{\{6\}}$
	MSE(β_2)	0.003322$^{\{3\}}$	0.002758$^{\{1\}}$	0.003304$^{\{2\}}$	0.003565$^{\{4\}}$	0.004347$^{\{6\}}$	0.004275$^{\{5\}}$
	MRE(β_1)	0.084238$^{\{4\}}$	0.082822$^{\{3\}}$	0.076818$^{\{1\}}$	0.082246$^{\{2\}}$	0.087517$^{\{6\}}$	0.087183$^{\{5\}}$
	MRE(β_2)	0.064149$^{\{3\}}$	0.060827$^{\{1\}}$	0.063184$^{\{2\}}$	0.070111$^{\{4\}}$	0.076090$^{\{6\}}$	0.074149$^{\{5\}}$
	D_{abs}	0.02575$^{\{6\}}$	0.02441$^{\{1\}}$	0.02523$^{\{3\}}$	0.02565$^{\{5\}}$	0.02762$^{\{4\}}$	0.02553$^{\{2\}}$
	D_{max}	0.04232$^{\{4\}}$	0.03933$^{\{1\}}$	0.04075$^{\{2\}}$	0.04174$^{\{3\}}$	0.04553$^{\{6\}}$	0.04238$^{\{5\}}$
	ASAE	0.01542$^{\{6\}}$	0.01477$^{\{3\}}$	0.01495$^{\{5\}}$	0.01322$^{\{2\}}$	0.01456$^{\{4\}}$	0.01280$^{\{1\}}$
	$\sum Ranks$	37$^{\{4\}}$	18$^{\{2\}}$	17$^{\{1\}}$	28$^{\{3\}}$	50$^{\{6\}}$	45$^{\{5\}}$
100	BIAS(β_1)	0.030189$^{\{4\}}$	0.030574$^{\{6\}}$	0.030155$^{\{3\}}$	0.028042$^{\{1\}}$	0.028246$^{\{2\}}$	0.030314$^{\{5\}}$
	BIAS(β_2)	0.030644$^{\{3\}}$	0.029209$^{\{2\}}$	0.037959$^{\{6\}}$	0.027781$^{\{1\}}$	0.034789$^{\{4\}}$	0.037482$^{\{5\}}$
	MSE(β_1)	0.001467$^{\{4\}}$	0.001470$^{\{5\}}$	0.001430$^{\{3\}}$	0.001257$^{\{2\}}$	0.001250$^{\{1\}}$	0.001494$^{\{6\}}$
	MSE(β_2)	0.001542$^{\{4\}}$	0.001336$^{\{2\}}$	0.001430$^{\{3\}}$	0.001248$^{\{1\}}$	0.001829$^{\{5\}}$	0.002226$^{\{6\}}$
	MRE(β_1)	0.060378$^{\{4\}}$	0.061149$^{\{6\}}$	0.060309$^{\{3\}}$	0.056084$^{\{1\}}$	0.056492$^{\{2\}}$	0.060628$^{\{5\}}$
	MRE(β_2)	0.043778$^{\{3\}}$	0.041727$^{\{2\}}$	0.054227$^{\{6\}}$	0.039687$^{\{1\}}$	0.049699$^{\{4\}}$	0.053546$^{\{5\}}$
	D_{abs}	0.01821$^{\{3\}}$	0.01904$^{\{5\}}$	0.01936$^{\{6\}}$	0.01760$^{\{2\}}$	0.01744$^{\{1\}}$	0.01887$^{\{4\}}$
	D_{max}	0.02920$^{\{3\}}$	0.03029$^{\{4\}}$	0.03195$^{\{6\}}$	0.02835$^{\{1\}}$	0.02896$^{\{2\}}$	0.03106$^{\{5\}}$
	ASAE	0.00913$^{\{4\}}$	0.00879$^{\{3\}}$	0.00972$^{\{5\}}$	0.00851$^{\{2\}}$	0.00986$^{\{6\}}$	0.00834$^{\{1\}}$
	$\sum Ranks$	32$^{\{3\}}$	35$^{\{5\}}$	41$^{\{6\}}$	12$^{\{2\}}$	33$^{\{4\}}$	4$^{\{1\}}$
200	BIAS(β_1)	0.023392$^{\{3\}}$	0.023033$^{\{2\}}$	0.021543$^{\{1\}}$	0.024213$^{\{4\}}$	0.026516$^{\{5\}}$	0.049531$^{\{6\}}$
	BIAS(β_2)	0.024547$^{\{2\}}$	0.027387$^{\{3\}}$	0.028945$^{\{4\}}$	0.022780$^{\{1\}}$	0.031777$^{\{5\}}$	0.040887$^{\{6\}}$
	MSE(β_1)	0.000856$^{\{3\}}$	0.000831$^{\{2\}}$	0.000766$^{\{1\}}$	0.022780$^{\{6\}}$	0.001083$^{\{5\}}$	0.000977$^{\{4\}}$
	MSE(β_2)	0.000994$^{\{2\}}$	0.001196$^{\{3\}}$	0.001359$^{\{5\}}$	0.000785$^{\{1\}}$	0.001690$^{\{6\}}$	0.001322$^{\{4\}}$
	MRE(β_1)	0.046784$^{\{3\}}$	0.046066$^{\{2\}}$	0.043086$^{\{1\}}$	0.048426$^{\{4\}}$	0.053033$^{\{6\}}$	0.049531$^{\{5\}}$
	MRE(β_2)	0.035068$^{\{2\}}$	0.039124$^{\{3\}}$	0.041350$^{\{4.5\}}$	0.032543$^{\{1\}}$	0.045395$^{\{6\}}$	0.040887$^{\{4.5\}}$
	D_{abs}	0.01429$^{\{3\}}$	0.01412$^{\{2\}}$	0.01358$^{\{1\}}$	0.01476$^{\{4\}}$	0.01591$^{\{6\}}$	0.01486$^{\{5\}}$
	D_{max}	0.02303$^{\{2\}}$	0.02325$^{\{3\}}$	0.02263$^{\{1\}}$	0.02366$^{\{4\}}$	0.02614$^{\{6\}}$	0.02432$^{\{5\}}$
	ASAE	0.00647$^{\{3\}}$	0.00681$^{\{4\}}$	0.00723$^{\{5\}}$	0.00613$^{\{1\}}$	0.00757$^{\{6\}}$	0.00625$^{\{2\}}$
	$\sum Ranks$	23$^{\{1\}}$	24$^{\{2\}}$	23.5$^{\{3\}}$	26$^{\{4\}}$	51$^{\{6\}}$	41.5$^{\{5\}}$
300	BIAS(β_1)	0.021546$^{\{4\}}$	0.018814$^{\{1\}}$	0.021932$^{\{5\}}$	0.022301$^{\{6\}}$	0.019639$^{\{2\}}$	0.020577$^{\{3\}}$
	BIAS(β_2)	0.022728$^{\{4\}}$	0.021988$^{\{2\}}$	0.023420$^{\{5\}}$	0.023309$^{\{3\}}$	0.025617$^{\{6\}}$	0.024347$^{\{1\}}$
	MSE(β_1)	0.000688$^{\{4\}}$	0.000556$^{\{1\}}$	0.000787$^{\{5\}}$	0.023309$^{\{6\}}$	0.000619$^{\{2\}}$	0.000623$^{\{3\}}$
	MSE(β_2)	0.000757$^{\{3\}}$	0.000702$^{\{1\}}$	0.000850$^{\{5\}}$	0.000819$^{\{4\}}$	0.001070$^{\{6\}}$	0.000909$^{\{2\}}$
	MRE(β_1)	0.043092$^{\{4\}}$	0.037627$^{\{2\}}$	0.043865$^{\{5\}}$	0.033299$^{\{1\}}$	0.039278$^{\{3\}}$	0.041155$^{\{6\}}$
	MRE(β_2)	0.032469$^{\{2\}}$	0.031411$^{\{1\}}$	0.033457$^{\{4\}}$	0.033299$^{\{3\}}$	0.036596$^{\{6\}}$	0.034781$^{\{5\}}$
	D_{abs}	0.01260$^{\{2\}}$	0.01135$^{\{1\}}$	0.01319$^{\{4\}}$	0.01356$^{\{6\}}$	0.01325$^{\{5\}}$	0.01308$^{\{3\}}$
	D_{max}	0.02062$^{\{2\}}$	0.01855$^{\{1\}}$	0.02147$^{\{3\}}$	0.02201$^{\{6\}}$	0.02180$^{\{5\}}$	0.02151$^{\{4\}}$
	ASAE	0.00554$^{\{3\}}$	0.00563$^{\{4\}}$	0.00638$^{\{6\}}$	0.00611$^{\{5\}}$	0.00595$^{\{2\}}$	0.00499$^{\{1\}}$
	$\sum Ranks$	28$^{\{3\}}$	14$^{\{1\}}$	42$^{\{5\}}$	40$^{\{4\}}$	47$^{\{6\}}$	29$^{\{2\}}$
400	BIAS(β_1)	0.017005$^{\{1\}}$	0.021569$^{\{5\}}$	0.019678$^{\{3\}}$	0.020153$^{\{4\}}$	0.023102$^{\{6\}}$	0.017360$^{\{2\}}$
	BIAS(β_2)	0.018571$^{\{1\}}$	0.021569$^{\{4\}}$	0.022879$^{\{6\}}$	0.020953$^{\{3\}}$	0.025550$^{\{5\}}$	0.019902$^{\{2\}}$
	MSE(β_1)	0.000451$^{\{1\}}$	0.000655$^{\{6\}}$	0.000623$^{\{4\}}$	0.000621$^{\{3\}}$	0.000845$^{\{5\}}$	0.000469$^{\{2\}}$
	MSE(β_2)	0.000549$^{\{\}}$	0.000777$^{\{\}}$	0.000832$^{\{\}}$	0.000693$^{\{\}}$	0.001021$^{\{\}}$	0.000582$^{\{\}}$
	MRE(β_1)	0.034010$^{\{1\}}$	0.041043$^{\{6\}}$	0.039356$^{\{4\}}$	0.040306$^{\{5\}}$	0.046204$^{\{3\}}$	0.034719$^{\{2\}}$
	MRE(β_2)	0.026530$^{\{1\}}$	0.030813$^{\{4\}}$	0.032684$^{\{6\}}$	0.029933$^{\{3\}}$	0.036500$^{\{5\}}$	0.028431$^{\{2\}}$
	D_{abs}	0.01117$^{\{1\}}$	0.01231$^{\{5\}}$	0.01218$^{\{4\}}$	0.01143$^{\{3\}}$	0.01392$^{\{6\}}$	0.01121$^{\{2\}}$
	D_{max}	0.01810$^{\{1\}}$	0.01991$^{\{5\}}$	0.02001$^{\{6\}}$	0.01863$^{\{3\}}$	0.02286$^{\{4\}}$	0.01833$^{\{2\}}$
	ASAE	0.00449$^{\{2\}}$	0.00498$^{\{4\}}$	0.00522$^{\{6\}}$	0.00488$^{\{3\}}$	0.00493$^{\{5\}}$	0.00444$^{\{1\}}$
	$\sum Ranks$	10$^{\{1\}}$	43$^{\{4\}}$	49$^{\{5\}}$	33$^{\{3\}}$	50$^{\{6\}}$	18$^{\{2\}}$

Table 5. Numerical values of the simulation evaluation for $\beta_1 = 1.5$, $\beta_2 = 1.7$.

n	Est.	δ_1	δ_2	δ_3	δ_4	δ_5	δ_6
30	BIAS(β_1)	0.140881$^{\{4\}}$	0.134746$^{\{1\}}$	0.153689$^{\{6\}}$	0.138076$^{\{2\}}$	0.146951$^{\{3\}}$	0.147838$^{\{5\}}$
	BIAS(β_2)	0.144189$^{\{2\}}$	0.138909$^{\{1\}}$	0.213291$^{\{6\}}$	0.150684$^{\{3\}}$	0.185187$^{\{4\}}$	0.205852$^{\{5\}}$
	MSE(β_1)	0.033602$^{\{3\}}$	0.028035$^{\{2\}}$	0.039716$^{\{6\}}$	0.027950$^{\{1\}}$	0.036164$^{\{5\}}$	0.034811$^{\{4\}}$
	MSE(β_2)	0.036761$^{\{2\}}$	0.031056$^{\{1\}}$	0.075680$^{\{6\}}$	0.036852$^{\{3\}}$	0.047889$^{\{4\}}$	0.068156$^{\{5\}}$
	MRE(β_1)	0.093921$^{\{3\}}$	0.089830$^{\{1\}}$	0.102459$^{\{1\}}$	0.092051$^{\{2\}}$	0.097967$^{\{4\}}$	0.098558$^{\{5\}}$
	MRE(β_2)	0.084817$^{\{2\}}$	0.081711$^{\{1\}}$	0.125466$^{\{6\}}$	0.088638$^{\{3\}}$	0.108934$^{\{4\}}$	0.121090$^{\{5\}}$
	D_{abs}	0.03566$^{\{1\}}$	0.03516$^{\{2\}}$	0.03880$^{\{4\}}$	0.03902$^{\{5\}}$	0.03648$^{\{3\}}$	0.04013$^{\{6\}}$
	D_{max}	0.05784$^{\{2\}}$	0.05630$^{\{1\}}$	0.06528$^{\{5\}}$	0.06180$^{\{4\}}$	0.06076$^{\{3\}}$	0.06643$^{\{6\}}$
	ASAE	0.02586$^{\{6\}}$	0.02323$^{\{1\}}$	0.02468$^{\{4\}}$	0.02387$^{\{2\}}$	0.02329$^{\{3\}}$	0.02481$^{\{5\}}$
	$\sum$ *Ranks*	25$^{\{2.5\}}$	11$^{\{1\}}$	44$^{\{5\}}$	25$^{\{2.5\}}$	33$^{\{4\}}$	46$^{\{6\}}$
70	BIAS(β_1)	0.088675$^{\{2\}}$	0.107243$^{\{4\}}$	0.109671$^{\{5\}}$	0.095263$^{\{3\}}$	0.111477$^{\{6\}}$	0.085562$^{\{1\}}$
	BIAS(β_2)	0.093172$^{\{1\}}$	0.117874$^{\{4\}}$	0.126861$^{\{6\}}$	0.103929$^{\{2\}}$	0.115699$^{\{3\}}$	0.116972$^{\{5\}}$
	MSE(β_1)	0.012260$^{\{2\}}$	0.018347$^{\{5\}}$	0.018559$^{\{6\}}$	0.015276$^{\{3\}}$	0.017770$^{\{4\}}$	0.011209$^{\{1\}}$
	MSE(β_2)	0.013826$^{\{1\}}$	0.019699$^{\{3\}}$	0.025349$^{\{6\}}$	0.017024$^{\{2\}}$	0.023959$^{\{5\}}$	0.022391$^{\{4\}}$
	MRE(β_1)	0.059117$^{\{2\}}$	0.071495$^{\{4\}}$	0.073114$^{\{5\}}$	0.063509$^{\{3\}}$	0.074318$^{\{6\}}$	0.057041$^{\{1\}}$
	MRE(β_2)	0.054807$^{\{1\}}$	0.069338$^{\{5\}}$	0.074624$^{\{6\}}$	0.061135$^{\{2\}}$	0.068058$^{\{3\}}$	0.068807$^{\{4\}}$
	D_{abs}	0.02445$^{\{1\}}$	0.02564$^{\{2.5\}}$	0.02819$^{\{5\}}$	0.02779$^{\{4\}}$	0.02840$^{\{6\}}$	0.02564$^{\{2.5\}}$
	D_{max}	0.03962$^{\{1\}}$	0.04217$^{\{3\}}$	0.04606$^{\{6\}}$	0.04366$^{\{4\}}$	0.04599$^{\{5\}}$	0.04153$^{\{2\}}$
	ASAE	0.01536$^{\{3\}}$	0.01505$^{\{2\}}$	0.01573$^{\{6\}}$	0.01540$^{\{4\}}$	0.01546$^{\{5\}}$	0.01498$^{\{1\}}$
	$\sum$ *Ranks*	14$^{\{1\}}$	32.5$^{\{4\}}$	51$^{\{6\}}$	27$^{\{3\}}$	43$^{\{5\}}$	21.5$^{\{2\}}$
100	BIAS(β_1)	0.064413$^{\{2\}}$	0.070516$^{\{3\}}$	0.071836$^{\{4\}}$	0.060834$^{\{1\}}$	0.078755$^{\{6\}}$	0.073663$^{\{5\}}$
	BIAS(β_2)	0.065384$^{\{1\}}$	0.074566$^{\{2\}}$	0.084264$^{\{5\}}$	0.079538$^{\{4\}}$	0.084365$^{\{6\}}$	0.076578$^{\{3\}}$
	MSE(β_1)	0.006304$^{\{2\}}$	0.007309$^{\{3\}}$	0.008868$^{\{5\}}$	0.005663$^{\{1\}}$	0.009173$^{\{6\}}$	0.008173$^{\{4\}}$
	MSE(β_2)	0.006753$^{\{1\}}$	0.008459$^{\{2\}}$	0.012359$^{\{1\}}$	0.009992$^{\{4\}}$	0.011014$^{\{5\}}$	0.009750$^{\{3\}}$
	MRE(β_1)	0.042942$^{\{2\}}$	0.047011$^{\{3\}}$	0.047890$^{\{4\}}$	0.040556$^{\{1\}}$	0.052504$^{\{6\}}$	0.049109$^{\{5\}}$
	MRE(β_2)	0.038461$^{\{1\}}$	0.043862$^{\{2\}}$	0.049567$^{\{6\}}$	0.046787$^{\{4\}}$	0.049626$^{\{5\}}$	0.045046$^{\{3\}}$
	D_{abs}	0.01746$^{\{1\}}$	0.01823$^{\{4\}}$	0.01811$^{\{3\}}$	0.01766$^{\{2\}}$	0.01977$^{\{6\}}$	0.01859$^{\{5\}}$
	D_{max}	0.02782$^{\{1\}}$	0.02958$^{\{3\}}$	0.02974$^{\{4\}}$	0.02889$^{\{2\}}$	0.03202$^{\{6\}}$	0.03016$^{\{5\}}$
	ASAE	0.01050$^{\{6\}}$	0.01017$^{\{4\}}$	0.01048$^{\{5\}}$	0.00987$^{\{1\}}$	0.01006$^{\{2\}}$	0.01013$^{\{3\}}$
	$\sum$ *Ranks*	17$^{\{1\}}$	26$^{\{3\}}$	37$^{\{5\}}$	20$^{\{2\}}$	48$^{\{6\}}$	36$^{\{4\}}$
200	BIAS(β_1)	0.064964$^{\{6\}}$	0.060226$^{\{5\}}$	0.059158$^{\{4\}}$	0.052603$^{\{2\}}$	0.050042$^{\{1\}}$	0.054877$^{\{3\}}$
	BIAS(β_2)	0.062547$^{\{3\}}$	0.060893$^{\{1\}}$	0.068252$^{\{4\}}$	0.061803$^{\{2\}}$	0.071409$^{\{5\}}$	0.072626$^{\{6\}}$
	MSE(β_1)	0.006198$^{\{6\}}$	0.005306$^{\{4\}}$	0.005411$^{\{5\}}$	0.004118$^{\{2\}}$	0.003805$^{\{1\}}$	0.004833$^{\{3\}}$
	MSE(β_2)	0.005730$^{\{1\}}$	0.005938$^{\{2\}}$	0.008169$^{\{4\}}$	0.005949$^{\{3\}}$	0.008356$^{\{6\}}$	0.008278$^{\{5\}}$
	MRE(β_1)	0.043309$^{\{6\}}$	0.040151$^{\{5\}}$	0.039439$^{\{4\}}$	0.035068$^{\{2\}}$	0.033362$^{\{1\}}$	0.036585$^{\{3\}}$
	MRE(β_2)	0.036792$^{\{3\}}$	0.035819$^{\{1\}}$	0.040148$^{\{4\}}$	0.036355$^{\{2\}}$	0.042005$^{\{5\}}$	0.042721$^{\{6\}}$
	D_{abs}	0.01667$^{\{6\}}$	0.01533$^{\{3\}}$	0.01583$^{\{5\}}$	0.01389$^{\{1\}}$	0.01438$^{\{2\}}$	0.01537$^{\{4\}}$
	D_{max}	0.02677$^{\{6\}}$	0.02485$^{\{3\}}$	0.02591$^{\{5\}}$	0.02245$^{\{1\}}$	0.02376$^{\{2\}}$	0.02529$^{\{4\}}$
	ASAE	0.00823$^{\{5\}}$	0.00762$^{\{1\}}$	0.00838$^{\{6\}}$	0.00801$^{\{2.5\}}$	0.00809$^{\{4\}}$	0.00801$^{\{2.5\}}$
	$\sum$ *Ranks*	42$^{\{6\}}$	25$^{\{2\}}$	41$^{\{5\}}$	17.5$^{\{1\}}$	26$^{\{3\}}$	36.5$^{\{4\}}$
300	BIAS(β_1)	0.050076$^{\{4\}}$	0.045969$^{\{2\}}$	0.059566$^{\{6\}}$	0.042283$^{\{1\}}$	0.051910$^{\{5\}}$	0.048075$^{\{3\}}$
	BIAS(β_2)	0.049690$^{\{2\}}$	0.051282$^{\{3\}}$	0.074500$^{\{6\}}$	0.055779$^{\{1\}}$	0.062622$^{\{5\}}$	0.054482$^{\{4\}}$
	MSE(β_1)	0.003993$^{\{4\}}$	0.003658$^{\{2\}}$	0.005465$^{\{6\}}$	0.002700$^{\{1\}}$	0.004040$^{\{5\}}$	0.003672$^{\{3\}}$
	MSE(β_2)	0.003560$^{\{1\}}$	0.003892$^{\{2\}}$	0.008194$^{\{6\}}$	0.004738$^{\{4\}}$	0.006130$^{\{5\}}$	0.004671$^{\{3\}}$
	MRE(β_1)	0.033384$^{\{4\}}$	0.030646$^{\{2\}}$	0.039711$^{\{6\}}$	0.028189$^{\{1\}}$	0.034607$^{\{5\}}$	0.032050$^{\{3\}}$
	MRE(β_2)	0.029229$^{\{1\}}$	0.030166$^{\{2\}}$	0.043824$^{\{6\}}$	0.032811$^{\{4\}}$	0.036836$^{\{5\}}$	0.032048$^{\{3\}}$
	D_{abs}	0.01282$^{\{3\}}$	0.01177$^{\{1\}}$	0.01437$^{\{6\}}$	0.01180$^{\{2\}}$	0.01323$^{\{4\}}$	0.01351$^{\{5\}}$
	D_{max}	0.02050$^{\{3\}}$	0.01926$^{\{1\}}$	0.02412$^{\{6\}}$	0.01942$^{\{2\}}$	0.02169$^{\{4\}}$	0.02184$^{\{5\}}$
	ASAE	0.00663$^{\{3\}}$	0.00653$^{\{1\}}$	0.00701$^{\{6\}}$	0.00664$^{\{4\}}$	0.00680$^{\{5\}}$	0.00657$^{\{2\}}$
	$\sum$ *Ranks*	25$^{\{3\}}$	16$^{\{1\}}$	54$^{\{6\}}$	20$^{\{2\}}$	43$^{\{5\}}$	31$^{\{4\}}$
400	BIAS(β_1)	0.037189$^{\{1\}}$	0.043222$^{\{3\}}$	0.048804$^{\{5\}}$	0.045928$^{\{4\}}$	0.053415$^{\{6\}}$	0.041111$^{\{2\}}$
	BIAS(β_2)	0.054353$^{\{4\}}$	0.046269$^{\{2\}}$	0.054886$^{\{5\}}$	0.044555$^{\{1\}}$	0.055852$^{\{6\}}$	0.051341$^{\{3\}}$
	MSE(β_1)	0.002109$^{\{1\}}$	0.002998$^{\{3\}}$	0.004085$^{\{5\}}$	0.003177$^{\{4\}}$	0.004293$^{\{6\}}$	0.002618$^{\{2\}}$
	MSE(β_2)	0.004520$^{\{4\}}$	0.003604$^{\{2\}}$	0.004858$^{\{5\}}$	0.003116$^{\{1\}}$	0.004929$^{\{6\}}$	0.004228$^{\{3\}}$
	MRE(β_1)	0.024793$^{\{5\}}$	0.028814$^{\{3\}}$	0.032536$^{\{5\}}$	0.030619$^{\{4\}}$	0.035610$^{\{6\}}$	0.027407$^{\{2\}}$
	MRE(β_2)	0.031972$^{\{4\}}$	0.027217$^{\{2\}}$	0.032286$^{\{5\}}$	0.026209$^{\{1\}}$	0.032854$^{\{6\}}$	0.030201$^{\{3\}}$
	D_{abs}	0.01058$^{\{1\}}$	0.01122$^{\{2\}}$	0.01242$^{\{5\}}$	0.01196$^{\{4\}}$	0.01298$^{\{6\}}$	0.01138$^{\{3\}}$
	D_{max}	0.01753$^{\{1\}}$	0.01820$^{\{2\}}$	0.02030$^{\{5\}}$	0.01914$^{\{4\}}$	0.02107$^{\{6\}}$	0.01858$^{\{3\}}$
	ASAE	0.00598$^{\{6\}}$	0.00573$^{\{2\}}$	0.00592$^{\{4\}}$	0.00582$^{\{3\}}$	0.00593$^{\{5\}}$	0.00563$^{\{1\}}$
	$\sum$ *Ranks*	27$^{\{4\}}$	21$^{\{1\}}$	44$^{\{5\}}$	26$^{\{3\}}$	53$^{\{6\}}$	22$^{\{2\}}$

Table 6. Numerical values of the simulation evaluation for $\beta_1 = 2.1,\ \beta_2 = 1.2$.

n	Est.	δ_1	δ_2	δ_3	δ_4	δ_5	δ_6
30	BIAS(β_1)	$0.231751^{\{5\}}$	$0.225366^{\{3\}}$	$0.280551^{\{6\}}$	$0.176933^{\{1\}}$	$0.199882^{\{2\}}$	$0.227671^{\{4\}}$
	BIAS(β_2)	$0.098975^{\{1\}}$	$0.108552^{\{3\}}$	$0.140167^{\{6\}}$	$0.099867^{\{2\}}$	$0.110004^{\{4\}}$	$0.133241^{\{5\}}$
	MSE(β_1)	$0.098197^{\{5\}}$	$0.076950^{\{3\}}$	$0.155109^{\{6\}}$	$0.048682^{\{1\}}$	$0.066991^{\{2\}}$	$0.082787^{\{4\}}$
	MSE(β_2)	$0.016848^{\{2\}}$	$0.017672^{\{3\}}$	$0.033116^{\{6\}}$	$0.015185^{\{1\}}$	$0.018684^{\{4\}}$	$0.028468^{\{5\}}$
	MRE(β_1)	$0.110357^{\{5\}}$	$0.107317^{\{3\}}$	$0.133596^{\{6\}}$	$0.084254^{\{1\}}$	$0.092594^{\{2\}}$	$0.108415^{\{4\}}$
	MRE(β_2)	$0.082479^{\{1\}}$	$0.090460^{\{3\}}$	$0.116805^{\{6\}}$	$0.083222^{\{2\}}$	$0.091768^{\{4\}}$	$0.111034^{\{5\}}$
	D_{abs}	$0.03716^{\{4\}}$	$0.03560^{\{2\}}$	$0.04060^{\{6\}}$	$0.03545^{\{1\}}$	$0.03698^{\{3\}}$	$0.03768^{\{5\}}$
	$D_{\max}$	$0.05921^{\{4\}}$	$0.05775^{\{3\}}$	$0.06733^{\{6\}}$	$0.05573^{\{1\}}$	$0.05809^{\{2\}}$	$0.06246^{\{5\}}$
	ASAE	$0.02481^{\{5\}}$	$0.02243^{\{2\}}$	$0.02485^{\{6\}}$	$0.02393^{\{3\}}$	$0.02428^{\{4\}}$	$0.02316^{\{1\}}$
	$\sum$ *Ranks*	$32^{\{4\}}$	$25^{\{2\}}$	$54^{\{6\}}$	$13^{\{1\}}$	$27^{\{3\}}$	$34^{\{5\}}$
70	BIAS(β_1)	$0.142763^{\{2\}}$	$0.181359^{\{5\}}$	$0.223506^{\{6\}}$	$0.137485^{\{1\}}$	$0.160294^{\{4\}}$	$0.142804^{\{3\}}$
	BIAS(β_2)	$0.070596^{\{1\}}$	$0.080046^{\{3\}}$	$0.108812^{\{6\}}$	$0.075467^{\{2\}}$	$0.087240^{\{4\}}$	$0.096997^{\{5\}}$
	MSE(β_1)	$0.034885^{\{3\}}$	$0.051439^{\{5\}}$	$0.101843^{\{6\}}$	$0.029713^{\{1\}}$	$0.041335^{\{4\}}$	$0.031040^{\{2\}}$
	MSE(β_2)	$0.008593^{\{1\}}$	$0.010966^{\{3\}}$	$0.019581^{\{6\}}$	$0.008917^{\{2\}}$	$0.011392^{\{4\}}$	$0.013391^{\{5\}}$
	MRE(β_1)	$0.067982^{\{2\}}$	$0.086361^{\{5\}}$	$0.106431^{\{6\}}$	$0.065469^{\{1\}}$	$0.074892^{\{4\}}$	$0.068002^{\{3\}}$
	MRE(β_2)	$0.058830^{\{1\}}$	$0.066705^{\{3\}}$	$0.090677^{\{6\}}$	$0.062889^{\{2\}}$	$0.071224^{\{4\}}$	$0.080831^{\{5\}}$
	D_{abs}	$0.02568^{\{2\}}$	$0.02739^{\{4\}}$	$0.03049^{\{6\}}$	$0.02542^{\{1\}}$	$0.02656^{\{3\}}$	$0.02827^{\{5\}}$
	$D_{\max}$	$0.04137^{\{2\}}$	$0.04420^{\{4\}}$	$0.05106^{\{6\}}$	$0.04052^{\{1\}}$	$0.04330^{\{3\}}$	$0.04689^{\{5\}}$
	ASAE	$0.01542^{\{3\}}$	$0.01434^{\{2\}}$	$0.01606^{\{6\}}$	$0.01601^{\{5\}}$	$0.01548^{\{4\}}$	$0.01427^{\{1\}}$
	$\sum$ *Ranks*	$17^{\{2\}}$	$34^{\{4\}}$	$54^{\{6\}}$	$16^{\{1\}}$	$34^{\{4\}}$	$34^{\{4\}}$
100	BIAS(β_1)	$0.113177^{\{4\}}$	$0.111792^{\{5\}}$	$0.118507^{\{6\}}$	$0.099234^{\{1\}}$	$0.101395^{\{2\}}$	$0.105504^{\{3\}}$
	BIAS(β_2)	$0.048108^{\{1\}}$	$0.051693^{\{3\}}$	$0.061349^{\{6\}}$	$0.050691^{\{2\}}$	$0.053298^{\{4\}}$	$0.057680^{\{5\}}$
	MSE(β_1)	$0.020512^{\{5\}}$	$0.019050^{\{4\}}$	$0.022578^{\{6\}}$	$0.014939^{\{1\}}$	$0.016430^{\{3\}}$	$0.016227^{\{2\}}$
	MSE(β_2)	$0.003956^{\{1\}}$	$0.004369^{\{3\}}$	$0.006070^{\{6\}}$	$0.004065^{\{2\}}$	$0.004474^{\{4\}}$	$0.004991^{\{5\}}$
	MRE(β_1)	$0.053894^{\{5\}}$	$0.053234^{\{4\}}$	$0.056432^{\{6\}}$	$0.047254^{\{2\}}$	$0.048681^{\{1\}}$	$0.050240^{\{3\}}$
	MRE(β_2)	$0.040090^{\{1\}}$	$0.043078^{\{3\}}$	$0.051124^{\{6\}}$	$0.042242^{\{2\}}$	$0.044073^{\{4\}}$	$0.048066^{\{5\}}$
	D_{abs}	$0.01825^{\{6\}}$	$0.01780^{\{5\}}$	$0.01722^{\{1\}}$	$0.01742^{\{3\}}$	$0.01737^{\{2\}}$	$0.01746^{\{4\}}$
	$D_{\max}$	$0.02944^{\{6\}}$	$0.02854^{\{4\}}$	$0.02844^{\{3\}}$	$0.02807^{\{2\}}$	$0.02790^{\{1\}}$	$0.02888^{\{5\}}$
	ASAE	$0.01014^{\{5\}}$	$0.00984^{\{4\}}$	$0.01027^{\{6\}}$	$0.00959^{\{1\}}$	$0.00971^{\{2\}}$	$0.00979^{\{3\}}$
	$\sum$ *Ranks*	$34^{\{3\}}$	$35^{\{5.5\}}$	$46^{\{6\}}$	$16^{\{1\}}$	$23^{\{2\}}$	$35^{\{5.5\}}$
200	BIAS(β_1)	$0.085301^{\{1\}}$	$0.092172^{\{4\}}$	$0.091146^{\{3\}}$	$0.096569^{\{6\}}$	$0.087810^{\{2\}}$	$0.094333^{\{5\}}$
	BIAS(β_2)	$0.041542^{\{1\}}$	$0.044535^{\{3\}}$	$0.049774^{\{5\}}$	$0.047617^{\{4\}}$	$0.043918^{\{2\}}$	$0.053579^{\{6\}}$
	MSE(β_1)	$0.011157^{\{1\}}$	$0.012944^{\{3\}}$	$0.013254^{\{4\}}$	$0.014525^{\{6\}}$	$0.012107^{\{2\}}$	$0.014101^{\{5\}}$
	MSE(β_2)	$0.002929^{\{1\}}$	$0.003176^{\{3\}}$	$0.004035^{\{5\}}$	$0.003292^{\{4\}}$	$0.003066^{\{2\}}$	$0.004173^{\{6\}}$
	MRE(β_1)	$0.040620^{\{2\}}$	$0.043891^{\{4\}}$	$0.043403^{\{3\}}$	$0.045985^{\{6\}}$	$0.041830^{\{1\}}$	$0.044921^{\{5\}}$
	MRE(β_2)	$0.034619^{\{1\}}$	$0.037112^{\{3\}}$	$0.041478^{\{5\}}$	$0.039681^{\{4\}}$	$0.036593^{\{2\}}$	$0.044649^{\{6\}}$
	D_{abs}	$0.01420^{\{4\}}$	$0.01366^{\{1\}}$	$0.01495^{\{5\}}$	$0.01469^{\{3\}}$	$0.01418^{\{1\}}$	$0.01500^{\{6\}}$
	$D_{\max}$	$0.02303^{\{3\}}$	$0.02234^{\{1\}}$	$0.02464^{\{5\}}$	$0.02406^{\{4\}}$	$0.02290^{\{2\}}$	$0.02486^{\{6\}}$
	ASAE	$0.00749^{\{2\}}$	$0.00771^{\{4\}}$	$0.00811^{\{6\}}$	$0.00788^{\{5\}}$	$0.00750^{\{3\}}$	$0.00719^{\{1\}}$
	$\sum$ *Ranks*	$16^{\{1\}}$	$26^{\{3\}}$	$41^{\{4\}}$	$42^{\{5\}}$	$17^{\{2\}}$	$46^{\{6\}}$
300	BIAS(β_1)	$0.071664^{\{1\}}$	$0.083764^{\{5\}}$	$0.080967^{\{4\}}$	$0.085707^{\{6\}}$	$0.078102^{\{2\}}$	$0.079613^{\{3\}}$
	BIAS(β_2)	$0.033862^{\{1\}}$	$0.037019^{\{4\}}$	$0.042924^{\{6\}}$	$0.037217^{\{5\}}$	$0.036235^{\{2\}}$	$0.036895^{\{3\}}$
	MSE(β_1)	$0.008292^{\{1\}}$	$0.011268^{\{6\}}$	$0.009273^{\{3\}}$	$0.010759^{\{5\}}$	$0.008699^{\{2\}}$	$0.009274^{\{4\}}$
	MSE(β_2)	$0.001960^{\{1\}}$	$0.002129^{\{5\}}$	$0.002709^{\{6\}}$	$0.002063^{\{3\}}$	$0.002002^{\{2\}}$	$0.002067^{\{4\}}$
	MRE(β_1)	$0.034126^{\{1\}}$	$0.039888^{\{5\}}$	$0.038556^{\{4\}}$	$0.040813^{\{6\}}$	$0.037008^{\{2\}}$	$0.037911^{\{3\}}$
	MRE(β_2)	$0.028219^{\{1\}}$	$0.030849^{\{4\}}$	$0.035770^{\{6\}}$	$0.031014^{\{5\}}$	$0.030108^{\{2\}}$	$0.030746^{\{3\}}$
	D_{abs}	$0.01298^{\{3\}}$	$0.01302^{\{4\}}$	$0.01285^{\{1\}}$	$0.01381^{\{5\}}$	$0.01286^{\{2\}}$	$0.01392^{\{6\}}$
	$D_{\max}$	$0.02083^{\{1\}}$	$0.02129^{\{4\}}$	$0.02116^{\{3\}}$	$0.02225^{\{5\}}$	$0.02101^{\{2\}}$	$0.02226^{\{6\}}$
	ASAE	$0.00635^{\{3\}}$	$0.00652^{\{5\}}$	$0.00636^{\{4\}}$	$0.00657^{\{6\}}$	$0.00621^{\{2\}}$	$0.00583^{\{1\}}$
	$\sum$ *Ranks*	$13^{\{1\}}$	$42^{\{6\}}$	$37^{\{5\}}$	$34^{\{4\}}$	$18^{\{2\}}$	$33^{\{3\}}$
400	BIAS(β_1)	$0.072708^{\{5\}}$	$0.078703^{\{6\}}$	$0.070650^{\{3\}}$	$0.058528^{\{1\}}$	$0.068470^{\{2\}}$	$0.071210^{\{4\}}$
	BIAS(β_2)	$0.032496^{\{4\}}$	$0.032374^{\{3\}}$	$0.040424^{\{6\}}$	$0.030482^{\{1\}}$	$0.031502^{\{2\}}$	$0.038274^{\{5\}}$
	MSE(β_1)	$0.008273^{\{5\}}$	$0.009101^{\{6\}}$	$0.007539^{\{3\}}$	$0.005648^{\{1\}}$	$0.007148^{\{2\}}$	$0.007576^{\{4\}}$
	MSE(β_2)	$0.001632^{\{2\}}$	$0.001746^{\{4\}}$	$0.002487^{\{6\}}$	$0.001547^{\{1\}}$	$0.001675^{\{3\}}$	$0.002239^{\{5\}}$
	MRE(β_1)	$0.034623^{\{5\}}$	$0.037478^{\{6\}}$	$0.033643^{\{4\}}$	$0.027871^{\{1\}}$	$0.032549^{\{2\}}$	$0.033910^{\{3\}}$
	MRE(β_2)	$0.027080^{\{4\}}$	$0.026978^{\{3\}}$	$0.033687^{\{6\}}$	$0.025402^{\{1\}}$	$0.026128^{\{2\}}$	$0.031895^{\{5\}}$
	D_{abs}	$0.01155^{\{4\}}$	$0.01206^{\{6\}}$	$0.01106^{\{2\}}$	$0.01088^{\{1\}}$	$0.01116^{\{3\}}$	$0.01140^{\{5\}}$
	$D_{\max}$	$0.01866^{\{4\}}$	$0.01935^{\{6\}}$	$0.01849^{\{3\}}$	$0.01752^{\{1\}}$	$0.01796^{\{2\}}$	$0.01890^{\{5\}}$
	ASAE	$0.00564^{\{4\}}$	$0.00536^{\{1\}}$	$0.00584^{\{6\}}$	$0.00569^{\{5\}}$	$0.00561^{\{3\}}$	$0.00547^{\{2\}}$
$\sum$ *Ranks*	$37^{\{3\}}$	$41^{\{6\}}$	$39^{\{5\}}$	$13^{\{1\}}$	$21^{\{2\}}$	$38^{\{4\}}$	

Table 7. Numerical values of the simulation evaluation for $\beta_1 = 1.7,\ \beta_2 = 3.2$.

n	Est.	δ_1	δ_2	δ_3	δ_4	δ_5	δ_6
30	BIAS(β_1)	$0.187659^{\{4\}}$	$0.188431^{\{5\}}$	$0.182689^{\{3\}}$	$0.171701^{\{1\}}$	$0.194039^{\{6\}}$	$0.173374^{\{2\}}$
	BIAS(β_2)	$0.284702^{\{2\}}$	$0.314128^{\{3\}}$	$0.349118^{\{5\}}$	$0.273745^{\{1\}}$	$0.367658^{\{6\}}$	$0.325210^{\{4\}}$
	MSE(β_1)	$0.058965^{\{3\}}$	$0.064934^{\{5\}}$	$0.068905^{\{6\}}$	$0.042010^{\{1\}}$	$0.060673^{\{4\}}$	$0.054281^{\{2\}}$
	MSE(β_2)	$0.144418^{\{2\}}$	$0.166440^{\{3\}}$	$0.211558^{\{6\}}$	$0.115919^{\{1\}}$	$0.210247^{\{5\}}$	$0.172632^{\{4\}}$
	MRE(β_1)	$0.110388^{\{4\}}$	$0.110841^{\{5\}}$	$0.107464^{\{3\}}$	$0.101000^{\{1\}}$	$0.114141^{\{6\}}$	$0.101985^{\{2\}}$
	MRE(β_2)	$0.088969^{\{2\}}$	$0.098165^{\{3\}}$	$0.109099^{\{4\}}$	$0.085545^{\{1\}}$	$0.114893^{\{5\}}$	$0.101628^{\{6\}}$
	D_{abs}	$0.03613^{\{1\}}$	$0.03842^{\{3\}}$	$0.03843^{\{4\}}$	$0.03924^{\{5\}}$	$0.04207^{\{6\}}$	$0.03667^{\{2\}}$
	D_{max}	$0.05815^{\{1\}}$	$0.06271^{\{4\}}$	$0.06402^{\{5\}}$	$0.06173^{\{3\}}$	$0.06850^{\{6\}}$	$0.06067^{\{2\}}$
	ASAE	$0.02539^{\{6\}}$	$0.02328^{\{1\}}$	$0.02362^{\{2\}}$	$0.02448^{\{5\}}$	$0.02392^{\{4\}}$	$0.02365^{\{3\}}$
	$\sum Ranks$	$25^{\{2\}}$	$32^{\{4\}}$	$38^{\{5\}}$	$19^{\{1\}}$	$48^{\{6\}}$	$27^{\{3\}}$
70	BIAS(β_1)	$0.107269^{\{2\}}$	$0.136901^{\{6\}}$	$0.125841^{\{5\}}$	$0.112822^{\{3\}}$	$0.120912^{\{4\}}$	$0.104972^{\{1\}}$
	BIAS(β_2)	$0.203163^{\{1\}}$	$0.210422^{\{2\}}$	$0.225646^{\{4\}}$	$0.225496^{\{3\}}$	$0.241919^{\{6\}}$	$0.232169^{\{5\}}$
	MSE(β_1)	$0.016909^{\{2\}}$	$0.026077^{\{5\}}$	$0.026259^{\{6\}}$	$0.018808^{\{3\}}$	$0.025015^{\{4\}}$	$0.019206^{\{1\}}$
	MSE(β_2)	$0.063993^{\{1\}}$	$0.068364^{\{2\}}$	$0.077894^{\{4\}}$	$0.073424^{\{3\}}$	$0.089511^{\{5\}}$	$0.106656^{\{6\}}$
	MRE(β_1)	$0.063099^{\{2\}}$	$0.080530^{\{6\}}$	$0.074024^{\{5\}}$	$0.066366^{\{3\}}$	$0.071125^{\{4\}}$	$0.061748^{\{1\}}$
	MRE(β_2)	$0.063489^{\{1\}}$	$0.065757^{\{2\}}$	$0.070514^{\{4\}}$	$0.070467^{\{3\}}$	$0.075600^{\{6\}}$	$0.072553^{\{5\}}$
	D_{abs}	$0.02645^{\{4\}}$	$0.02883^{\{6\}}$	$0.02718^{\{5\}}$	$0.02639^{\{3\}}$	$0.02538^{\{1\}}$	$0.02599^{\{2\}}$
	D_{max}	$0.04307^{\{4\}}$	$0.04585^{\{6\}}$	$0.04470^{\{5\}}$	$0.04233^{\{3\}}$	$0.04214^{\{2\}}$	$0.04198^{\{1\}}$
	ASAE	$0.01662^{\{6\}}$	$0.01602^{\{5\}}$	$0.01524^{\{1\}}$	$0.01559^{\{4\}}$	$0.01533^{\{2\}}$	$0.01537^{\{3\}}$
	$\sum Ranks$	$23^{\{1\}}$	$40^{\{6\}}$	$38^{\{5\}}$	$28^{\{3\}}$	$34^{\{4\}}$	$25^{\{2\}}$
100	BIAS(β_1)	$0.090307^{\{5\}}$	$0.080436^{\{3\}}$	$0.090022^{\{4\}}$	$0.068355^{\{1\}}$	$0.098995^{\{6\}}$	$0.079156^{\{2\}}$
	BIAS(β_2)	$0.133847^{\{1\}}$	$0.144293^{\{3\}}$	$0.198379^{\{6\}}$	$0.144705^{\{4\}}$	$0.177196^{\{5\}}$	$0.140288^{\{2\}}$
	MSE(β_1)	$0.012106^{\{4\}}$	$0.010023^{\{3\}}$	$0.014439^{\{5\}}$	$0.007693^{\{1\}}$	$0.015427^{\{6\}}$	$0.009404^{\{2\}}$
	MSE(β_2)	$0.028238^{\{1\}}$	$0.034123^{\{4\}}$	$0.057433^{\{6\}}$	$0.030276^{\{2\}}$	$0.050482^{\{5\}}$	$0.030976^{\{3\}}$
	MRE(β_1)	$0.053122^{\{5\}}$	$0.047316^{\{3\}}$	$0.052954^{\{4\}}$	$0.040209^{\{1\}}$	$0.058232^{\{6\}}$	$0.046562^{\{2\}}$
	MRE(β_2)	$0.041827^{\{1\}}$	$0.045092^{\{3\}}$	$0.061993^{\{6\}}$	$0.045220^{\{4\}}$	$0.055374^{\{5\}}$	$0.043840^{\{2\}}$
	D_{abs}	$0.01902^{\{4\}}$	$0.01677^{\{1\}}$	$0.01968^{\{5\}}$	$0.01764^{\{2\}}$	$0.02104^{\{6\}}$	$0.01859^{\{3\}}$
	D_{max}	$0.03037^{\{4\}}$	$0.02740^{\{1\}}$	$0.03300^{\{5\}}$	$0.02878^{\{2\}}$	$0.03437^{\{6\}}$	$0.03015^{\{3\}}$
	ASAE	$0.01105^{\{6\}}$	$0.01024^{\{3\}}$	$0.01005^{\{2\}}$	$0.01052^{\{5\}}$	$0.00984^{\{1\}}$	$0.01049^{\{4\}}$
	$\sum Ranks$	$31^{\{4\}}$	$24^{\{3\}}$	$43^{\{5\}}$	$22^{\{1\}}$	$46^{\{6\}}$	$23^{\{2\}}$
200	BIAS(β_1)	$0.070123^{\{3\}}$	$0.074385^{\{6\}}$	$0.071756^{\{5\}}$	$0.062716^{\{1\}}$	$0.067923^{\{2\}}$	$0.071427^{\{4\}}$
	BIAS(β_2)	$0.099689^{\{1\}}$	$0.119422^{\{3\}}$	$0.173332^{\{6\}}$	$0.118102^{\{2\}}$	$0.128552^{\{5\}}$	$0.126266^{\{4\}}$
	MSE(β_1)	$0.007370^{\{3\}}$	$0.007730^{\{4\}}$	$0.007814^{\{5\}}$	$0.006587^{\{1\}}$	$0.006923^{\{2\}}$	$0.007919^{\{6\}}$
	MSE(β_2)	$0.017062^{\{1\}}$	$0.022514^{\{2\}}$	$0.041835^{\{6\}}$	$0.024107^{\{3\}}$	$0.027773^{\{5\}}$	$0.025258^{\{4\}}$
	MRE(β_1)	$0.041249^{\{3\}}$	$0.043756^{\{6\}}$	$0.042210^{\{5\}}$	$0.036892^{\{1\}}$	$0.039955^{\{2\}}$	$0.042016^{\{4\}}$
	MRE(β_2)	$0.031153^{\{1\}}$	$0.037319^{\{3\}}$	$0.054166^{\{6\}}$	$0.036907^{\{2\}}$	$0.040172^{\{5\}}$	$0.039458^{\{4\}}$
	D_{abs}	$0.01496^{\{2\}}$	$0.01596^{\{6\}}$	$0.01472^{\{1\}}$	$0.01540^{\{3\}}$	$0.01543^{\{4\}}$	$0.01571^{\{5\}}$
	D_{max}	$0.02404^{\{1\}}$	$0.02573^{\{6\}}$	$0.02544^{\{4\}}$	$0.02462^{\{2\}}$	$0.02528^{\{3\}}$	$0.02546^{\{5\}}$
	ASAE	$0.00799^{\{2\}}$	$0.00825^{\{4\}}$	$0.00802^{\{3\}}$	$0.00842^{\{6\}}$	$0.00775^{\{1\}}$	$0.00841^{\{5\}}$
	$\sum Ranks$	$17^{\{1\}}$	$40^{\{4\}}$	$41^{\{5.5\}}$	$21^{\{2\}}$	$29^{\{3\}}$	$41^{\{5.5\}}$
300	BIAS(β_1)	$0.051610^{\{1\}}$	$0.056124^{\{4\}}$	$0.063921^{\{5\}}$	$0.053606^{\{3\}}$	$0.069504^{\{6\}}$	$0.052772^{\{2\}}$
	BIAS(β_2)	$0.092383^{\{1\}}$	$0.107779^{\{3\}}$	$0.126277^{\{5\}}$	$0.097704^{\{2\}}$	$0.116645^{\{4\}}$	$0.115272^{\{6\}}$
	MSE(β_1)	$0.004038^{\{1\}}$	$0.005326^{\{4\}}$	$0.006883^{\{5\}}$	$0.004512^{\{3\}}$	$0.007872^{\{6\}}$	$0.004168^{\{2\}}$
	MSE(β_2)	$0.013233^{\{1\}}$	$0.020655^{\{4\}}$	$0.023226^{\{6\}}$	$0.014942^{\{2\}}$	$0.020056^{\{3\}}$	$0.022492^{\{5\}}$
	MRE(β_1)	$0.030359^{\{1\}}$	$0.033014^{\{4\}}$	$0.037600^{\{5\}}$	$0.031533^{\{3\}}$	$0.040885^{\{6\}}$	$0.031042^{\{2\}}$
	MRE(β_2)	$0.028870^{\{1\}}$	$0.033681^{\{3\}}$	$0.039462^{\{6\}}$	$0.030533^{\{2\}}$	$0.036452^{\{5\}}$	$0.036023^{\{4\}}$
	D_{abs}	$0.01218^{\{2\}}$	$0.01316^{\{5\}}$	$0.01297^{\{4\}}$	$0.01201^{\{1\}}$	$0.01502^{\{6\}}$	$0.01265^{\{3\}}$
	D_{max}	$0.01970^{\{2\}}$	$0.02151^{\{4\}}$	$0.02157^{\{5\}}$	$0.01965^{\{1\}}$	$0.02437^{\{6\}}$	$0.02067^{\{3\}}$
	ASAE	$0.00736^{\{6\}}$	$0.00662^{\{1\}}$	$0.00710^{\{5\}}$	$0.00707^{\{4\}}$	$0.00706^{\{3\}}$	$0.00704^{\{2\}}$
	$\sum Ranks$	$16^{\{1\}}$	$32^{\{4\}}$	$46^{\{6\}}$	$21^{\{2\}}$	$45^{\{5\}}$	$29^{\{3\}}$
400	BIAS(β_1)	$0.044765^{\{2\}}$	$0.053342^{\{5\}}$	$0.052305^{\{4\}}$	$0.044389^{\{1\}}$	$0.063939^{\{6\}}$	$0.052042^{\{3\}}$
	BIAS(β_2)	$0.082558^{\{1\}}$	$0.096510^{\{3\}}$	$0.105358^{\{5\}}$	$0.084396^{\{2\}}$	$0.106201^{\{6\}}$	$0.104150^{\{4\}}$
	MSE(β_1)	$0.003208^{\{2\}}$	$0.004643^{\{5\}}$	$0.004527^{\{4\}}$	$0.003175^{\{1\}}$	$0.006388^{\{6\}}$	$0.004086^{\{3\}}$
	MSE(β_2)	$0.010995^{\{1\}}$	$0.014770^{\{3\}}$	$0.018122^{\{6\}}$	$0.011751^{\{2\}}$	$0.016065^{\{4\}}$	$0.017208^{\{5\}}$
	MRE(β_1)	$0.026332^{\{2\}}$	$0.031377^{\{5\}}$	$0.030768^{\{4\}}$	$0.026111^{\{1\}}$	$0.037611^{\{6\}}$	$0.030613^{\{3\}}$
	MRE(β_2)	$0.025799^{\{1\}}$	$0.030159^{\{3\}}$	$0.032924^{\{5\}}$	$0.026374^{\{2\}}$	$0.033188^{\{6\}}$	$0.032547^{\{4\}}$
	D_{abs}	$0.01071^{\{1\}}$	$0.01128^{\{3\}}$	$0.01157^{\{4\}}$	$0.01103^{\{2\}}$	$0.01345^{\{6\}}$	$0.01336^{\{5\}}$
	D_{max}	$0.01733^{\{1\}}$	$0.01857^{\{3\}}$	$0.01916^{\{4\}}$	$0.01778^{\{2\}}$	$0.02214^{\{6\}}$	$0.02160^{\{5\}}$
	ASAE	$0.00606^{\{5\}}$	$0.00595^{\{2\}}$	$0.00601^{\{4\}}$	$0.00609^{\{6\}}$	$0.00599^{\{3\}}$	$0.00592^{\{1\}}$
	$\sum Ranks$	$16^{\{1\}}$	$32^{\{3\}}$	$40^{\{5\}}$	$19^{\{2\}}$	$49^{\{6\}}$	$33^{\{4\}}$

Table 8. Numerical values of the simulation evaluation for $\beta_1 = 2.7,\ \beta_2 = 1.2$.

n	Est.	δ_1	δ_2	δ_3	δ_4	δ_5	δ_6
30	BIAS(β_1)	$0.326529^{\{3\}}$	$0.314338^{\{2\}}$	$0.491706^{\{6\}}$	$0.288435^{\{1\}}$	$0.377449^{\{5\}}$	$0.340399^{\{4\}}$
	BIAS(β_2)	$0.097608^{\{1\}}$	$0.109169^{\{2\}}$	$0.147600^{\{6\}}$	$0.112435^{\{3\}}$	$0.143113^{\{5\}}$	$0.119420^{\{4\}}$
	MSE(β_1)	$0.189773^{\{3\}}$	$0.174201^{\{2\}}$	$0.483171^{\{6\}}$	$0.123135^{\{1\}}$	$0.257628^{\{5\}}$	$0.192085^{\{4\}}$
	MSE(β_2)	$0.014373^{\{1\}}$	$0.020535^{\{3\}}$	$0.036426^{\{6\}}$	$0.018509^{\{2\}}$	$0.031914^{\{5\}}$	$0.025386^{\{4\}}$
	MRE(β_1)	$0.120937^{\{3\}}$	$0.116421^{\{2\}}$	$0.182113^{\{6\}}$	$0.106828^{\{1\}}$	$0.139796^{\{5\}}$	$0.126074^{\{4\}}$
	MRE(β_2)	$0.081340^{\{1\}}$	$0.090974^{\{2\}}$	$0.123000^{\{6\}}$	$0.093696^{\{3\}}$	$0.119261^{\{5\}}$	$0.099516^{\{4\}}$
	D_{abs}	$0.03586^{\{2\}}$	$0.03398^{\{1\}}$	$0.04280^{\{6\}}$	$0.03652^{\{3\}}$	$0.03937^{\{5\}}$	$0.03753^{\{4\}}$
	D_{max}	$0.05815^{\{2\}}$	$0.05614^{\{1\}}$	$0.07079^{\{6\}}$	$0.05907^{\{3\}}$	$0.06552^{\{5\}}$	$0.06081^{\{4\}}$
	ASAE	$0.02489^{\{4\}}$	$0.02448^{\{3\}}$	$0.02560^{\{6\}}$	$0.02324^{\{2\}}$	$0.02516^{\{5\}}$	$0.02243^{\{1\}}$
	$\sum$ Ranks	$20^{\{3\}}$	$18^{\{1\}}$	$54^{\{6\}}$	$19^{\{2\}}$	$45^{\{5\}}$	$33^{\{4\}}$
70	BIAS(β_1)	$0.233254^{\{4\}}$	$0.222870^{\{3\}}$	$0.235241^{\{5\}}$	$0.221870^{\{2\}}$	$0.280309^{\{6\}}$	$0.216156^{\{1\}}$
	BIAS(β_2)	$0.077990^{\{3\}}$	$0.071920^{\{1\}}$	$0.092433^{\{6\}}$	$0.072741^{\{2\}}$	$0.091576^{\{5\}}$	$0.085223^{\{4\}}$
	MSE(β_1)	$0.097679^{\{5\}}$	$0.079608^{\{2\}}$	$0.090270^{\{4\}}$	$0.072194^{\{1\}}$	$0.128846^{\{6\}}$	$0.083318^{\{3\}}$
	MSE(β_2)	$0.009342^{\{3\}}$	$0.008265^{\{2\}}$	$0.012911^{\{6\}}$	$0.008055^{\{1\}}$	$0.012878^{\{5\}}$	$0.012370^{\{4\}}$
	MRE(β_1)	$0.086390^{\{4\}}$	$0.082544^{\{3\}}$	$0.087126^{\{5\}}$	$0.082174^{\{2\}}$	$0.103818^{\{6\}}$	$0.080058^{\{1\}}$
	MRE(β_2)	$0.064991^{\{3\}}$	$0.059933^{\{1\}}$	$0.077027^{\{6\}}$	$0.060617^{\{2\}}$	$0.076313^{\{5\}}$	$0.071019^{\{4\}}$
	D_{abs}	$0.02621^{\{4\}}$	$0.02538^{\{2\}}$	$0.02634^{\{5\}}$	$0.02546^{\{3\}}$	$0.02728^{\{6\}}$	$0.02498^{\{1\}}$
	D_{max}	$0.04302^{\{4\}}$	$0.04083^{\{2\}}$	$0.04368^{\{5\}}$	$0.04048^{\{1\}}$	$0.04489^{\{6\}}$	$0.04123^{\{3\}}$
	ASAE	$0.01500^{\{4\}}$	$0.01496^{\{3\}}$	$0.01602^{\{5\}}$	$0.01439^{\{1\}}$	$0.01632^{\{6\}}$	$0.01477^{\{2\}}$
	$\sum$ Ranks	$34^{\{4\}}$	$19^{\{2\}}$	$47^{\{5\}}$	$13^{\{1\}}$	$51^{\{6\}}$	$23^{\{3\}}$
100	BIAS(β_1)	$0.155229^{\{2\}}$	$0.145562^{\{1\}}$	$0.178444^{\{6\}}$	$0.161473^{\{3\}}$	$0.174864^{\{5\}}$	$0.164851^{\{4\}}$
	BIAS(β_2)	$0.048879^{\{1\}}$	$0.050273^{\{3\}}$	$0.063274^{\{5\}}$	$0.049851^{\{2\}}$	$0.069715^{\{6\}}$	$0.057060^{\{4\}}$
	MSE(β_1)	$0.041120^{\{1\}}$	$0.032546^{\{1\}}$	$0.053032^{\{6\}}$	$0.040669^{\{2\}}$	$0.052871^{\{5\}}$	$0.051291^{\{4\}}$
	MSE(β_2)	$0.004035^{\{3\}}$	$0.003975^{\{2\}}$	$0.005978^{\{5\}}$	$0.003966^{\{1\}}$	$0.007676^{\{6\}}$	$0.005417^{\{4\}}$
	MRE(β_1)	$0.057492^{\{2\}}$	$0.053912^{\{1\}}$	$0.066090^{\{6\}}$	$0.059805^{\{3\}}$	$0.064764^{\{5\}}$	$0.061056^{\{4\}}$
	MRE(β_2)	$0.040733^{\{1\}}$	$0.041894^{\{3\}}$	$0.052728^{\{5\}}$	$0.041543^{\{2\}}$	$0.058096^{\{6\}}$	$0.047550^{\{4\}}$
	D_{abs}	$0.01904^{\{3\}}$	$0.01981^{\{5\}}$	$0.02090^{\{6\}}$	$0.01919^{\{4\}}$	$0.01879^{\{2\}}$	$0.01852^{\{1\}}$
	D_{max}	$0.03034^{\{1\}}$	$0.03141^{\{4\}}$	$0.03380^{\{6\}}$	$0.03068^{\{3\}}$	$0.03166^{\{5\}}$	$0.03040^{\{2\}}$
	ASAE	$0.00986^{\{4\}}$	$0.00968^{\{3\}}$	$0.01002^{\{5\}}$	$0.00925^{\{2\}}$	$0.01038^{\{6\}}$	$0.00898^{\{1\}}$
	$\sum$ Ranks	$18^{\{1\}}$	$23^{\{3\}}$	$50^{\{6\}}$	$22^{\{2\}}$	$46^{\{5\}}$	$28^{\{4\}}$
200	BIAS(β_1)	$0.129023^{\{3\}}$	$0.128423^{\{2\}}$	$0.172346^{\{6\}}$	$0.099934^{\{1\}}$	$0.144469^{\{5\}}$	$0.136795^{\{4\}}$
	BIAS(β_2)	$0.039171^{\{1\}}$	$0.042142^{\{2\}}$	$0.052021^{\{5\}}$	$0.045987^{\{4\}}$	$0.053960^{\{6\}}$	$0.043745^{\{3\}}$
	MSE(β_1)	$0.027715^{\{2.5\}}$	$0.027715^{\{2.5\}}$	$0.048656^{\{6\}}$	$0.016484^{\{1\}}$	$0.032278^{\{5\}}$	$0.028785^{\{4\}}$
	MSE(β_2)	$0.003141^{\{2.5\}}$	$0.003141^{\{2.5\}}$	$0.004494^{\{5\}}$	$0.003022^{\{4\}}$	$0.004847^{\{6\}}$	$0.002690^{\{1\}}$
	MRE(β_1)	$0.047756^{\{3\}}$	$0.047564^{\{2\}}$	$0.063832^{\{6\}}$	$0.037012^{\{1\}}$	$0.053507^{\{5\}}$	$0.050665^{\{4\}}$
	MRE(β_2)	$0.031792^{\{1\}}$	$0.035118^{\{2\}}$	$0.043350^{\{5\}}$	$0.038323^{\{4\}}$	$0.044967^{\{6\}}$	$0.036455^{\{3\}}$
	D_{abs}	$0.01439^{\{1.5\}}$	$0.01439^{\{1.5\}}$	$0.01695^{\{5\}}$	$0.01459^{\{3\}}$	$0.01756^{\{6\}}$	$0.01658^{\{4\}}$
	D_{max}	$0.02305^{\{1.5\}}$	$0.02305^{\{1.5\}}$	$0.02795^{\{5\}}$	$0.02372^{\{3\}}$	$0.02870^{\{6\}}$	$0.02664^{\{4\}}$
	ASAE	$0.00729^{\{1.5\}}$	$0.00729^{\{1.5\}}$	$0.00794^{\{6\}}$	$0.00781^{\{5\}}$	$0.00771^{\{4\}}$	$0.00750^{\{3\}}$
	$\sum$ *Ranks*	$17.5^{\{1.5\}}$	$17.5^{\{1.5\}}$	$49^{\{5.5\}}$	$26^{\{3\}}$	$49^{\{5.5\}}$	$30^{\{4\}}$
300	BIAS(β_1)	$0.085842^{\{1\}}$	$0.114236^{\{3\}}$	$0.135437^{\{6\}}$	$0.109338^{\{2\}}$	$0.126799^{\{5\}}$	$0.122139^{\{4\}}$
	BIAS(β_2)	$0.032346^{\{1\}}$	$0.034052^{\{2\}}$	$0.047801^{\{6\}}$	$0.039724^{\{3\}}$	$0.042805^{\{5\}}$	$0.039737^{\{4\}}$
	MSE(β_1)	$0.021574^{\{2\}}$	$0.040669^{\{6\}}$	$0.029567^{\{5\}}$	$0.018704^{\{1\}}$	$0.024502^{\{4\}}$	$0.021964^{\{3\}}$
	MSE(β_2)	$0.001835^{\{1\}}$	$0.003966^{\{6\}}$	$0.003579^{\{5\}}$	$0.002442^{\{3\}}$	$0.002660^{\{4\}}$	$0.002360^{\{2\}}$
	MRE(β_1)	$0.031356^{\{1\}}$	$0.042310^{\{3\}}$	$0.050162^{\{6\}}$	$0.040495^{\{2\}}$	$0.046963^{\{5\}}$	$0.045237^{\{4\}}$
	MRE(β_2)	$0.026876^{\{1\}}$	$0.028377^{\{2\}}$	$0.039834^{\{6\}}$	$0.033103^{\{3\}}$	$0.035671^{\{5\}}$	$0.033114^{\{4\}}$
	D_{abs}	$0.01250^{\{2.5\}}$	$0.01250^{\{2.5\}}$	$0.01415^{\{6\}}$	$0.01229^{\{4\}}$	$0.01294^{\{5\}}$	$0.01186^{\{1\}}$
	D_{max}	$0.02043^{\{3.5\}}$	$0.02043^{\{3.5\}}$	$0.02352^{\{6\}}$	$0.02005^{\{2\}}$	$0.02130^{\{5\}}$	$0.01967^{\{1\}}$
	ASAE	$0.00647^{\{3.5\}}$	$0.00647^{\{3.5\}}$	$0.00677^{\{6\}}$	$0.00637^{\{2\}}$	$0.00671^{\{5\}}$	$0.00611^{\{1\}}$
	$\sum$ Ranks	$16.5^{\{1\}}$	$31.5^{\{4\}}$	$52^{\{6\}}$	$22^{\{2\}}$	$43^{\{5\}}$	$24^{\{3\}}$
400	BIAS(β_1)	$0.340399^{\{6\}}$	$0.115643^{\{4\}}$	$0.105898^{\{2\}}$	$0.098022^{\{1\}}$	$0.120638^{\{5\}}$	$0.108066^{\{3\}}$
	BIAS(β_2)	$0.119420^{\{6\}}$	$0.037393^{\{3\}}$	$0.036925^{\{2\}}$	$0.032426^{\{1\}}$	$0.041630^{\{5\}}$	$0.038210^{\{4\}}$
	MSE(β_1)	$0.021466^{\{4\}}$	$0.040669^{\{6\}}$	$0.018225^{\{3\}}$	$0.015093^{\{1\}}$	$0.022926^{\{5\}}$	$0.017765^{\{2\}}$
	MSE(β_2)	$0.002225^{\{4\}}$	$0.003966^{\{6\}}$	$0.002131^{\{2\}}$	$0.001619^{\{1\}}$	$0.002740^{\{5\}}$	$0.002231^{\{3\}}$
	MRE(β_1)	$0.042831^{\{4.5\}}$	$0.042831^{\{4.5\}}$	$0.039222^{\{2\}}$	$0.036305^{\{1\}}$	$0.044681^{\{6\}}$	$0.040025^{\{3\}}$
	MRE(β_2)	$0.031161^{\{3.5\}}$	$0.031161^{\{3.5\}}$	$0.030771^{\{2\}}$	$0.027022^{\{1\}}$	$0.034692^{\{6\}}$	$0.031841^{\{5\}}$
	D_{abs}	$0.01277^{\{5.5\}}$	$0.01277^{\{5.5\}}$	$0.01167^{\{2\}}$	$0.01060^{\{1\}}$	$0.01186^{\{3\}}$	$0.01220^{\{4\}}$
	D_{max}	$0.02068^{\{5.5\}}$	$0.02068^{\{5.5\}}$	$0.01903^{\{2\}}$	$0.01722^{\{1\}}$	$0.01955^{\{3\}}$	$0.02010^{\{4\}}$
	ASAE	$0.00546^{\{3.5\}}$	$0.00546^{\{3.5\}}$	$0.00572^{\{5\}}$	$0.00543^{\{2\}}$	$0.00583^{\{6\}}$	$0.00535^{\{1\}}$
	$\sum$ *Ranks*	$42^{\{5\}}$	$41.5^{\{4\}}$	$22^{\{2\}}$	$10^{\{1\}}$	$44^{\{6\}}$	$29^{\{3\}}$

Table 9. Relative and comprehensive rankings of all estimation techniques for the proposed distribution across varying model parameter values.

Parameters	n	δ_1	δ_2	δ_3	δ_4	δ_5	δ_6
$\beta_1 = 0.5,\ \beta_2 = 0.7$	30	3.5	1.0	5.0	3.5	6.0	2.0
	70	4.0	2.0	1.0	3.0	6.0	5.0
	100	3.0	5.0	6.0	2.0	4.0	1.0
	200	1.0	2.0	3.0	4.0	6.0	5.0
	300	3.0	1.0	5.0	4.0	6.0	2.0
	400	1.0	4.0	5.0	3.0	6.0	2.0
$\beta_1 = 1.5,\ \beta_2 = 1.7$	30	2.5	1.0	5.0	2.5	4.0	6.0
	70	1.0	4.0	6.0	3.0	5.0	2.0
	100	1.0	3.0	5.0	2.0	6.0	4.0
	200	6.0	2.0	5.0	1.0	3.0	4.0
	300	3.0	1.0	6.0	2.0	5.0	4.0
	400	4.0	1.0	5.0	3.0	6.0	2.0
$\beta_1 = 2.1,\ \beta_2 = 1.2$	30	4.0	2.0	6.0	1.0	3.0	5.0
	70	2.0	4.0	6.0	1.0	4.0	4.0
	100	3.0	5.5	6.0	1.0	2.0	5.5
	200	1.0	3.0	4.0	5.0	2.0	6.0
	300	1.0	6.0	5.0	4.0	2.0	3.0
	400	3.0	6.0	5.0	1.0	2.0	4.0
$\beta_1 = 1.7,\ \beta_2 = 3.2$	30	2.0	4.0	5.0	1.0	6.0	3.0
	70	1.0	6.0	5.0	3.0	4.0	2.0
	100	4.0	3.0	5.0	1.0	6.0	2.0
	200	1.0	4.0	5.5	2.0	3.0	5.5
	300	1.0	4.0	6.0	2.0	5.0	3.0
	400	1.0	3.0	5.0	2.0	6.0	4.0
$\beta_1 = 2.7,\ \beta_2 = 1.2$	30	3.0	1.0	6.0	2.0	5.0	4.0
	70	4.0	2.0	5.0	1.0	6.0	3.0
	100	1.0	3.0	6.0	2.0	5.0	4.0
	200	1.5	1.5	5.5	3.0	5.5	4.0
	300	1.0	4.0	6.0	2.0	5.0	3.0
	400	5.0	4.0	2.0	1.0	6.0	3.0
$\sum$ Ranks		72.5	93	150	68	140.5	106.5
Overall Rank		2.0	6.0	3.0	1.0	5.0	4.0

5. Bayesian inference

Bayesian estimation is an effective approach for estimating the parameters of a distributed model. This method creates a posterior distribution for an existing lifespan distribution by utilizing prior information. From a Bayesian standpoint, there is no hard and fast method for choosing priors because one cannot clearly assert that one prior is superior to another. When there is insufficient interpretive information about the unknown parameter, a non-informative prior is frequently adopted. In contrast, if considerable information about the parameter(s) is available, an informative prior is generally more effective. The likelihood function based on the PDF of the HS-PHLD, as provided in Eq (1.13), is used to generate the posterior distribution.

Bayesian estimation leverages prior distributions to include information about the parameters β_1 and β_2. We assume that β_1 and β_2 adhere to independent Gamma priors,

$$\beta_1 \sim \text{Gamma}(\sigma_1, \omega_1), \text{ and } \beta_2 \sim \text{Gamma}(\sigma_2, \omega_2).$$

The parameters $\sigma_1, \omega_1, \sigma_2, \omega_2$ serve as hyperparameters in this context.

$$\pi(\beta_1|\sigma_1, \omega_1) = \frac{\omega_1^{\sigma_1}}{\Gamma(\sigma_1)} \beta_1^{\sigma_1 - 1} e^{-\omega_1 \beta_1}; \;\; \beta_1 > 0,$$
$$\pi(\beta_2|\sigma_2, \omega_2) = \frac{\omega_2^{\sigma_2}}{\Gamma(\sigma_2)} \beta_2^{\sigma_2 - 1} e^{-*\omega_2 \beta_2}; \;\; \beta_2 > 0.$$

If prior knowledge is not sufficient, then small values of these hyperparameters result in weakly informative priors. This ensures that the results are data-driven. For our study, we have used a value of 1.5 for these hyperparameters to obtain slightly informative priors. This is because we want to use prior knowledge to some extent. If prior knowledge is available, then these hyperparameters can be set to obtain informative priors. This results in more precise estimates. The choice of hyperparameters is also crucial to obtain numerically stable results when Marckov chain monte Carlo (MCMC) is used to obtain the estimates. If these hyperparameters are set to large values, then numerical instability is likely to result. Thus, we obtain the joint prior-distribution of β_1 and β_2 as follows:

$$\pi(\beta_1, \beta_2) = \frac{\omega_1^{\sigma_1} \omega_2^{\sigma_2}}{\Gamma(\sigma_1)\Gamma(\sigma_2)} \beta_1^{\sigma_1 - 1} \beta_2^{\sigma_2 - 1} e^{-(\omega_1 \beta_1 + \omega_2 \beta_2)}.$$

Based on Bayes' theorem, the joint posterior density of β_1 and β_2 is formulated as

$$\pi(\beta_1, \beta_2|x) = \frac{L(x|\beta_1, \beta_2)\, \pi(\beta_1, \beta_2)}{\int_0^\infty \int_0^\infty L(x|\beta_1, \beta_2)\, \pi(\beta_1, \beta_2) d\beta_1 d\beta_2}.$$

Currently, we utilize three distinct loss functions-the squared error loss function (SELF), the linear-exponential loss function (LELF), and the generalized entropy loss function (GELF); see [16] and [20].

5.1. Estimation under SELF

The SELF measures the discrepancy between the predicted and true values by taking the square of their difference. and is stated as

$$L(\alpha, \hat{\alpha}) = (\alpha - \hat{\alpha})^2.$$

Under squared error loss, the Bayesian estimator is given by the mean of the posterior distribution.

$$\hat{\alpha}_{SELF} = E[\alpha|X] = \int \alpha\, \pi(\alpha|X) d\alpha.$$

5.2. Estimation under LELF

The LELF can be formulated as

$$L(\alpha, \hat{\alpha}) = e^{c(\alpha-\hat{\alpha})} - c(\alpha - \hat{\alpha}) - 1, \quad c \neq 0.$$

The Bayesian estimator under the LELF is described as

$$\hat{\alpha}_{LELF} = -\frac{1}{c} \ln \mathbb{E}[e^{-c\alpha}|X].$$

Analogous to the SELF approach, the expectation $\mathbb{E}[e^{-c\alpha} \mid X]$ is estimated by averaging the appropriately transformed samples from the MCMC chain, where the hyperparameters v_1 and v_2 (defined in Table 10) correspond to the values of c for different scenarios or model parameters. Bayesian estimation under the GELF can be formulated as follows

$$L(\alpha, \hat{\alpha}) = \frac{\left(\hat{\alpha}^k - \alpha^k\right)}{k}, \quad k \neq 0.$$

The Bayesian estimator derived under GELF is expressed as

$$\hat{\alpha}_{GELF} = \mathbb{E}[\alpha^k|X]^{\frac{1}{k}}.$$

The expectation $\mathbb{E}[\alpha^k \mid X]$ is computed by averaging the k-th power of the samples from the MCMC chain. The hyperparameters p_1 and p_2 (see Table 10) determine the value of k for different scenarios or parameters. The posterior expectations for these estimators are evaluated using Monte Carlo methods, as closed-form solutions are not obtainable.

Table 10. Summary of hyperparameters, their values, and purposes used in the simulation study for Bayesian MCMC estimation of the HS-PHLD model.

Parameter/setting	Values	Description
n	25, 50, 75, 100	Sample sizes for simulation
$\sigma_1, \omega_1, \sigma_2, \omega_2$	1.5, 1.5, 1.5, 1.5	Shape and rate parameters for gamma priors
v_1, v_2	−0.5, 0.5	Linear exponential loss hyperparameters
p_1, p_2	−0.5, 0.5	Generalized entropic loss hyperparameters
N_{sim}	500	Number of Monte Carlo data replicates
T	2500	Number of MCMC iterations per replicate
sd	0.01, 0.01	Proposed distribution standard deviations in MCMC
MCMC burn-in	20% (last 80% samples used)	Discard initial MCMC samples for estimation

We use a Metropolis- Hastings algorithm within a Gibbs sampler to obtain the posterior distributions of the parameters β_1 and β_2 since the posterior is not able to be solved analytically. The MCMC algorithm is as follows.

(1) **Initialization:** Choose starting values $\beta_1^{(0)}$ and $\beta_2^{(0)}$.
(2) **Iterative sampling:** For each iteration $t = 1, 2, \ldots, T$:
  (a) **Sample $\beta_1^{(t)}$ conditional on $\beta_2^{(t-1)}$:**
   - Propose a candidate β_1^* from a proposed distribution $q_1(\beta_1^* \mid \beta_1^{(t-1)})$, tuned to ensure valid proposals and efficient sampling (e.g., a gamma distribution with the mean centered at $\beta_1^{(t-1)}$).
   - Compute the acceptance probability:

$$\alpha_1 = \min\left(1, \frac{\pi(\beta_1^*, \beta_2^{(t-1)} \mid X)}{\pi(\beta_1^{(t-1)}, \beta_2^{(t-1)} \mid X)} \times \frac{q_1(\beta_1^{(t-1)} \mid \beta_1^*)}{q_1(\beta_1^* \mid \beta_1^{(t-1)})}\right),$$

   where $\pi(\cdot \mid X)$ denotes the unnormalized posterior density.
   - Accept β_1^* with probability α_1; otherwise, retain $\beta_1^{(t)} = \beta_1^{(t-1)}$.

  (b) **Sample $\beta_2^{(t)}$ conditional on $\beta_1^{(t)}$:**
   - Propose a candidate β_2^* from a proposed distribution $q_2(\beta_2^* \mid \beta_2^{(t-1)})$, similarly tuned for efficient sampling.
   - Compute the acceptance probability:

$$\alpha_2 = \min\left(1, \frac{\pi(\beta_1^{(t)}, \beta_2^* \mid X)}{\pi(\beta_1^{(t)}, \beta_2^{(t-1)} \mid X)} \times \frac{q_2(\beta_2^{(t-1)} \mid \beta_2^*)}{q_2(\beta_2^* \mid \beta_2^{(t-1)})}\right).$$

   - Accept β_2^* with probability α_2; otherwise, retain $\beta_2^{(t)} = \beta_2^{(t-1)}$.

(3) **Repeat:** Steps (a) and (b) for T iterations to generate a Markov chain $\{(\beta_1^{(t)}, \beta_2^{(t)})\}_{t=1}^{T}$.
(4) **Burn-in period:** Remove the initial part of the chain, which is normally around 20%, to reduce the impact of the initial values. This allows the chain to converge to the stationary distribution. The remainder of the chain is then used for inference.
(5) **Convergence diagnostics:** Convergence can also be checked visually with plots such as trace plots and autocorrelation plots. The effective sample size should also be computed, and if multiple chains were run, the Gelman-Rubin diagnostic should be used to ensure that the chains have mixed well and converged to the target posterior distribution.
(6) **Posterior estimation:** Bayesian estimates (e.g., posterior means, credible intervals) are computed from the post-burn-in samples $\{(\beta_1^{(t)}, \beta_2^{(t)})\}_{t=\text{burn-in}+1}^{T}$.

This approach balances computational feasibility with accurate approximation of the posterior distribution within the Bayesian MCMC framework.

5.3. Simulation study for Bayesian estimation

In order to check the effectiveness of Bayesian MCMC estimators, we conducted a Monte Carlo simulation with $N_{\text{sim}} = 500$ repetitions. In each replication, we obtained a random sample from the HS-PHLD model. We used the Metropolis–Hastings within the Gibbs sampler for parameter estimation. We performed $T = 2500$ iterations. We avoided the impact of starting values and ensured convergence of the Metropolis-Hastings algorithm by discarding 20% of the sample for burn-in. We obtained the results from the remaining sample. We repeated this for all replications. We checked the effectiveness of the Bayesian estimators using measures such as Bias, MSE, and coverage probability. We also obtained average estimated bias and root mean squared error (RMSE) for Bayesian methods for the HS-PHLD model for various sample sizes, i.e., $n = 25, 50, 75, 100$, as obtained in the simulation for the following cases:

- Case I: $\beta_1 = 0.5$, $\beta_2 = 1.2$;
- Case II: $\beta_1 = 0.75$, $\beta_2 = 1.5$.

The results of the simulations in Tables 11 and 13 provide insight into the performance of the Bayesian estimation approaches for the HS-PHLD parameter estimates β_1 and β_2 for various sample sizes and true parameter values. The performance can be measured in terms of the estimation accuracy and reliability through the assessment of the bias, RMSE, highest posterior density (HPD) intervals, and coverage probabilitity (CP) of each method. The study assesses their accuracy, efficiency, and reliability, allowing for a comprehensive comparative evaluation for each estimation approach. A prominent and clear pattern in the results of the simulations in both tables for all estimation approaches is that the estimation accuracy increases as the sample size n increases.

- In all cases, the pattern for both β_1 and β_2 is the same: As the sample size goes from 25 to 100, bias and RMSE decrease. This illustrates the property of consistency for all estimators: Estimates get closer to the true values as the sample size increases. This holds for both MLE and all Bayesian estimators under the varying loss functions.
- In general, the Bayesian estimators reduce the bias to a greater extent than the MLE. This difference is evident in the case of β_2 in both tables, where the bias value has reduced significantly. For instance, when $\beta_2 = 1.2$ and $n = 25$, the bias value for MLE is 0.083606 , whereas for BE_{GELF2}, it is 0.076034. This suggests that by utilizing prior knowledge in the Bayesian method, even when using non-informative priors, the estimates are, on average, closer to the truth and hence less biased.
- Efficiency, based on the value of RMSE, depends on the values of the parameters. For β_1, the maximum likelihood method is often comparable to or only marginally suboptimal compared with Bayesian methods, particularly when the sample size is small. However, for β_2 in both tables, the Bayesian estimators always have the lowest value of RMSE. This indicates that Bayesian estimators are more efficient and reliable for estimating β_2, as they provide a better trade-off between bias and variance to obtain more accurate estimates.
- The HPD intervals provide us with valuable insights into the precision of our estimates. Across the board, for all parameters and all methods, the average interval length (AIL) decreases as the sample size increases. One of the most striking observations is that the Bayesian estimators are more likely to provide HPD intervals that are shorter than the confidence intervals obtained using MLE. For example, when $\beta_2 = 1.5$ and $n = 75$, the AIL for MLE is 0.53355, whereas that of BE_{LELF2} is 0.51631, demonstrating the improved precision of Bayesian methods.
- The CP remains at the nominal level of 95.2% for all methods and for all sample sizes and parameter values. This indicates that both MLE and Bayesian estimators produce valid interval estimates that contain the parameter within the intended CP, with Bayesian methods generally producing shorter intervals, which indicate greater efficiency in interval estimation.
- The BEGELF2 and BELELF2 estimators are particularly distinguished by their accuracy and efficiency. With their sharper HPD intervals, through remaining within nominal coverage, they

clearly represent the best choice for practical application and further research on the HS-PHLD . The asymmetric loss functions achieve the best possible compromise of bias reduction, precision, and reliable interval estimation for both parameters for all sample sizes considered.

- The convergence is examined by applying the Gelman-Rubin test and the findings in Tables 12–14 are based on three parallel chains. These tables indicates the convergence behavior of the MCMC chains for the parameters β_1 and β_2 across different samples, We observed that the point estimate of the potential scale reduction factor ($\hat{R}$) falls within the acceptance range $\hat{R} < 1.1$. Specifically the values 1.00 and 1.02 strongly suggests that the Markov chains have converged to the target posterior distribution. Moreover the upper confidence limits also remain below 1.1, which indicates the stability of the chains. The multivariate potential scale reduction factor (PSRF) values near unity further suggests good mixing among the chains. Overall, the results demonstrates stable and reliable posterior estimation.
- The diagnostic plots for MCMC which are shown in Figures 6–13. These figures show that the trace plots, the marginal posterior densities the auto-correlation plots for the estimated parameters. In order to check whether our MCMC algorithm worked properly and yielded proper results, we used several diagnostics plots based on our simulated draws where we excluded the first 50% as a burn-in phase. The trace plots of our simulation results can be seen in Figures 6–13; together with the autocorrelation plots, these plots prove to be a good illustration of how well our chain converged with no signs of high correlations between simulations at different lags.

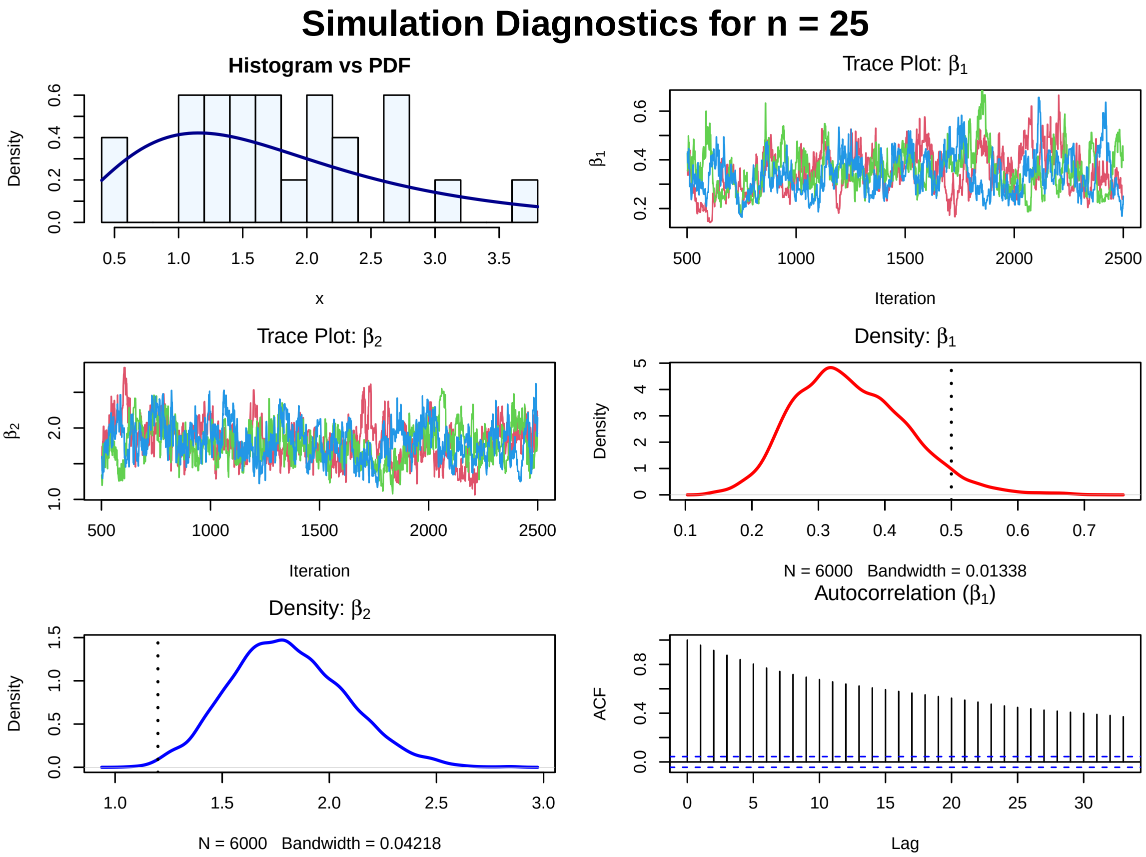

Figure 6. Simulation diagnostics from Table-11 of the HS-PHLD for n= 25.

Table 11. Simulation values for $\beta_1 = 0.5$, $\beta_2 = 1.2$ including bias, RMSE, HPD intervals, and coverage.

Parameter	Metric	MLE	BE_{SELF}	BE_{LELF1}	BE_{LELF2}	BE_{GELF1}	BE_{GELF2}
β_1	Bias (n = 25)	0.083606	0.061061	0.058822	0.063266	0.066050	0.076034
	Bias (n = 50)	0.081066	0.069584	0.068466	0.070694	0.072155	0.077295
	Bias (n = 75)	0.079237	0.071518	0.070773	0.072259	0.073245	0.076700
	Bias (n = 100)	0.081102	0.075195	0.074642	0.075746	0.076490	0.079083
	RMSE (n = 25)	0.126803	0.108673	0.107842	0.109533	0.111488	0.117563
	RMSE (n = 50)	0.106911	0.096935	0.096263	0.097610	0.098786	0.102580
	RMSE (n = 75)	0.096387	0.089349	0.088811	0.089888	0.090736	0.093544
	RMSE (n = 100)	0.093009	0.087400	0.086955	0.087844	0.088514	0.090760
	HPD_lower (n = 25)	0.210399	0.237248	0.238461	0.236052	0.232275	0.222321
	HPD_lower (n = 50)	0.297447	0.316738	0.317598	0.315886	0.314056	0.308693
	HPD_lower (n = 75)	0.312716	0.328326	0.328931	0.327725	0.326513	0.322904
	HPD_lower (n = 100)	0.332904	0.339694	0.340141	0.337278	0.336416	0.333814
	HPD_upper (n = 25)	0.596597	0.597705	0.600822	0.594641	0.592600	0.582425
	HPD_upper (n = 50)	0.563177	0.571713	0.573116	0.570321	0.569290	0.564473
	HPD_upper (n = 75)	0.525583	0.538290	0.539338	0.537248	0.536356	0.532874
	HPD_upper (n = 100)	0.507882	0.512792	0.513424	0.510181	0.509453	0.506477
	AIL (n = 25)	0.386197	0.360457	0.362361	0.358589	0.360325	0.360104
	AIL (n = 50)	0.265730	0.254974	0.255519	0.254436	0.255235	0.255781
	AIL (n = 75)	0.212868	0.209964	0.210407	0.209523	0.209844	0.209970
	AIL (n = 100)	0.174978	0.173098	0.173283	0.172903	0.173037	0.172664
	CP (n = 25)	95.200000	95.200000	95.200000	95.200000	95.200000	95.200000
	CP (n = 50)	95.200000	95.200000	95.200000	95.200000	95.200000	95.200000
	CP (n = 75)	95.200000	95.200000	95.200000	95.200000	95.200000	95.200000
	CP (n = 100)	95.200000	95.200000	95.200000	95.200000	95.200000	95.200000
β_2	Bias (n = 25)	0.405509	0.331873	0.345072	0.318864	0.323402	0.306277
	Bias (n = 50)	0.365259	0.330389	0.336915	0.323908	0.326159	0.317652
	Bias (n = 75)	0.349708	0.326778	0.331095	0.322480	0.323965	0.318319
	Bias (n = 100)	0.344378	0.327144	0.330376	0.323923	0.325036	0.320807
	RMSE (n = 25)	0.458080	0.382253	0.395380	0.369364	0.374398	0.358610
	RMSE (n = 50)	0.392039	0.356672	0.363154	0.350243	0.352619	0.344480
	RMSE (n = 75)	0.366901	0.343706	0.348003	0.339431	0.340970	0.335483
	RMSE (n = 100)	0.356807	0.339357	0.342575	0.336150	0.337292	0.333151
	HPD_lower (n = 25)	1.240176	1.191548	1.199007	1.184135	1.185247	1.172467
	HPD_lower (n = 50)	1.299940	1.300536	1.305150	1.295945	1.296986	1.289849
	HPD_lower (n = 75)	1.353808	1.337646	1.341094	1.333920	1.334895	1.329174
	HPD_lower (n = 100)	1.380279	1.365899	1.368211	1.363207	1.363921	1.360821
	HPD_upper (n = 25)	2.029883	1.919153	1.937805	1.900822	1.909478	1.889940
	HPD_upper (n = 50)	1.830751	1.794795	1.803967	1.786299	1.789787	1.780650
	HPD_upper (n = 75)	1.780362	1.747530	1.753450	1.741689	1.744182	1.737744
	HPD_upper (n = 100)	1.717555	1.691443	1.695175	1.687726	1.689238	1.685254
	AIL (n = 25)	0.789707	0.727605	0.738798	0.716687	0.724231	0.717473
	AIL (n = 50)	0.530810	0.494259	0.498818	0.490354	0.492801	0.490801
	AIL (n = 75)	0.426554	0.409885	0.412356	0.407769	0.409288	0.408570
	AIL (n = 100)	0.337276	0.325545	0.326965	0.324518	0.325317	0.324433
	CP (n = 25)	95.200000	95.200000	95.200000	95.200000	95.200000	95.200000
	CP (n = 50)	95.200000	95.200000	95.200000	95.200000	95.200000	95.200000
	CP (n = 75)	95.200000	95.200000	95.200000	95.200000	95.200000	95.200000
	CP (n = 100)	95.200000	95.200000	95.200000	95.200000	95.200000	95.200000

Table 12. Gelman-Rubin diagnostic for MCMC convergence.

Sample size	Parameter β_1			Parameter β_2	
	Point est.	Upper confidence interval.	Multivariate PSRF	Point est.	Upper confidence interval.
n = 25	1.01	1.03	1.01	1.00	1.00
n = 50	1.02	1.07	1.02	1.01	1.05
n = 75	1.00	1.00	1.01	1.01	1.02
n = 100	1.01	1.02	1.00	1.00	1.00

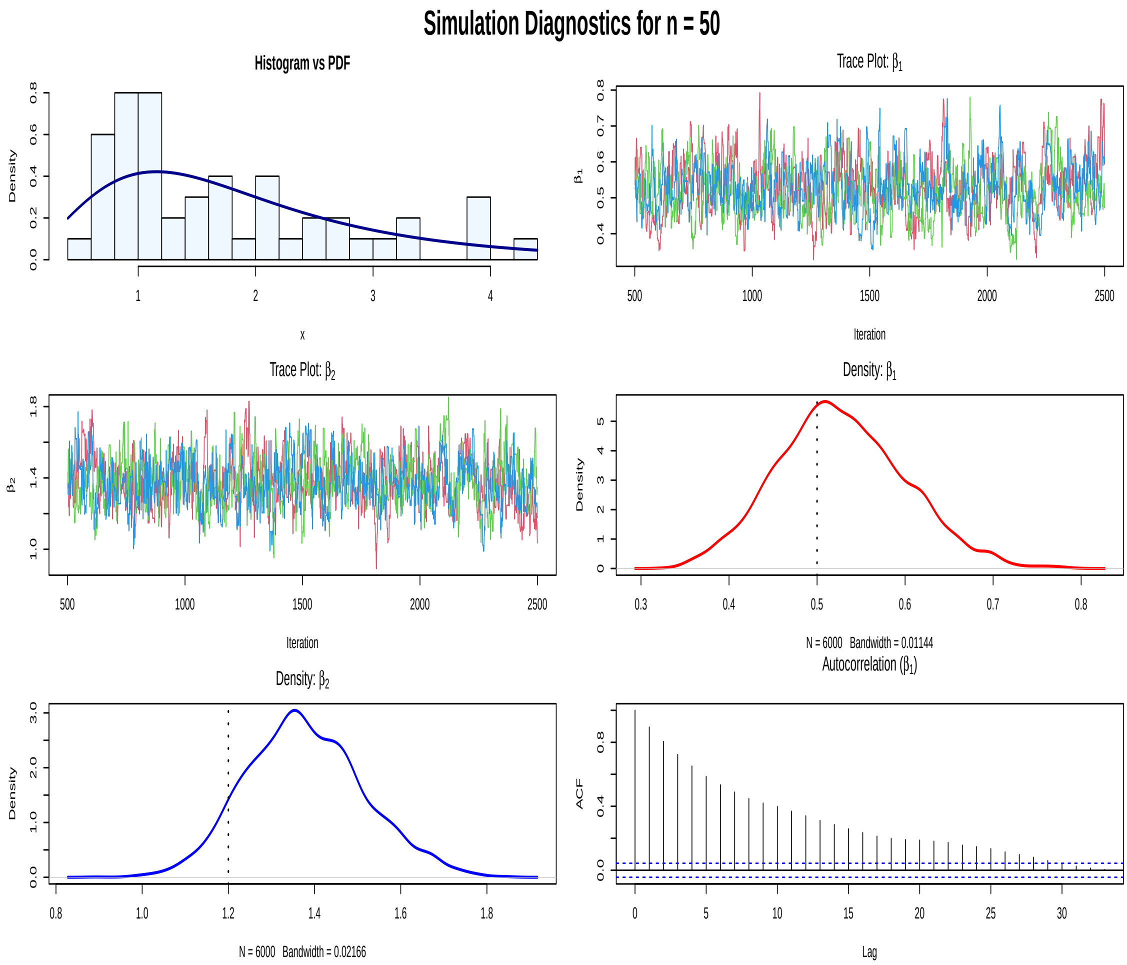

Figure 7. Simulation diagnostics from Table-11 of HS-PHLD for n= 50.

Table 13. Simulation values for $\beta_1 = 0.75$, $\beta_2 = 1.5$ including Bias, RMSE, HPD intervals, and coverage.

Parameter	Metric	MLE	BE_{SELF}	BE_{LELF1}	BE_{LELF2}	BE_{GELF1}	BE_{GELF2}
β_1	Bias (n = 25)	0.03926	0.02818	0.02420	0.03209	0.03355	0.04428
	Bias (n = 50)	0.04214	0.03612	0.03415	0.03808	0.03886	0.04432
	Bias (n = 75)	0.04155	0.03755	0.03623	0.03887	0.03939	0.04307
	Bias (n = 100)	0.04539	0.04226	0.04128	0.04324	0.04364	0.04640
	RMSE (n = 25)	0.14656	0.13239	0.13253	0.13238	0.13337	0.13595
	RMSE (n = 50)	0.10696	0.10061	0.10023	0.10103	0.10154	0.10359
	RMSE (n = 75)	0.08776	0.08359	0.08315	0.08404	0.08439	0.08610
	RMSE (n = 100)	0.07868	0.07554	0.07508	0.07600	0.07630	0.07787
	HPD_lower (n = 25)	0.39982	0.44873	0.45141	0.44610	0.45052	0.44145
	HPD_lower (n = 50)	0.54611	0.55768	0.55922	0.55615	0.55494	0.54946
	HPD_lower (n = 75)	0.55241	0.56327	0.56203	0.56233	0.56158	0.55807
	HPD_lower (n = 100)	0.58310	0.58942	0.59025	0.58859	0.58801	0.58517
	HPD_upper (n = 25)	0.96389	0.96289	0.96919	0.95673	0.96403	0.95177
	HPD_upper (n = 50)	0.92944	0.92532	0.92825	0.92242	0.92219	0.91595
	HPD_upper (n = 75)	0.85580	0.86128	0.86055	0.85956	0.85928	0.85529
	HPD_upper (n = 100)	0.82623	0.82397	0.82512	0.82282	0.82258	0.81981
	AIL (n = 25)	0.56407	0.51417	0.51778	0.51063	0.51351	0.51032
	AIL (n = 50)	0.38333	0.36764	0.36903	0.36627	0.36725	0.36649
	AIL (n = 75)	0.30339	0.29800	0.29852	0.29723	0.29770	0.29723
	AIL (n = 100)	0.24313	0.23455	0.23487	0.23423	0.23457	0.23464
	CP (n = 25)	95.20	95.20	95.20	95.20	95.20	95.20
	CP (n = 50)	95.20	95.20	95.20	95.20	95.20	95.20
	CP (n = 75)	95.20	95.20	95.20	95.20	95.20	95.20
	CP (n = 100)	95.20	95.20	95.20	95.20	95.20	95.20
β_2	Bias (n = 25)	0.50687	0.39613	0.41696	0.37570	0.38536	0.36358
	Bias (n = 50)	0.45658	0.40386	0.41409	0.39373	0.39854	0.38784
	Bias (n = 75)	0.43712	0.40259	0.40937	0.39586	0.39905	0.39195
	Bias (n = 100)	0.43048	0.40478	0.40987	0.39971	0.40212	0.39678
	RMSE (n = 25)	0.57258	0.46039	0.48101	0.44027	0.45048	0.43056
	RMSE (n = 50)	0.49005	0.43725	0.44740	0.42721	0.43216	0.42194
	RMSE (n = 75)	0.45862	0.42404	0.43077	0.41735	0.42060	0.41371
	RMSE (n = 100)	0.44601	0.42031	0.42538	0.41527	0.41771	0.41248
	HPD_lower (n = 25)	1.55018	1.46350	1.47501	1.45214	1.45565	1.43979
	HPD_lower (n = 50)	1.62490	1.61639	1.62340	1.60942	1.61205	1.60319
	HPD_lower (n = 75)	1.69209	1.66222	1.66697	1.66678	1.65882	1.64888
	HPD_lower (n = 100)	1.72530	1.70443	1.70775	1.70077	1.70227	1.69794
	HPD_upper (n = 25)	2.53735	2.35819	2.38842	2.32849	2.34538	2.31938
	HPD_upper (n = 50)	2.28824	2.23489	2.24874	2.22118	2.22871	2.21628
	HPD_upper (n = 75)	2.22563	2.18070	2.18908	2.18229	2.17685	2.16520
	HPD_upper (n = 100)	2.14683	2.11075	2.11633	2.10446	2.10776	2.10183
	AIL (n = 25)	0.98717	0.89468	0.91341	0.87635	0.88973	0.87959
	AIL (n = 50)	0.66333	0.61850	0.62534	0.61177	0.61666	0.61309
	AIL (n = 75)	0.53355	0.51847	0.52211	0.51551	0.51803	0.51631
	AIL (n = 100)	0.42152	0.40632	0.40858	0.40369	0.40548	0.40390
	CP (n = 25)	95.20	95.20	95.20	95.20	95.20	95.20
	CP (n = 50)	95.20	95.20	95.20	95.20	95.20	95.20
	CP (n = 75)	95.20	95.20	95.20	95.20	95.20	95.20
	CP (n = 100)	95.20	95.20	95.20	95.20	95.20	95.20

Table 14. Gelman-Rubin diagnostic: Potential scale reduction factors (PSRFs).CI, confidence interval.

Sample size	Parameter β_1		Parameter β_2		Multivariate PSRF
	Point Est.	Upper CI, confidence interval.	Point Est.	Upper CI, confidence interval.	
n = 25	1.02	1.07	1.01	1.01	1.02
n = 50	1.00	1.00	1.01	1.01	1.00
n = 75	1.00	1.00	1.00	1.00	1.00
n = 100	1.01	1.02	1.00	1.01	1.01

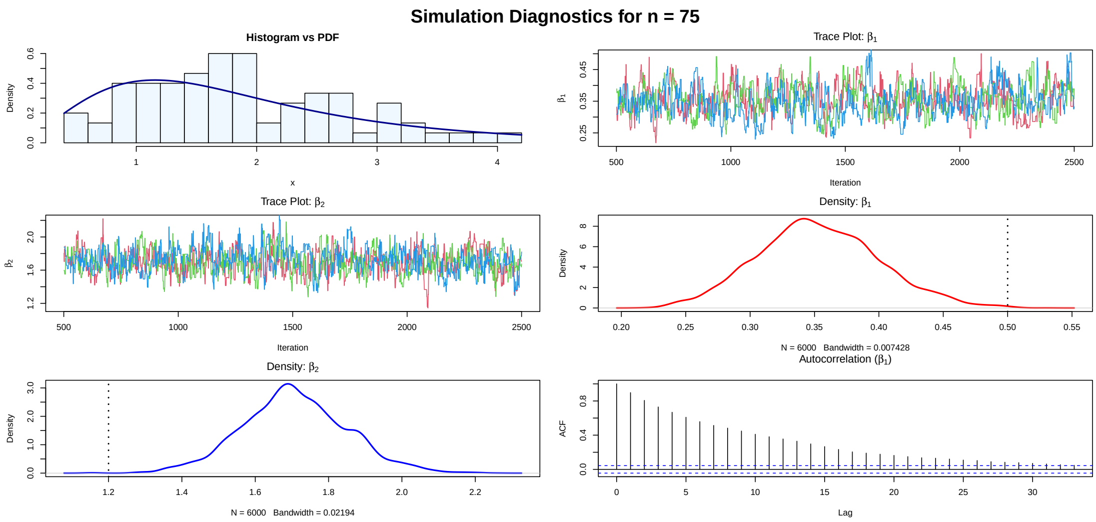

Figure 8. Simulation diagnostics from Table-11 of the HS-PHLD for n=75.

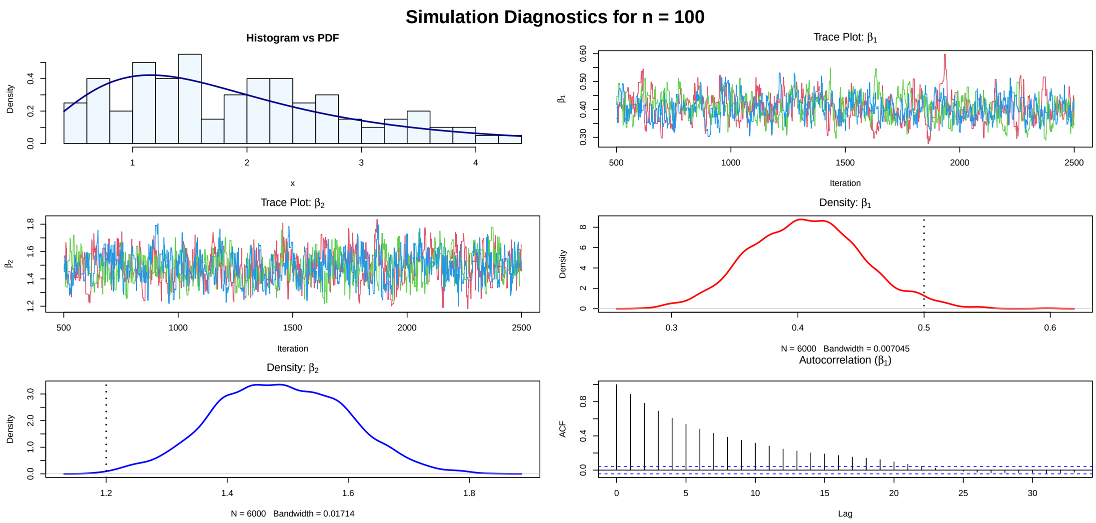

Figure 9. Simulation diagnostics from Table-11 of the HS-PHLD for n= 100.

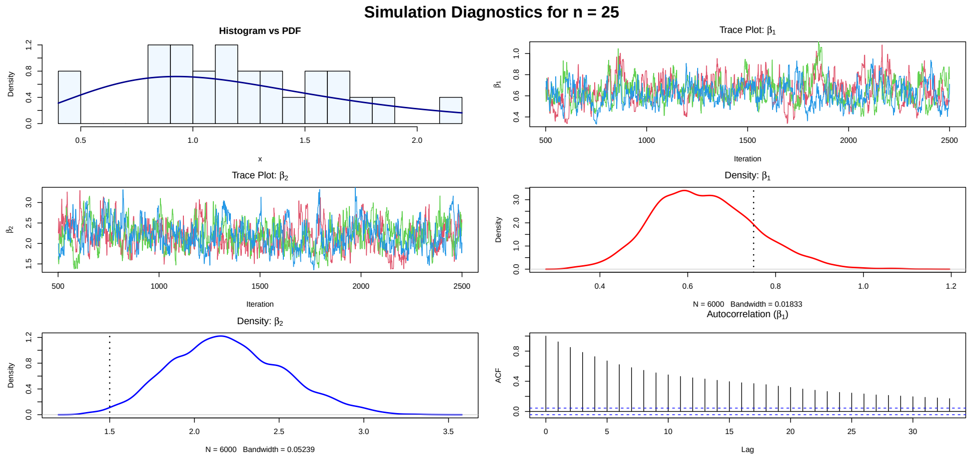

Figure 10. Simulation diagnostics from Table-13 of the HS-PHLD for n= 25.

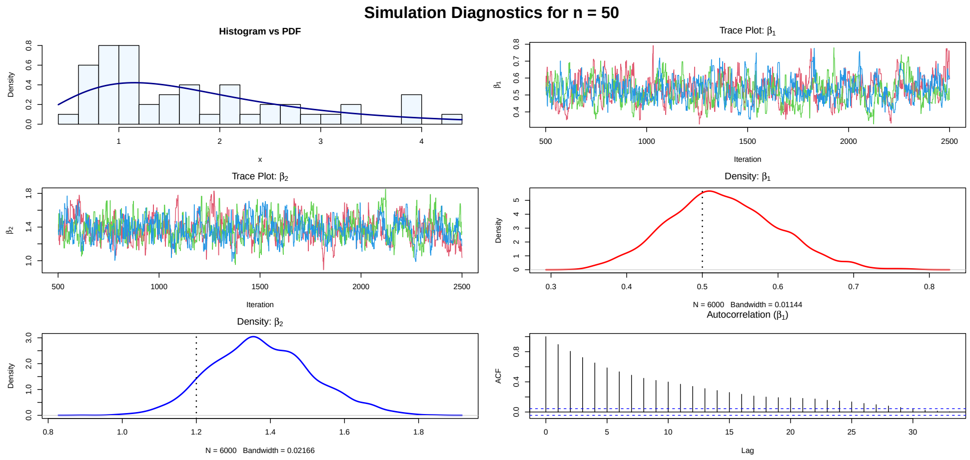

Figure 11. Simulation diagnostics Table-13 of HS-PHLD for n=50.

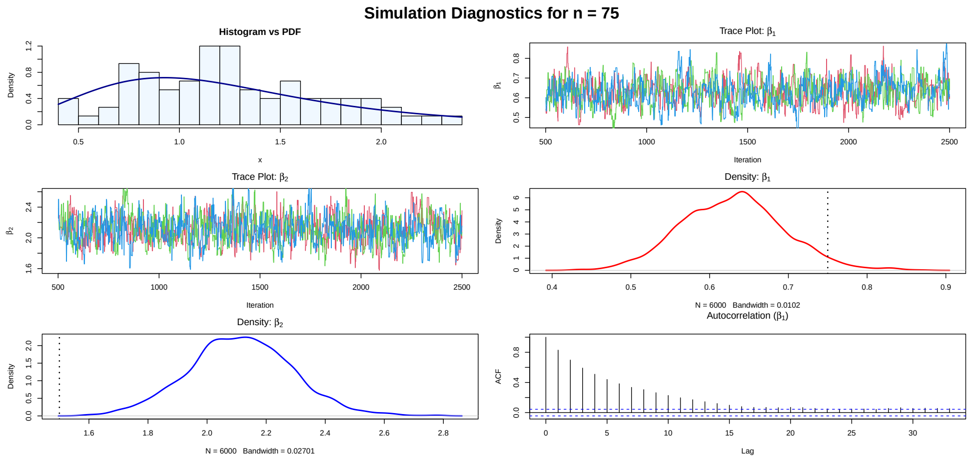

Figure 12. Simulation diagnostics from Table-13 of the HS-PHLD for n= 75.

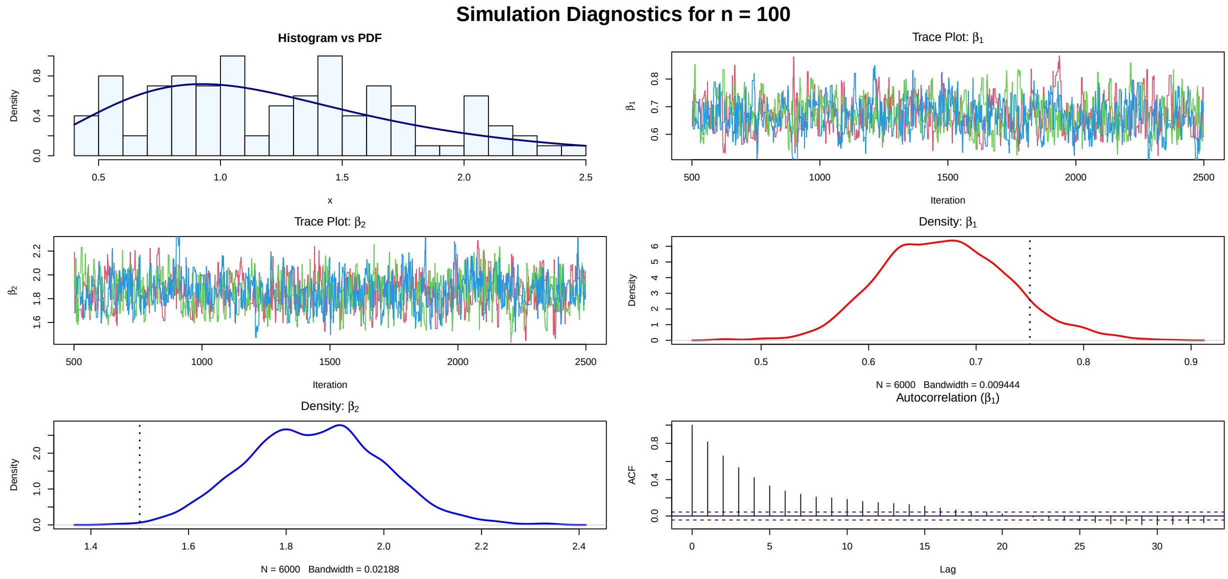

Figure 13. Simulation diagnostics from Table-13 of the HS-PHLD for n= 100

6. Data analysis

This segment analyzes real-world datasets to determine the HS-PHLD's flexibility and performance. We investigate three datasets: The first depicts the drought-related death rate in Canada in 2020, the second illustrates the crude mortality rate (CMR) among persons who inject drugs, and the third gives information on the breaking stress of carbon fibers (measured in GPa) with 50- mm lengths. To determine the HS-PHLD's adaptability, we compare its goodness-of-fit against several competing distributions, including the PHLD, the Chen distribution (Chen-D), the Gompertz distribution (Gomp-D), the Weibull distribution (WD), the novel cot Fréchet distribution (NCFD) of [12], the novel sin Lomax distribution (NSLD) of [18], the Kumaraswamy power Fréchet distribution (KPFD) of [19], and the exponentiated Weibull distribution (EWD).

The effectiveness of these distributions is evaluated via a variety of statistical criteria, including the Akaike information criterion (AIC), the consistent Akaike information criterion (CAIC), the Bayesian information criterion (BIC), and the Hannan- Quinn information Criterion (HQIC). Non-parametric tests, comprising the Kolmogorov-Smirnov test (K-S), the Anderson-Darling test (A), and the Cramér-von Mises test (W), are additionally used, along with their respective p-values. A distribution is considered preferable if it offers lower values across these criteria while delivering higher p-values. Moreover eHS-PHLD achieved the highest AIC weight, indicating it is the most plausible model among those considered.

Tables 15, 17, and 19 provide the maximum likelihood (ML) estimates and the accompanying standard errors for the datasets. Furthermore, Tables 16, 18, and 19 offers the goodness-of-fit findings for the established HS-PHLD model. Throughout all datasets, the HS-PHLD outperforms other models, demonstrating greater flexibility and robustness.

Data set I: The dataset contains COVID-19 mortality rates in Canada over 36 days, spanning from April 10 to May 15, 2020. The data was sourced from the World Health Organization (WHO) COVID-19 dashboard, available at `https://covid19.who.int/`. It specifically focuses on daily

mortality rates during this timeframe.
3.1091, 3.3825,3.1444, 3.2135, 2.4946, 3.5146, 4.9274, 3.3769, 6.8686, 3.0914, 4.9378, 3.1091, 3.2823, 3.8594, 4.0480,4.1685, 3.6426, 3.2110, 2.8636, 3.2218, 2.9078, 3.6346, 2.7957, 4.2781, 4.2202, 1.5157, 2.6029, 3.3592,2.8349, 3.1348, 2.5261, 1.5806, 2.7704, 2.1901, 2.4141, 1.9048.

The dataset has a minimum value of 1.516 and a maximum of 6.869, with a mean of 3.282. The first quartile is 2.789, the median is 3.178, and the third quartile is 3.637, while the skewness of 1.214 and kurtosis of 6.152 indicate a right-skewed distribution with heavy tails. The data are positively skewed with a longer right tail and exhibits leptokurtic behaviour, suggesting sharper peaks and heavier tails than a normal distribution.

Table 15. The ML estimates (standard errors in parentheses) for Dataset I.

Model	$\hat{\beta}_1$	$\hat{\beta}_2$	$\hat{\theta}$	$\hat{\lambda}$
HS-PHLD	0.04082619	2.66283115	...	...
	(0.01692528)	(0.30598892)	...	...
PHLD	0.04077727	2.80790072		
	(0.02043209)	(0.33570052)		...
Chen-D	0.04703544	0.86001544	...	...
	(0.01445551)	(0.04552483)		...
Gomp-D	0.08416981	0.68242851	...	...
	(0.04087310)	(0.09611306)	...	...
WD	0.014131457	3.301459384	...	...
	(0.007696221)	(0.361802341)	...	...
KPFD	1.1244832	0.8655848	15.0952652	23.1005287
	(1.2696637)	(3.7614936)	(83.3398154)	(63.8541435)
NSLD	0.007537349	41.865277232	...	...
	(0.004824443)	(27.158144301)	...	...
NCFD	24.3570505	3.2376784	...	...
	(8.4551548)	(0.3722326)	...	...
EWD	0.4397237	1.5109548	8.1871738	...
	(0.5025900)	(0.6033351)	(9.3109098)	...

Table 16. Comparison criterion and goodness-of-fit statistics for Dataset I.

Model	-ℓ	AIC	CAIC	HQIC	BIC
HS-PHLD	**48.49331**	**100.98663**	**101.35027**	**102.09201**	**104.15367**
PHLD	51.72174	107.44347	107.80711	108.54885	110.61051
Chen-D	57.73274	119.46548	119.82911	120.57086	122.63251
Gomp-D	58.23414	120.46827	120.83191	121.57365	123.63531
WD	51.47482	106.94964	107.31328	108.05502	110.11668
KPFD	49.05649	104.11298	105.40330	106.32374	110.44706
NSLD	71.42355	146.8471	147.2107	147.9525	150.0141
NCFD	53.3288	110.6576	111.0213	111.7630	113.8247
EWD	49.0936	102.18721	102.93721	103.84528	106.937775
Model	K-S statistic (p-value)	A*(p-value)	W*(p-value)	ΔAIC	AIC-weights
HS-PHLD	**0.12689 (0.6081)**	**0.59089 (0.6555)**	**0.1049 (0.5638)**	**0.00**	**0.5386**
PHLD	0.14029 (0.478)	1.1374 (0.2922)	0.18968 (0.2892)	6.46	0.0213
Chen-D	0.18442 (0.1727)	2.4405 (0.05358)	0.41467 (0.06557)	18.48	0.0001
Gomp-D	0.1863 (0.1642)	2.5277 (0.04824)	0.43043 (0.05956)	19.48	0.0000
WD	0.14844 (0.4058)	1.1447 (0.2892)	0.19782 (0.2724)	5.96	0.0273
KPFD	0.10827 (0.4926)	0.52938 (0.5159)	0.089601 (0.5411)	3.13	0.1128
NSLD	0.32013 (0.001249)	6.2558 (0.0007595)	1.2009 (0.0007264)	45.86	0.0000
NCFD	0.18423 (0.1735)	1.7458 (0.1276)	0.30466 (0.1309)	9.67	0.0043
EWD	0.15535 (0.4192)	0.6274 (0.6179)	0.188875 (0.445)	1.20	0.295

Table 17. The ML estimates (standard errors in parentheses) for Dataset II.

Model	$\hat{\beta}_1$	$\hat{\beta}_2$	$\hat{\theta}$	$\hat{\lambda}$
HS-PHLD	0.3504077	1.1705704	...	...
	(0.0530392)	(0.1080019)	...	...
PHLD	0.32892160	1.34435944	...	...
	(0.07153829)	(0.13331681)	...	...
Chen-D	0.13872491	0.62706868	...	...
	(0.02748465)	(0.03620812)	...	...
Gomp-D	0.95820922	0.22628131		
	(0.44164336)	(0.06212107)	...	...
WD	0.16787656	1.59666384	...	...
	(0.04105938)	(0.15017099)		...
KPFD	0.5079914	0.1650593	45.9875188	37.6292093
	(0.3810671)	(1.1976295)	(343.9863784)	(92.9217465)
NSLD	0.010258565	40.491299218	...	...
	(0.007023009)	(27.611474649)	...	...
NCFD	1.8141978	1.4695052	...	...
	(0.2296868)	(0.1315385)	...	...
EWD	0.9278107	0.8354858	4.0020797	...
	(0.7628670)	(0.3493109)	(4.0253753)	...

Table 18. Comparison criterion and goodness-of-fit statistics for Dataset II.

Model	$-\ell$	AIC	CAIC	HQIC	BIC
HS-PHLD	**119.1122**	**242.2245**	**242.4180**	**243.9403**	**246.5732**
PHLD	121.4353	246.8706	247.0642	248.5865	251.2194
Chen-D	126.5859	257.1719	257.3654	258.8877	261.5206
Gomp-D	124.2617	252.5234	252.7170	254.2393	256.8722
WD	120.4257	244.8515	245.0450	246.5673	249.2002
KPFD	119.9552	245.9105	246.5771	249.3422	254.6080
NSLD	122.1297	248.2594	248.4530	249.9753	252.6082
NCFD	125.5849	255.1699	255.3634	256.8857	259.5186
EWD	119.9552	243.9103	244.3037	246.4841	250.4335
Model	K-S statistic (p-value)	A* (p-value)	W* (p-value)	ΔAIC	AIC-weights
HS-PHLD	**0.063724 (0.9545)**	**0.27905 (0.9529)**	**0.041663(0.9258)**	**0.00**	**0.4969**
PHLD	0.10054 (0.527)	0.62275 (0.6261)	0.090885 (0.633)	4.65	0.0487
Chen-D	0.11784 (0.3274)	1.5772 (0.1591)	0.22647 (0.2217)	14.95	0.0003
Gomp-D	0.10411 (0.4816)	1.2726 (0.2413)	0.17489 (0.3224)	10.30	0.0029
WD	0.095577 (0.5927)	0.50873 (0.7373)	0.078017 (0.7051)	2.63	0.1336
KPFD	0.064564 (0.9493)	0.27233 (0.9573)	0.041628 (0.926)	3.69	0.0787
NSLD	0.11281 (0.3798)	0.98869 (0.3629)	0.14694 (0.3999)	6.03	0.0243
NCFD	0.1559 (0.08489)	1.5128 (0.1735)	0.25894 (0.1773)	12.95	0.0008
EWD	0.067129 (0.9314)	0.27274 (0.957)	0.041665 (0.9258)	1.69	0.2139

Table 19. The ML estimates (standard error in parentheses) for Dataset III.

Model	$\hat{\beta}_1$	$\hat{\beta}_2$	$\hat{\theta}$	$\hat{\lambda}$
HS-PHLD	0.02871884	4.31733972	...	...
	(0.01031335)	(0.39792396)	...	...
PHLD	0.017521171	5.033480151	...	...
	(0.008255227)	(0.479658710)	...	...
Chen-D	0.02279975	1.48857145	...	...
	(0.00658317)	(0.06094416)	...	...
Gomp-D	0.003935951	2.280767454	...	...
	(0.001125466)	(0.113966747)	...	...
WD	0.006211121	5.790988664	...	...
	(0.002453684)	(0.412544107)	...	...
KPFD	1.2666693	0.1690586	103.0996905	170.7613848
	(0.6475164)	(0.2642516)	(167.2390565)	(518.0522582)
NSLD	0.008331224	54.494829735	...	...
	(0.004330322)	(28.666868504)	...	...
NCFD	33.5891704	5.1241263	...	...
	(9.7580911)	(0.4505964)		...
EWD	0.08356755	3.59876118	2.79296592	...
	(0.13609829)	(1.37755300)	(2.33583388)	...

Table 20. Comparison criterion and goodness-of-fit statistics for Dataset III.

Model	$-\ell$	AIC	CAIC	HQIC	BIC
HS-PHLD	**34.69502**	**73.39004**	**73.58677**	**75.09103**	**77.70781**
PHLD	36.05506	76.11012	76.30684	77.81110	80.42788
Chen-D	40.45630	84.91259	85.10931	86.61358	89.23036
Gomp-D	39.10220	82.20440	82.40112	83.90539	86.52217
WD	35.39935	74.79871	74.99543	76.49969	79.11647
KPFD	35.37198	76.74395	77.42192	80.14593	85.37949
NSLD	101.8267	207.6533	207.8501	209.3543	211.9711
NCFD	43.49945	90.99889	91.19561	92.69988	95.31666
EWD	35.45494	74.90988	75.30988	77.46135	81.38652
Model	K.S statistic (p-value)	A* (p-value)	W* (p-value)	ΔAIC	AIC-weights
HS-PHLD	**0.06971 (0.9149)**	**0.24352 (0.9737)**	**0.036022 (0.9537)**	**0.00**	**0.4130**
PHLD	0.071387 (0.8959)	0.34537 (0.9002)	0.032125 (0.9696)	2.72	0.1060
Chen-D	0.092798 (0.64)	1.0409 (0.3362)	0.11555 (0.5151)	11.52	0.0013
Gomp-D	0.093371 (0.6323)	0.85487 (0.4426)	0.0856 (0.6617)	8.81	0.0050
WD	0.071221 (0.8961)	0.27163 (0.9577)	0.042357 (0.7946)	1.41	0.2042
KPFD	0.077078 (0.8356)	0.29599 (0.9487)	0.038136 (0.9226)	3.35	0.0772
NSLD	0.36648 (6.837e-08)	14.644 (9.375e-06)	2.8842 (6.948e-08)	134.26	0.0000
NCFD	0.12799 (0.2452)	1.69 (0.1371)	0.27229 (0.1621)	17.61	0.0001
EWD	0.077158 (0.905)	0.25801 (0.9481)	0.038488 (0.9216)	1.52	0.1932

In Figure 14, the plots reveal the data distribution, skewness, and tail behaviour. PP-plots (probability-probability plots), QQ-plots assess normality, while the survival function shows event's probability over time. The TTT-plot compares the theoretical vs. empirical fits. Where the PP-plots is Probability-Probability Plot (sometimes called a Percent-Percent Plot). A graphical tool used to compare the empirical cumulative distribution function (CDF) of a dataset against the theoretical CDF of a specified probability distribution. The PP-plots are highly sensitive to discrepancies in the middle (the bulk) of the distribution, rather than the tails. The QQ-Plot (Quantile-Quantile Plot) a graphical tool that compares the quantiles of our empirical data against the quantiles of a theoretical distribution, and TTT-Plot (Total Time on Test Plot) A foundational graphical tool used in reliability and survival analysis to identify the shape of the empirical hazard rate (failure rate) function of a dataset before we even choose a model. It plots the empirical scaled TTT transform against the cumulative proportion of failures. Both axes range from 0 to 1. The x-axis represents the fraction of failures: k/n. The y-axis represents the scaled TTT statistic: $\phi_n(k/n) = \frac{T(x_{(k)})}{T(x_{(n)})}$, where $T(x_{(k)})$ is the total time accumulated on the test up to the k-th failure.

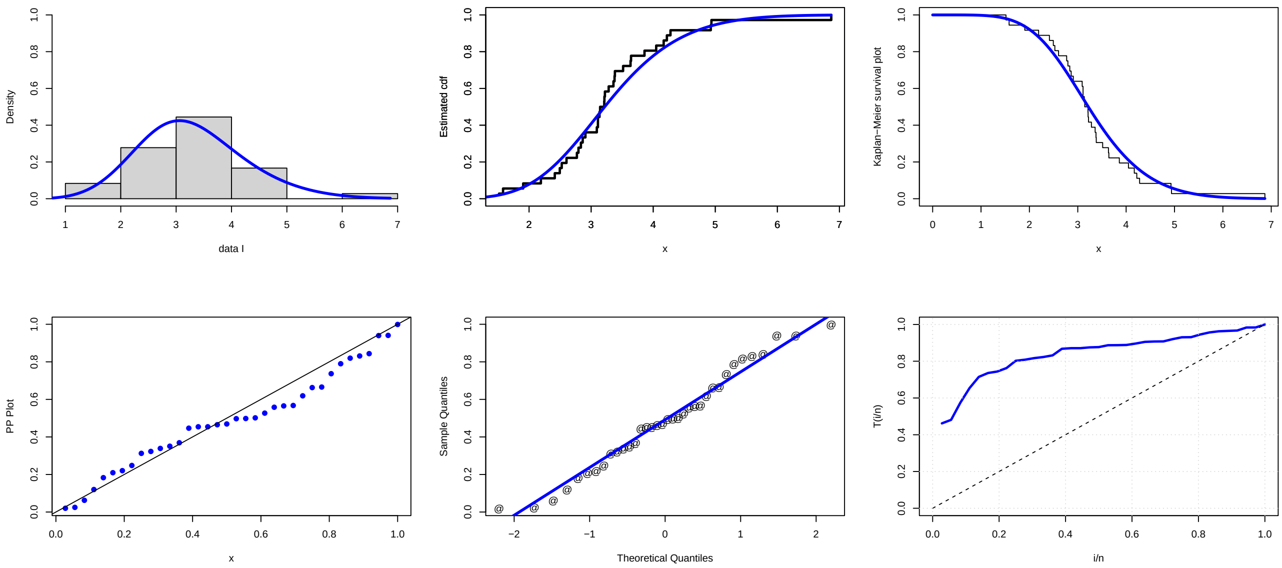

Figure 14. Histogram, empirical CDF, survival function, PP-plot, QQ-plot, and TTT-plot for the HS-PHLD Dataset I.

Data set II: The dataset, sourced from Mathers et al. [17], provides information on the crude mortality rate (CMR) in individuals who inject drugs. It includes the following observations:
2.01, 6.32, 3.52, 2.15, 5.42, 2.04, 2.77, 2.26, 1.95, 1.00, 2.45, 0.74, 0.98, 1.27, 2.77, 3.68, 1.18, 1.09,1.60, 0.57, 3.33, 0.91, 7.14, 2.08, 3.85, 1.99, 7.76, 2.52, 1.57, 4.67, 4.22, 1.92, 1.59, 4.08, 2.02, 0.84,6.85, 2.18, 2.04, 1.05, 2.91, 1.37, 2.43, 2.28, 3.74, 1.30, 1.59, 1.83, 3.85, 6.30, 4.83, 0.50, 3.40, 2.33,4.25, 3.49, 2.12, 0.83, 0.54, 3.23, 4.50, 0.71, 0.48, 2.30, 7.73.

The dataset's second column has a minimum value of 0.480 and a maximum of 7.760, with a mean of 2.726. The first quartile is 1.370, the median is 2.180, and the third quartile is 3.680. The skewness of 1.125 indicates a right-skewed distribution, while the kurtosis of 3.693 suggests slightly heavier tails than a normal distribution. The data is right-skewed with a moderate spread, as most values lie between 1.370 and 3.680. The mean that is higher than the median confirms the skewness. The kurtosis suggests that the distribution has slightly thicker tails compared to a normal distribution.

In Figure 15, the plots reveal the data distribution, skewness, and tail behaviour. The PP-plot and QQ-plots assess normality, while the survival function shows event's probability over time. The TTT-plot compares the theoretical vs. empirical fit.

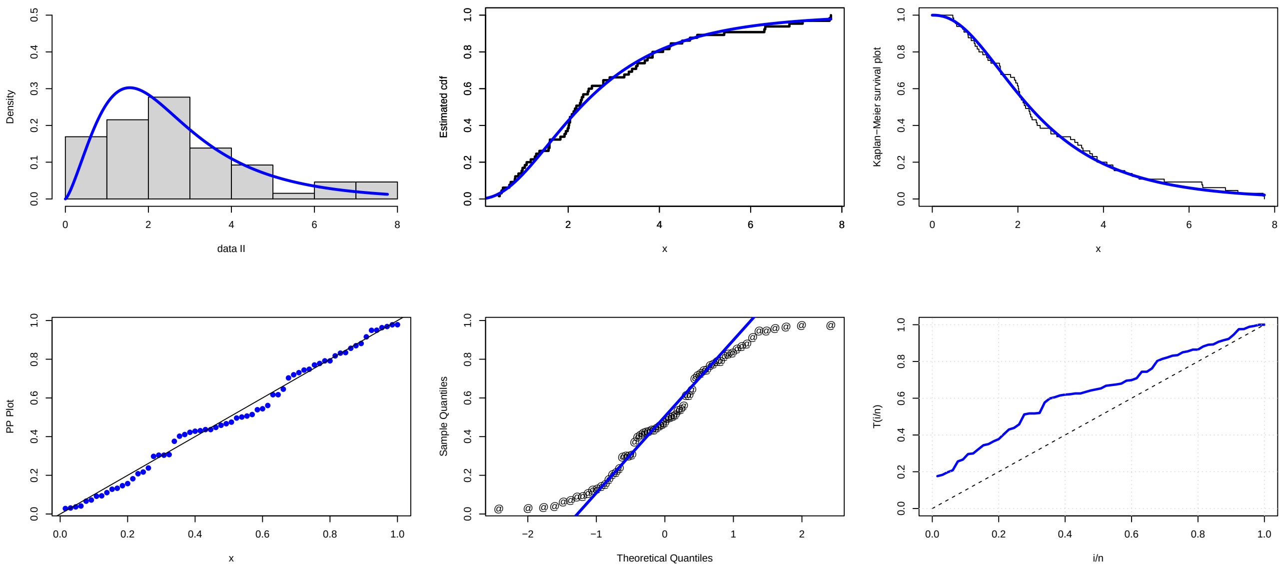

Figure 15. Histogram, empirical CDF, survival function, PP-plot, QQ-plot, and TTT-plot for the HS-PHLD Dataset II.

Data-set III: The dataset provides measurements of the breaking stress (in GPa) for carbon fibers with a length of 50 mm. This data were originally collected and published by Bader and Priest [21]. The observations are as follows:
1.339, 1.434, 1.549, 1.574, 1.589, 1.613, 1.746, 1.753, 1.764, 1.807, 1.812, 1.84, 1.852, 1.852, 1.862, 1.864, 1.931, 1.952, 1.974, 2.019, 2.051, 2.055, 2.058, 2.088, 2.125, 2.162, 2.171, 2.172, 2.18, 2.194, 2.211, 2.27, 2.272, 2.28, 2.299, 2.308, 2.335, 2.349, 2.356, 2.386, 2.39, 2.41, 2.43, 2.458, 2.471, 2.497, 2.514, 2.558, 2.577, 2.593, 2.601, 2.604, 2.62, 2.633, 2.67, 2.682, 2.699, 2.705, 2.735, 2.785, 3.02, 3.042, 3.116, 3.174.

The dataset has a minimum value of 1.339 and a maximum of 3.174, with a mean of 2.241. The first quartile is 1.914, the median is 2.271, and the third quartile is 2.563, while the skewness (0.042) and kurtosis (2.527) suggest a nearly symmetric and moderately light-tailed distribution. The data is nearly symmetric (low skewness) and has lighter tails than a normal distribution (lower kurtosis). The median and mean are close, suggesting fairly balanced data as shown in Table 20.

In Figure 16, the plots the reveal data distribution, skewness, and tail behavior. The PP-plots and QQ-plots assess normality, while the survival function shows event's probability over time. The TTT-plot compares the theoretical vs. empirical fits.

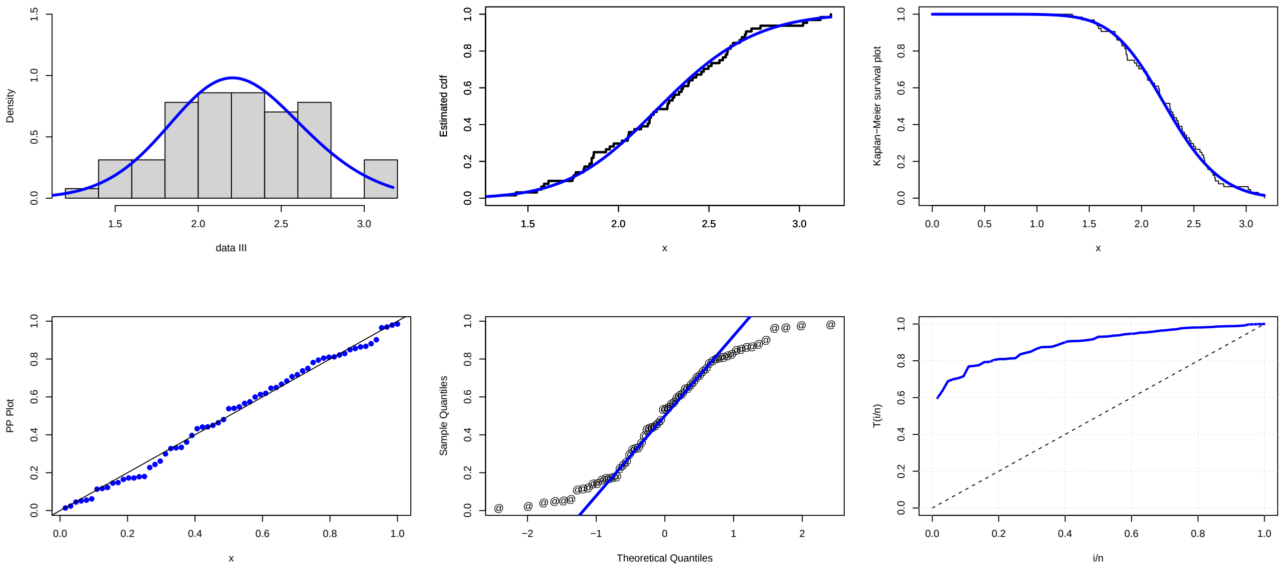

Figure 16. Histogram, empirical CDF, survival function, PP-plot, QQ-plot, and TTT-plot for the HS-PHLD Dataset III.

Figure 17 provides information on the estimated PDFs of the fitted models over histograms for Datasets I, II, and III.

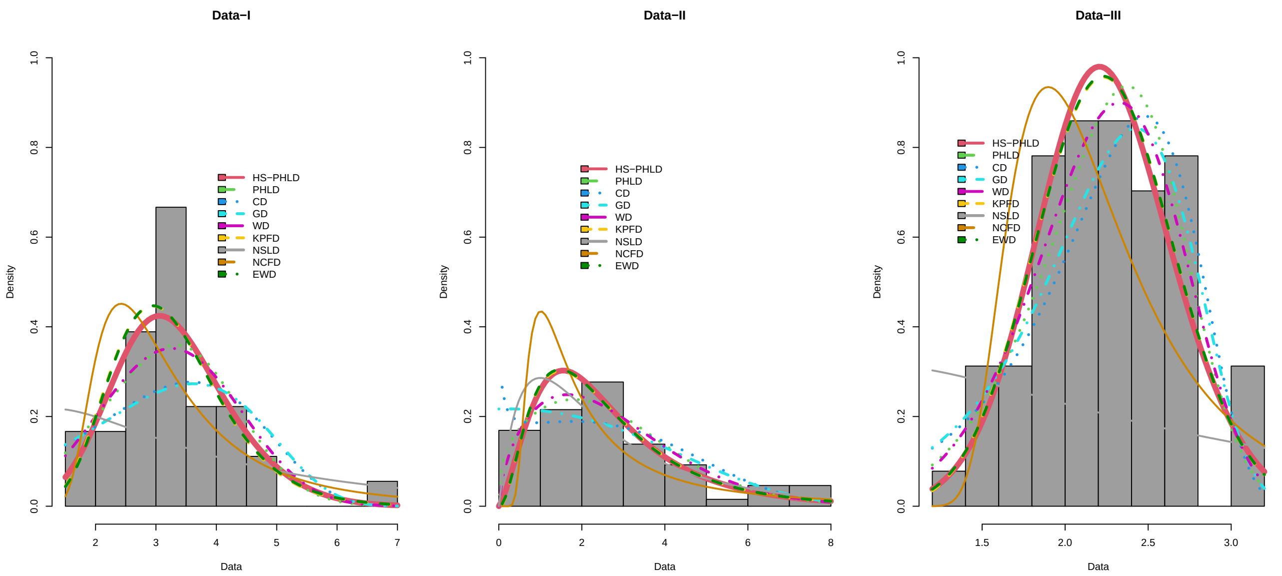

Figure 17. Estimated PDFs of the fitted models for Datasets I, II, and III.

7. Conclusions

In the present article, we establish a novel family of distributions based on the hyperbolic secant function, known as the hyperbolic secant-B (HS-B) family. This framework, which utilizes the properties of the hyperbolic secant function, enables the creation of new trigonometric distributions based on existing baselines. We demonstrate that the proposed family outperforms its baseline competitors, providing greater flexibility for modelling complicated data. The HS-HLPD is a particular instance within this family that is thoroughly investigated. We determine its CDF, PDF, and series expansions, as well as conducting a thorough study of its moments, actuarial risk measures, and other related statistical functions. The model parameters are computed via both non-Bayesian and Bayesian techniques to provide robust inference. To validate its applicability, we present the proposed distribution to three real-world datasets: COVID-19-related data, CMR among individuals who inject drugs, and the breaking stress (in GPa) of 50-mm carbon fibers. The empirical results corroborate the model's capacity to capture complicated data patterns, indicating that it might be useful in a variety of domains such as actuarial science, reliability analysis, and biological research. We hypothesize that this distribution may be applied to different areas that require flexible and tractable probabilistic modeling.

Author contributions

Aijaz Ahmad: Conceptualization, formal analysis, data curation, writing – review & editing; Ahmed R. El-Saeed: Software, formal analysis, writing – review & editing, funding acquisition; Taha Radwan: Methodology, software, funding acquisition; Manzoor A. Khanday: Methodology, resources; Ahlam H. Tolba: Methodology, validation, formal analysis, investigation, writing – review & editing. visualization. All authors have read and approved the final version of the manuscript for publication.

Use of Generative-AI tools declaration

The authors declare that they have not used Artificial Intelligence (AI) tools in the creation of this article.

Acknowledgments

The researchers would like to thank the Deanship of Graduate Studies and Scientific Research at Qassim University for financial support (QU-APC-2026).

Conflict of interest

The authors declare no conflict of interest

References

1. A. Hassan1, I. H. Dar, M. A. Lone, A novel family of generating distributions based on trigonometric functions with an application to exponential distribution, *J. Sci. Res.*, **65** (2021), 172–179. https://doi.org/10.37398/JSR.2021.650519
2. M. A. Alomair, Z. Ahmad, G. S. Rao, H. Al-Mofleh, S. K. Khosa, A. S. Al Naim, A new trigonometric modification of the Weibull distribution: Control chart and applications in quality control, *PLoS One*, **18** (2023), e0286593. https://doi.org/10.1371/journal.pone.0286593

3. C. Chesneau, H. S. Bakouch, T. Hussain, A new class of probability distributions via cosine and sine functions with applications, *Commun. Stat. Simul. Comput.*, **48** (2019), 2287–2300. https://doi.org/10.1080/03610918.2018.1440303

4. L. Souza, W. R. O. Junior, C. C. R. Brito, C. Chesneau, T. A. E. Ferreira, L. G. M. Soares, General properties of cos-G class of distributions with applications, *Eurasian Bull. Math.*, **2** (2019), 63–79.

5. F. Jamal, C. Chesneau, A new family of polyno-expo-trigonometric distributions with applications, *Infin. Dimens. Anal. Quantum Probab. Relat. Top.*, **22** (2019), 1950027. https://doi.org/10.1142/S0219025719500279

6. D. Kumar, U. Singh, S. K. Singh, A new distribution using sine function–its application to bladder cancer patients data, *J. Stat. Appl. Pro.*, **4** (2015), 417–427. http://dx.doi.org/10.12785/jsap/040309

7. M. A. Lone, I. H. Dar, T. R. Jan, A new method for generating distributions with an application to Weibull distribution, *Reliab. Theory Appl.*, **17** (2022), 223–239.

8. M. Jallal, A. Ahmad, R. Tripathi, Weibull inverse power Rayleigh distribution with applications related to distinct fields of science, *Reliab. Theory Appl.*, **17** (2022), 272–290.

9. H. O. Odhah, H. M. Alshanari, Z. Ahmad, F. Khan, A. A. A. H. El-Bagoury, A novel probabilistic approach based on trigonometric function: Model theory with practical applications, *Symmetry*, **15** (2023), 1528. https://doi.org/10.3390/sym15081528

10. Z. Mahmood, T. Jawa, N. Sayed-Ahmed, E. M. Khalil, A. H. Muse, A. H. Tolba, An extended cosine generalized family of distributions for reliability modeling: Characteristics and applications with simulation study, *Math. Probl. Eng.*, **2022** (2022), 3634698. https://doi.org/10.1155/2022/3634698

11. A. T. Ramadan, A. H. Tolba, B. S. El-Desouky, A unit half-logistic geometric distribution and its application in insurance, *Axioms*, **11** (2022), 676. https://doi.org/10.3390/axioms11120676

12. A. Ahmad, A. A. Rather, Y. A. Tashkady, M. E. Bakr, M. M. M. El-Din, A. M. Gemeay, et al., Deriving the new cotangent Frechet distribution with real data analysis, *Alex. Eng. J.*, **105** (2024), 12–24. https://doi.org/10.1016/j.aej.2024.06.038

13. A. Ahmad, N. Alsadat, M. N. Atchadé, S. Q. ul-Ain, A. M. Gemeay, M. A. Meraou, et al., A new hyperbolic sine-generator with an example of Rayleigh distribution: Simulation and data analysis in industry, *Alex. Eng. J.*, **73** (2023), 415–426. https://doi.org/10.1016/j.aej.2023.04.048

14. A. Ahmad, F. M. Alghamdi, A. Ahmad, O. Albalawi, A. A. Zaagan, M. Zakarya, et al., New arctan-generator family of distributions with an example of Frechet distribution: simulation and analysis related to strength of glass carbon fiber, *Alex. Eng. J.*, **100** (2024), 42–52. https://doi.org/10.1016/j.aej.2024.05.021

15. L. Souza, W. R. O. Junior, C. C. R. Brito, C. Chesneau, R. Fernandes, T. A. E. Ferreira, Sec-G class of distributions: Properties and applications, *Symmetry*, **14** (2022), 299. http://dx.doi.org/10.3390/sym14020299

16. R. L. Smith, J. C. Naylor, A comparison of maximum likelihood and Bayesian estimation for the three parameter Weibull distribution, *J. R. Stat. Soc. Ser. C-Appl. Stat.*, **36** (1987), 358–369. https://doi.org/10.2307/2347795

17. B. M. Mathers, L. Degenhardt, C. Bucello, J. Lemon, L. Wiessing, M. Hickman, Mortality among people who inject drugs: A systematic review and meta-analysis, *Bull. World Health Organ.*, **91** (2013), 102–123. https://doi.org/10.2471/BLT.12.108282

18. A. Ahmad, A. A. Rather, A. M. Gemeay, M. Nagy, L. P. Sapkota, A. H. Mansi, Novel sin-G class of distributions with an illustration of Lomax distribution: Properties and data analysis, *AIP Adv.*, **14** (2024), 035132. https://doi.org/10.1063/5.0180263

19. N. Alsadat, A. Ahmad, M. Jallal, A. M. Gemeay, M. A. Meraou, E. Hussam, et al., The novel Kumaraswamy power Frechet distribution with data analysis related to diverse scientific areas, *Alex. Eng. J.*, **70** (2023), 651–664. https://doi.org/10.1016/j.aej.2023.03.003

20. S. Nadarajah, *The model for fracture toughness*, *J. Mech. Sci. Technol.*, **22** (2008), 1255–1258. https://doi.org/10.1007/s12206-007-1049-y

21. M. G. Bader, A. M. Priest, Statistical Aspects of Fibre and Bundle Strength in Hybrid Composites, In: *Progress in science and engineering of composites*, 1982, 1129–1136. https://doi.org/10.5281/zenodo.15402867

A. Appendix

Theorem A.1. *Let $B(x;\Theta)$ be a baseline CDF with survival function $\bar{B}(x;\Theta) = 1 - B(x;\Theta)$, $\Theta > 0$. Define*

$$F(x;\Theta) = \frac{e^{2\bar{e}} + 1}{(e^{\bar{e}} - 1)^2} \int_0^{\left(e - e^{\bar{B}(x;\Theta)}\right)} \operatorname{sech}(t)\tanh(t)\, dt, \quad x \in \mathbb{R},\ 2 < e < 3.$$

Then $F(x;\Theta)$ is a valid CDF.

Proof. **Step 1: Range.** Since $0 \le B(x;\Theta) \le 1$, we have $0 \le \bar{B}(x;\Theta) \le 1$, which implies

$$e^{\bar{B}(x;\Theta)} \in [1, e] \ \Rightarrow\ e - e^{\bar{B}(x;\Theta)} \in [0, e-1].$$

As $\operatorname{sech}(t)\tanh(t) \ge 0$ for $t \ge 0$, and

$$\int_0^m \operatorname{sech}(t)\tanh(t)\, dt = 1 - \operatorname{sech}(m),$$

it follows that

$$0 \le F(x;\Theta) \le \frac{e^{2\bar{e}} + 1}{(e^{\bar{e}} - 1)^2} (1 - \operatorname{sech}(e-1)) = 1.$$

Step 2: Boundary Conditions. Since $B(x;\Theta)$ is a valid CDF,

$$\lim_{x\to-\infty} B(x;\Theta) = 0, \quad \lim_{x\to+\infty} B(x;\Theta) = 1.$$

Thus,

$$\lim_{x\to-\infty} \bar{B}(x;\Theta) = 1, \quad \lim_{x\to+\infty} \bar{B}(x;\Theta) = 0.$$

Hence,

$$e^{\bar{B}(x;\Theta)} \to e \text{ as } x \to -\infty, \quad e^{\bar{B}(x;\Theta)} \to 1 \text{ as } x \to +\infty.$$

Using

$$F(x;\Theta) = \frac{e^{2\bar{e}} + 1}{(e^{\bar{e}} - 1)^2}\Big(1 - \operatorname{sech}(e - e^{\bar{B}(x;\Theta)})\Big),$$

we get

$$\lim_{x\to-\infty} F(x;\Theta) = 0, \quad \lim_{x\to+\infty} F(x;\Theta) = 1.$$

Step 3: Monotonicity. Differentiating,

$$f(x;\Theta) = \frac{e^{2\bar{e}} + 1}{(e^{\bar{e}} - 1)^2} \operatorname{sech}\Big(e - e^{\bar{B}(x;\Theta)}\Big) \tanh\Big(e - e^{\bar{B}(x;\Theta)}\Big) \cdot \frac{d}{dx}\Big(e - e^{\bar{B}(x;\Theta)}\Big) \geq 0,$$

which shows that $F(x;\Theta)$ is non-decreasing. Continuity follows from that of $B(x;\Theta)$. Hence, $F(x;\Theta)$ is a valid CDF. □